



# Enumeration and analysis of models of planar maps via the bijective method

Collet Gwendal

## ► To cite this version:

Collet Gwendal. Enumeration and analysis of models of planar maps via the bijective method. Combinatorics [math.CO]. École Polytechnique, 2014. English. NNT: . tel-01084964

HAL Id: tel-01084964

<https://pastel.hal.science/tel-01084964>

Submitted on 20 Nov 2014

**HAL** is a multi-disciplinary open access archive for the deposit and dissemination of scientific research documents, whether they are published or not. The documents may come from teaching and research institutions in France or abroad, or from public or private research centers.

L'archive ouverte pluridisciplinaire **HAL**, est destinée au dépôt et à la diffusion de documents scientifiques de niveau recherche, publiés ou non, émanant des établissements d'enseignement et de recherche français ou étrangers, des laboratoires publics ou privés.



**THÈSE DE DOCTORAT DE  
L'ÉCOLE POLYTECHNIQUE**

Spécialité

**Informatique**

École doctorale de l'École Polytechnique

Présentée par

**Gwendal COLLET**

Pour obtenir le grade de  
**DOCTEUR de l'ÉCOLE POLYTECHNIQUE**

Sujet de la thèse :

**Énumération et analyse de modèles de cartes  
planaires par la méthode bijective**

soutenue le 18 novembre 2014

devant le jury composé de :

M. Éric FUSY	Directeur de thèse
M. Gilles SCHAEFFER	Directeur de thèse
M. Konstantinos PANAGIOTOU	Rapporteur
M. Jean-François MARCKERT	Rapporteur
M. Michael DRMOTA	Examinateur
M. Emmanuel GUITTER	Examinateur
Mme Michèle SORIA	Examinatrice



# Contents

<b>1</b>	<b>Préliminaires</b>	<b>7</b>
1.1	Classes combinatoires et séries génératrices . . . . .	7
1.1.1	Classes combinatoires . . . . .	7
1.1.2	Séries génératrices et méthode symbolique . . . . .	8
1.1.3	Génération aléatoire . . . . .	9
1.1.4	Énumération bijective . . . . .	11
1.2	Graphes, surfaces et cartes . . . . .	11
1.2.1	Graphes, plongements et cartes topologiques . . . . .	11
1.2.2	Cartes combinatoires : étiquetées ou enracinées . . . . .	13
1.2.3	Familles classiques de cartes . . . . .	15
1.2.4	Bijections classiques sur les cartes . . . . .	17
1.3	Distances et convergence . . . . .	18
1.3.1	Profil des distances dans les cartes . . . . .	18
1.3.2	Résultats de convergence . . . . .	19
1.4	Organisation de la thèse . . . . .	21
<b>2</b>	<b>Bijection for bipartite and quasi-bipartite maps</b>	<b>25</b>
2.1	Introduction . . . . .	25
2.2	Bijection between vertex-pointed maps and mobiles . . . . .	28
2.3	Bipartite case . . . . .	30
2.4	Quasi-bipartite case . . . . .	33
2.4.1	Blossoming trees and mobiles . . . . .	33
2.4.2	Decomposing along the middle-path . . . . .	35
<b>3</b>	<b>Extension to <math>p</math>-constellations and quasi-<math>p</math>-constellations</b>	<b>39</b>
3.1	Introduction . . . . .	39
3.2	From vertex-pointed hypermaps to hypermobiles . . . . .	41
3.3	Proof of Theorem 7 for $p$ -constellations . . . . .	43
3.4	Proof of Theorem 7 for quasi $p$ -constellations . . . . .	45
3.4.1	Blossoming $p$ -trees and $p$ -mobiles . . . . .	47
3.4.2	Decomposing along the alternating middle-path . . . . .	48
3.4.3	Degree transfer lemma . . . . .	50

<b>4 A bijection for simple maps</b>	<b>53</b>
4.1 Introduction . . . . .	53
4.2 The bijection . . . . .	58
4.2.1 Canonical orientations for outer-triangular simple maps.	58
4.2.2 Canonical orientations for eulerian triangulations. . .	58
4.2.3 From outer-triang. simple maps to eulerian triang. . .	59
4.2.4 Bijection with oriented binary trees. . . . .	62
4.3 Counting results . . . . .	63
4.3.1 Exact counting. . . . .	63
4.3.2 Asymptotic counting. . . . .	67
4.4 Application to random generation of simple maps . . . . .	69
4.4.1 Sampling rooted simple maps by edges. . . . .	69
4.4.2 Sampling rooted simple maps by vertices and edges. .	70
4.5 A simpler formulation from trees to maps . . . . .	71
<b>5 Distance-profile in random rooted simple maps</b>	<b>75</b>
5.1 Introduction . . . . .	75
5.2 Bijection and transfer of canonical paths . . . . .	77
5.3 The profile of random rooted eulerian triang. . . . .	79
5.3.1 Profile with respect to the root-vertex . . . . .	79
5.3.2 Profile with respect to the outer face . . . . .	80
5.4 The profile of random rooted simple maps . . . . .	80
5.4.1 Profile of random rooted outer-triangular simple maps	80
5.4.2 Profile of random rooted simple maps . . . . .	83
5.5 Further results . . . . .	85
5.5.1 The profile of random rooted loopless and general maps	85
5.5.2 Towards convergence to the Brownian map . . . . .	86
<b>6 Conclusion et perspectives</b>	<b>91</b>
6.1 Cartes avec bords . . . . .	91
6.2 Cartes simples et distances . . . . .	92
<b>Bibliographie</b>	<b>93</b>

# Remerciements

Je tiens à remercier en premier lieu mes deux directeurs de thèse Gilles Schaeffer et Éric Fusy. Ce sont eux qui m'ont initié aux trésors de la combinatoire, en me faisant découvrir toute la richesse des bijections lors des cours du MPRI, puis en me guidant dans le vaste univers des cartes. Grâce à leur enthousiasme et le foisonnement de leurs idées, j'ai pu entrevoir toute une variété de problèmes stimulants. Je dois beaucoup à Éric qui a su, par sa gentillesse et son soutien sans faille, me donner confiance en mon travail.

Je remercie Konstantinos Panagiotou et Jean-François Marckert pour leur relecture attentive de mon manuscrit. Merci également à Michèle Soria, Emmanuel Guitter et Michael Drmota d'avoir accepté de faire partie de mon jury.

Si ces années se sont si bien déroulées, c'est avant tout car j'ai eu la chance de m'intégrer dans une communauté chaleureuse et ouverte d'esprit. Partout où j'ai pu m'aventurer, j'ai trouvé des gens agréables et accueillants. Je remercie donc tous ceux que j'ai pu croiser au LIX, et qui ont contribué à en faire un cadre épanouissant : Luca, Marie, Vincent, Guillaume, Dominique, Katya, Maks, Thibaut, Clément, Étienne... Mais aussi Corinne et Sylvie, toujours souriantes et efficaces, grâce à qui tout s'est déroulé tranquillement.

Je pense également à tous les jeunes du groupe ALEA, de Paris à Luminy, en passant par Bordeaux et Oxford, qui m'ont poussé à quitter ma coquille : Alice et Axel pour plein de choses, Adeline et notre escapade japonaise, Élie dont je n'arrive décidément pas à me débarrasser, Julien et son poulpe, Jérémie et Dalida, les chansons avec Julien, Cécile, Matthieu, Thu Hien, Basile, Fiona, Adrien, et j'en oublie...

J'ai beaucoup appris au cours des – toujours enrichissantes – journées Cartes, avec entre autres Jérémie Bouttier et Jérémie Bettinelli, ou lors de mes séjours en Espagne avec Juanjo Rué et Marc Noy.

Et comme il n'y a pas que la recherche, je me dois de remercier mes colocataires qui ont réussi à me supporter pendant tout ce temps.

Enfin je n'exprimerai jamais assez toute l'affection que j'éprouve pour ma famille, mon père, ma mère, mon frère et ma sœur à qui je dois tout et qui ont toujours été à mes côtés quoi que je fasse.



# Chapter 1

## Préliminaires

### 1.1 Classes combinatoires et séries génératrices

#### 1.1.1 Classes combinatoires

La combinatoire énumérative s'intéresse à des ensembles d'objets (permutations, arbres, graphes, cartes...) et cherche à répondre à la question suivante : *combien existe-t-il d'objets d'une taille donnée ?* Pour que cette question ait un sens, nous allons considérer des familles appelées *classes combinatoires*. Une *classe combinatoire*  $(\mathcal{C}, |\cdot|)$  est une collection d'objets  $\mathcal{C}$  munie d'un paramètre de taille  $|\cdot| : \mathcal{C} \rightarrow \mathbb{N}$  (longueur, nombre de sommets, d'arêtes...), tel que :

$$\forall n \geq 0, c_n = \#\{c \in \mathcal{C} : |c|=n\} \text{ est fini.}$$

Ainsi nous essayerons d'évaluer, pour une classe donnée  $\mathcal{C}$ , ses coefficients  $c_n (n \geq 0)$  de manière exacte ou approchée.

Considérons par exemple l'ensemble des permutations comptées selon la longueur. L'ensemble  $\mathfrak{S}_n (n \geq 1)$  des permutations à  $n$  éléments est l'ensemble des manières d'ordonner ces éléments. Un simple raisonnement par récurrence nous donne l'expression exacte suivante :

$$\#\mathfrak{S}_n = n \cdot (n - 1) \cdots 2 \cdot 1 = n! .$$

La formule de Stirling nous donne également une formule approchée pour ce nombre :

$$n! \underset{n \rightarrow \infty}{\sim} \sqrt{2\pi n} \left(\frac{n}{e}\right)^n .$$

Cette formule asymptotique facilite notamment la comparaison avec d'autres classes d'objets.

On peut également définir d'autres paramètres que la taille sur une classe combinatoire, pourvu qu'ils satisfassent la même contrainte. Extrêmement

variés, ces paramètres dépendent de la structure considérée et des informations que l'on souhaite en extraire : nombre de cycles dans une permutation, de composantes connexes dans un graphe, hauteur d'un arbre... .

### 1.1.2 Séries génératrices et méthode symbolique

Afin de manipuler plus facilement les coefficients d'une classe, nous allons introduire un outil fondamental de la combinatoire énumérative : *la série génératrice*. Soit  $(\mathcal{C}, |\cdot|)$  une classe combinatoire et ses coefficients  $c_n (n \geq 0)$ . La série génératrice  $C(z)$  associée à  $\mathcal{C}$  est une série formelle définie ainsi :

$$C(z) = \sum_{c \in \mathcal{C}} z^{|c|} = \sum_{n \geq 0} c_n z^n.$$

Outre la représentation élégante de tous les coefficients d'une classe dans un même objet mathématique, la série génératrice se révèle être un outil particulièrement adapté pour un grand nombre de classes combinatoires. En effet, de nombreuses opérations sur les classes se traduisent directement en opérations sur les séries associées. On va alors chercher à décomposer une classe à l'aide d'opérations élémentaires, les traduire automatiquement à l'aide d'un *dictionnaire* pour obtenir des équations sur les séries : c'est la méthode symbolique décrite dans l'excellent ouvrage de Flajolet et Sedgewick [34]. Si nous ne pouvons ici être exhaustifs, voici quelques opérations importantes – des *briques de base* – et leur traduction sur les séries :

- Atome neutre  $\mathcal{E}$  de taille 0 :  $E(z) = z^0 = 1$ ,
- Atome unitaire  $\mathcal{Z}$  de taille 1 :  $Z(z) = z$ ,
- Union disjointe  $\mathcal{C} = \mathcal{A} + \mathcal{B}$  :  $C(z) = A(z) + B(z)$ ,
- Produit cartésien  $\mathcal{C} = \mathcal{A} \times \mathcal{B}$  :  $C(z) = A(z) \cdot B(z)$ ,
- Séquence : si  $\mathcal{A}$  n'a pas d'élément neutre,  $\mathcal{C} = \sum_{k \geq 0} \mathcal{A}^k = Seq(\mathcal{A})$  :

$$C(z) = \frac{1}{1 - A(z)}.$$

Afin d'éclaircir notre propos, nous allons détailler l'exemple des *arbres binaires*, structure essentielle en combinatoire (et dans cette thèse). Un arbre binaire est une structure récursive définie ainsi : soit une feuille, soit un sommet interne relié à un fils gauche et un fils droit qui sont eux-mêmes des arbres binaires. Si on note  $\mathcal{B}$  l'ensemble des arbres binaires comptés selon le nombre de sommets internes, on obtient alors directement la décomposition suivante :

$$\mathcal{B} = \{\circ\} + \{\bullet\} \cdot \mathcal{B} \cdot \mathcal{B} \Rightarrow B(z) = 1 + zB^2(z) \Rightarrow B(z) = \frac{1 - \sqrt{1 - 4z}}{2z}.$$

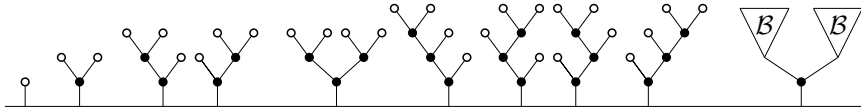


Figure 1.1: Arbres binaires ayant au plus 3 sommets internes  $\bullet$ , et leur décomposition générique.

Un développement en série nous donne la valeur des coefficients de  $B(z)$  :  $[z^n]B(z) = \frac{1}{n+1} \binom{2n}{n} = \text{Cat}(n)$ . Ce sont les nombres de Catalan (dont les premiers termes sont : 1,1,2,5,14,42...) qui apparaissent dans un grand nombre de structures combinatoires. La formule de Stirling nous donne également un équivalent :

$$\text{Cat}(n) \underset{n \rightarrow \infty}{\sim} 4^n n^{-3/2}.$$

**Remarque 1** (Nombres de Catalan généralisés). *Si nous avons décrit ici le cas des arbres binaires, on peut facilement étendre ce raisonnement aux arbres  $m$ -aires ( $m \geq 2$ ), où les sommets internes ont degré  $m+1$ . On obtient alors une expression similaire pour le nombre d'arbres  $m$ -aires à  $n$  sommets internes :*

$$Cat_m(n) = \frac{1}{(m-1)n+1} \binom{mn}{n}.$$

On appelle ces coefficients les nombres de Catalan généralisés, et on retrouve les nombres de Catalan pour  $m = 2$ .

Lorsqu'une classe combinatoire est munie de plusieurs paramètres (outre la taille), on peut définir sa série génératrice multivariée. Soit une classe  $(\mathcal{C}, |\cdot|, u(\cdot))$  munie d'un paramètre  $u(\cdot)$ , si  $x$  représente la taille et  $z$  le paramètre  $u(\cdot)$ , alors sa série génératrice bivariée s'exprime ainsi :

$$C(x, z) = \sum_{c \in \mathcal{C}} x^{|c|} z^{u(c)} = \sum_{i, j \geq 0} c_{i,j} x^i z^j.$$

où le coefficient  $c_{i,j}$  est le nombre d'objets dans  $\mathcal{C}$  de taille  $i$  et tels que le paramètre  $u$  vaut  $j$ .

### 1.1.3 Génération aléatoire

Un générateur aléatoire pour une classe combinatoire  $\mathcal{C}$  est un algorithme qui tire aléatoirement un objet  $c \in \mathcal{C}$  selon une distribution donnée. On parlera le plus souvent de génération aléatoire uniforme en taille exacte lorsque l'on souhaite obtenir un objet d'une taille donnée, de façon à ce que tous les objets de même taille soient équiprobables. Cela permet d'avoir un aperçu du comportement typique des objets de grandes tailles, de vérifier la validité

d'un modèle, ou encore d'étudier la complexité d'algorithmes sur de grandes instances.

Outre les méthodes *ad hoc*, spécifiques à certaines classes, il existe deux méthodes générales pour concevoir des générateurs aléatoires uniformes. La première, et la plus naturelle, est la *méthode récursive* [52] [35] : si l'on sait décomposer un objet d'une taille donnée en objets de plus petite taille, il suffit de tirer aléatoirement ces objets et de les recombiner. Par exemple si  $\mathcal{C} = \mathcal{A} \times \mathcal{B}$ , pour tirer un objet de  $c \in \mathcal{C}$  de taille  $n$ , il faut tirer deux objets  $a \in \mathcal{A}$  et  $b \in \mathcal{B}$  dont la somme des tailles est égale à  $n$ . Pour conserver l'uniformité en taille, il faut pouvoir calculer la probabilité pour que  $a$  soit de taille  $k$  et  $b$  de taille  $n - k$  :

$$\mathbb{P}(|a|=k \text{ et } |b|=n-k : a \in \mathcal{A}, b \in \mathcal{B}, |(a,b)|=n) = \frac{a_k b_{n-k}}{\sum_{i=0}^n a_i b_{n-i}}.$$

Cela suppose d'évaluer un grand nombre de coefficients et peut s'avérer coûteux.

La deuxième méthode permet d'éviter cet écueil, en mettant à profit les séries génératrices : ce sont les *générateurs de Boltzmann* introduits dans [32]. Soit une classe combinatoire  $\mathcal{C}$ , un *générateur de Boltzmann* de  $\mathcal{C}$ , noté  $\Gamma\mathcal{C}(x)$ , tire aléatoirement un élément  $c \in \mathcal{C}$  avec probabilité :

$$\mathbb{P}(c) = \frac{x^{|c|}}{C(x)}.$$

Pour que cette expression ait un sens, il faut choisir  $x$  positif et dans le rayon de convergence de la série. On note que si deux objets de même taille sont bien équiprobables, un tel générateur ne garantit pas la taille de l'objet obtenu. On peut toutefois biaiser le générateur en choisissant un paramètre  $x$  adapté afin de viser une taille donnée. En effet, l'espérance de la taille de l'objet généré est :

$$\mathbb{E}_x(|c|) = x \frac{C'(x)}{C(x)}.$$

On peut alors obtenir un *générateur de Boltzmann en taille exacte* (respectivement *en taille approchée*) en utilisant une technique de rejet : on rejette l'objet tiré tant qu'il n'est pas de la bonne taille (resp. dans un intervalle de taille donné  $[n(1 - \epsilon), n(1 + \epsilon)]$ ), puis on recommence jusqu'à obtenir satisfaction. La propriété d'uniformité est bien conservée, et de tels générateurs sont souvent efficaces en pratique (en général linéaire en taille approchée).

Les générateurs de Boltzmann s'étendent naturellement au cas des séries génératrices bivariées. Soit une classe  $(\mathcal{C}, |\cdot|, u(\cdot))$  munie d'un second paramètre  $u$ , son générateur de Boltzmann bivarié  $\Gamma\mathcal{C}(x, z)$  tire un objet  $c \in \mathcal{C}$  avec probabilité :

$$\mathbb{P}(c) = \frac{x^{|c|} z^{u(c)}}{C(x, z)}.$$

À condition de pouvoir déterminer des valeurs adaptées pour les paramètres  $x, z$ , on génère alors efficacement des objets en contrôlant leur taille et un second paramètre (voir Chapitre 4 pour un exemple de générateur bivarié).

#### 1.1.4 Énumération bijective

La méthode bijective consiste à établir une bijection  $\Phi$  entre la classe combinatoire considérée  $\mathcal{C}$  et une classe  $\mathcal{C}'$  que l'on sait déjà énumérer. De plus, il faut que cette bijection “préserve” la taille, au sens où, pour un entier donné  $n$ , tous les objets de taille  $n$  dans  $\mathcal{C}$  s'envoient par  $\Phi$  sur des objets d'une même taille  $n$  dans  $\mathcal{C}'$ . On a alors égalité des coefficients  $c_n, c'_n$  et donc des séries génératrices  $C(z), C'(z)$ . Réciproquement, si deux familles ont la même série génératrice, cela implique l'existence d'une bijection entre ces deux familles : en effet, on peut toujours définir une bijection entre deux ensembles finis de même cardinal (en numérotant chacun des éléments d'une taille donnée). Toutefois, on cherchera dans la mesure du possible à établir une bijection *constructive*, à construire de manière automatique l'image dans  $\mathcal{C}'$  d'un objet de  $\mathcal{C}$ . Cela se prête notamment bien aux algorithmes de génération aléatoire : si l'on sait générer uniformément un objet de  $\mathcal{C}'$ , alors une bijection constructive nous donne son image qui sera également uniforme dans  $\mathcal{C}$ .

Une bijection consiste à faire correspondre un objet d'une classe  $\mathcal{C}$  avec un objet dans une autre classe  $\mathcal{C}'$ . De manière moins contraignante, on peut également utiliser des correspondances *many-to-many*. On cherche alors à faire correspondre des sous-ensembles de  $\mathcal{C}$  d'une taille donnée  $r$  avec des sous-ensembles de  $\mathcal{C}'$  d'une taille donnée  $s$  : il s'agit d'une correspondance *r-to-s* (le cas  $r = s = 1$  serait donc une bijection). Cela se traduit naturellement par la relation suivante sur les séries génératrices :  $s \cdot C(z) = r \cdot C'(z)$ . De plus, lorsque  $r = s$ , on a égalité des séries génératrices et donc l'existence d'une bijection.

## 1.2 Graphes, surfaces et cartes

### 1.2.1 Graphes, plongements et cartes topologiques

Nous abordons ici des notions classiques de la théorie des graphes. Un *graphe*  $G = (V, E)$  est un couple formé d'un ensemble fini  $V$  de *sommets* et d'un ensemble fini  $E \subseteq V \times V$  de paires de sommets, appelées *arêtes*. En toute généralité, nous autorisons une arête à joindre un sommet à lui-même, formant une *boucle*, ainsi que les *arêtes multiples* (plusieurs arêtes peuvent joindre les deux mêmes sommets :  $E$  est donc en réalité un multi-ensemble). Un graphe est dit *simple* lorsqu'il ne contient ni boucle ni arête multiple. Soit  $e = (u, v)$  une arête de  $G$ , alors  $e$  est *incidente* aux sommets  $u, v$  et les sommets  $u$  et  $v$  sont dits *adjacents*.

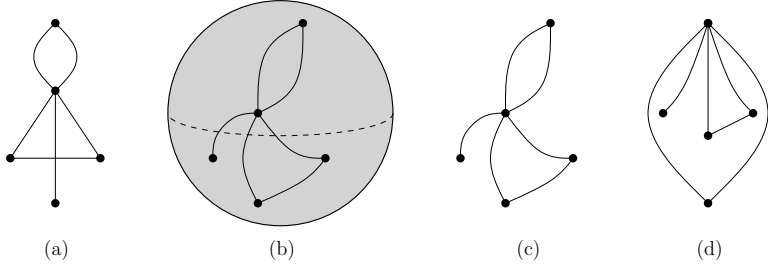


Figure 1.2: (a) Un graphe planaire  $G$ , (b) un plongement de  $G$  sur la sphère et (c),(d) deux projections planaires de ce plongement.

Une surface désigne ici une surface compacte orientable sans bord. À déformation continue près, une surface  $\mathbb{S}$  est uniquement déterminée par son *genre*  $g \in \mathbb{N}$  : l’unique surface de genre 0 est la sphère, et l’unique surface de genre  $g \geq 1$  est le tore à  $g$  trous.

Si un graphe  $G$  peut être dessiné sur une surface  $\mathbb{S}$  sans qu’il y ait d’intersection d’arêtes, on obtient alors un *plongement* de  $G$  dans  $\mathbb{S}$ . Les composantes connexes de  $\mathbb{S}$  privé de l’image de  $G$  sont appelées des *faces*. Lorsque toutes les faces du plongement sont homéomorphes à un disque ouvert, on parle d’un *plongement cellulaire*. Apparaissent alors deux nouvelles relations d’incidence : arête-face et sommet-face, à la frontière des composantes connexes.

Dans le cas particulier de la sphère, un plongement est nécessairement cellulaire si le graphe est connexe. Un graphe connexe qui peut être plongé sur la sphère est alors appelé *graphe planaire*. Cette dénomination s’explique en remarquant que la sphère peut se projeter sur le plan en envoyant un point à l’infini. Par la suite, tous les dessins se feront dans le plan. Notons que le choix du point envoyé à l’infini perturbe la représentation du plongement mais non le plongement lui-même. L’énumération des graphes planaires fait l’objet de recherches actives qui culminent avec l’obtention de formules d’énumération asymptotique par Giménez et Noy [39].

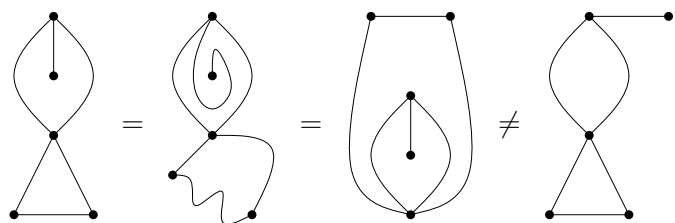


Figure 1.3: Trois représentations d’une même carte topologique, et une carte distincte (face de degré 2) ayant le même graphe sous-jacent.

Un graphe admet une infinité de plongements cellulaires. Pour en faire

l'énumération, on va donc les considérer à homotopie près : deux plongements d'un même graphe sont dits équivalents s'il existe une déformation continue qui permet de passer de l'un à l'autre. Une *carte topologique* est alors une classe d'équivalence des plongements cellulaires de graphes. Pour un graphe donné  $G$ , il existe alors un nombre fini de cartes topologiques ayant  $G$  pour graphe sous-jacent : il s'agit bien d'une classe combinatoire.

### 1.2.2 Cartes combinatoires : étiquetées ou enracinées

Les cartes peuvent aussi se définir de manière purement combinatoires à l'aide d'un encodage des différentes relations d'incidence. Une *carte combinatoire étiquetée* à  $n$  arêtes est un triplet  $G = (\alpha, \sigma, \phi)$  de permutations de  $\llbracket 1, \dots, 2n \rrbracket$  (vu comme l'ensemble des *demi-arêtes* de  $G$ ), qui représentent les arêtes, les sommets et les faces, et respectent les conditions suivantes :

- $\alpha$  est une involution sans point fixe,
- $\phi = \sigma\alpha$ ,
- (Connexité) le groupe engendré par  $\alpha, \sigma$  et  $\phi$  agit transitivement sur  $\llbracket 1, \dots, 2n \rrbracket$ .

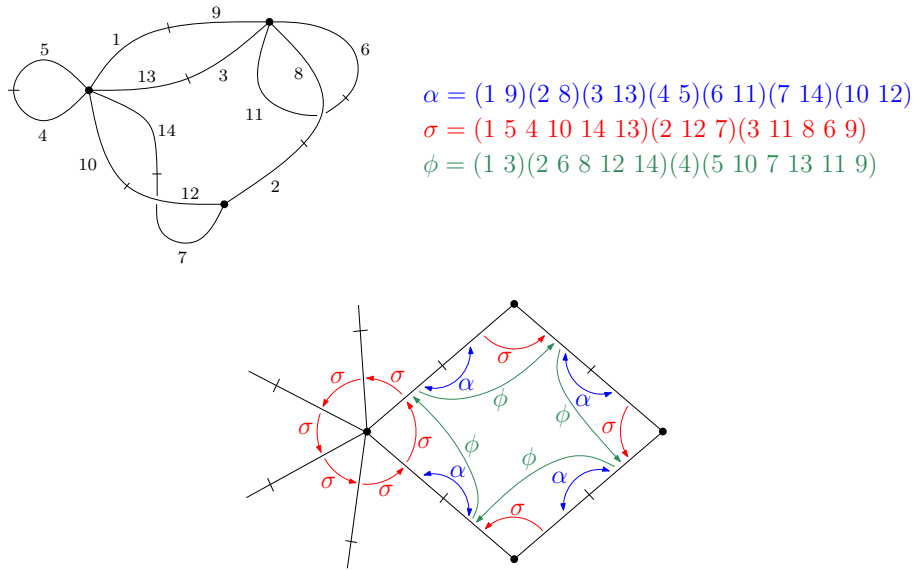


Figure 1.4: Une carte combinatoire avec ses demi-arêtes étiquetées, et la représentation des permutations  $\alpha, \sigma$  et  $\phi$ .

Les cycles de  $\sigma$  et  $\phi$  forment respectivement les sommets et les faces de la carte combinatoire. La longueur des cycles définit le *degré* (ou nombre de demi-arêtes incidentes) des sommets et des faces. On peut ainsi représenter

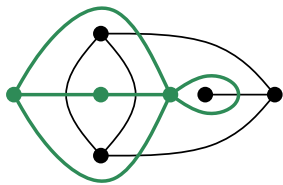


Figure 1.5: Une carte (5 arêtes, 4 sommets, 3 faces) et sa duale (5 arêtes, 3 sommets, 4 faces).

graphiquement une carte combinatoire en plaçant un sommet pour chaque cycle de  $\sigma$ , puis en représentant les demi-arêtes incidentes dans l'ordre antihoraire associé au cycle, enfin  $\alpha$  nous donne les paires de demi-arêtes à connecter (voir Figure 1.4).

Avec une telle définition, on ne voit plus apparaître le genre de la carte. Le genre d'une carte combinatoire est pourtant bien défini car il est donné par la fameuse relation d'Euler qui est l'un des premiers résultats obtenus sur les cartes.

**Theorem 2** (Relation d'Euler). *Soit une carte  $G$  avec  $a$  arêtes,  $s$  sommets et  $f$  faces, le genre  $g$  de  $G$  est défini par la relation suivante :*

$$s + f = a + 2 - 2g$$

Sur la figure 1.4, la carte possède 7 arêtes, 3 sommets et 4 faces. Son genre est donc :  $g = \frac{1}{2}(e + 2 - s - f) = \frac{1}{2}(7 + 2 - 3 - 4) = 1$ . Cela signifie que cette carte peut être dessinée sur le tore sans croisement d'arêtes de façon à ce que les faces soient homéomorphes au disque ouvert.

**Remarque 3** (Dualité). *Soit une carte  $C = (\alpha, \sigma, \phi)$ . Il est intéressant de noter le rôle symétrique joué par  $\sigma$  et  $\phi$ . La carte obtenue en échangeant le rôle des sommets et des faces s'écrit  $C^* = (\alpha, \phi, \sigma)$  : c'est la carte duale de  $C$  (qui prend alors le nom de carte primaire). Une bijection simple permet de passer de l'une à l'autre (voir la figure 1.5). Il suffit de placer un sommet dans chacune des faces de la carte, puis de tracer une nouvelle arête joignant les sommets de part et d'autre de chacune des arêtes de la carte : c'est l'opération de dualité. Toutefois pour retrouver les permutations  $\phi$  et  $\sigma$  sur les sommets et les faces de la carte duale, il faut à présent lire les demi-arêtes dans le sens horaire autour des sommets (antihoraire dans la carte primaire). Au prix de cette convention, on retrouve l'expression de la carte duale.*

On remarque que plusieurs cartes étiquetées peuvent avoir la même structure : degrés, relations d'incidence entre faces et sommets... Il est donc d'usage de considérer plutôt des cartes *enracinées*. Une carte *enracinée* est une carte combinatoire munie d'une demi-arête distinguée appelée *racine*,

modulo réétiquetage des demi-arêtes préservant la racine. L’arête contenant la racine et le sommet incident à la racine sont appelés *arête racine* et *sommet racine*. On représentera généralement une carte enracinée comme une carte topologique où l’arête racine est orientée depuis le sommet racine.

**Remarque 4.** *Dans la littérature, une carte enracinée peut également désigner une carte avec un coin marqué, où un coin désigne la section délimitée par deux arêtes consécutives incidentes au même sommet. Cette définition est équivalente à l’enracinement sur une arête orientée.*

*La présence d’une racine permet de briser les symétries pouvant apparaître dans les cartes et posant problème lorsque l’on veut les dénombrer. Les cartes étiquetées et enracinées sont des objets de même nature. Une fois fixée la racine, vue comme la demi-arête d’étiquette 1, il suffit d’étiqueter les autres demi-arêtes. Pour une carte enracinée à  $n$  arêtes, il y a donc  $(2n - 1)!$  cartes étiquetées correspondantes.*

Dans la suite, nous nous intéresserons essentiellement aux cartes planaires (genre égal à 0). L’énumération des cartes planaires enracinées est connue depuis les travaux de Tutte [62].

### 1.2.3 Familles classiques de cartes

Outre les cartes planaires générales, de nombreuses familles de cartes planaires possèdent de belles propriétés énumératives. On définit souvent une sous-famille de cartes à l’aide d’un ensemble de contraintes, locales ou globales, dont nous allons décrire les plus communes.

**Contraintes de degrés (des faces ou des sommets).** Une carte planaire dont toutes les faces sont de degré  $p$  ( $p \geq 3$ ) est une *p-angulation*. Les cas  $p = 3, 4$  – correspondant aux *triangulations* et aux *quadrangulations* – sont les premières familles de cartes à avoir été étudiées. Notons par ailleurs que les quadrangulations à  $n$  faces sont en bijection avec les cartes planaires générales à  $n$  arêtes. On peut également donner une certaine liberté au degré des faces : une carte *bipartie* est une carte dont les faces ont degré pair. Prescrire le degré des faces est équivalent, par dualité, à prescrire le degré des sommets : les cartes *p-valentes* sont les duals des *p-angulations*, les cartes *eulériennes* (qui tirent leur nom de l’existence d’un parcours eulérien sur ces cartes) sont les duals des cartes biparties. Les cartes biparties cubiques, ou *bicubiques*, duals des *triangulations eulériennes*, cumulent contrainte sur le degré des sommets et des faces.

Les cartes eulériennes ont également la propriété d’admettre un coloriage propre de leurs faces en deux couleurs : *faces sombres* et *faces claires*. Comme le degré autour de chaque sommet est pair, il suffit d’y alterner entre faces claires et sombres. Il y a donc deux colorages possibles pour une carte eulérienne. Dans le cas d’une carte enracinée, on pourra définir

le coloriage canonique comme celui qui présente une face sombre (ou claire selon la convention) à droite de la racine. Les cartes eulériennes coloriées peuvent alors être considérées comme des *hypercartes*, où les faces claires jouent le rôle d'*hyperfaces* et les faces sombres d'*hyperarêtes* (les sommets sont inchangés). Les *hypercartes* peuvent se voir comme une généralisation naturelle des cartes, au sens où elles sont des hypercartes avec des hyperarêtes de degré 2 : les hyperarêtes sont alors contractées en les arêtes de la carte. Notons qu'il ne s'agit là que d'une des représentations des hypercartes, dont on peut trouver plusieurs définitions équivalentes dans [51],[59].

Nous nous intéresserons aussi à une famille particulière d'hypercartes : les constellations. Soit  $p \geq 2$ , une  $p$ -*constellation* est une hypercarte où les hyperarêtes sont de degré  $p$  et les hyperfaces de degré multiple de  $p$ .

**Contraintes de maille.** La maille  $m(m \geq 1)$  d'une carte est le degré du plus petit cycle du graphe sous-jacent. Une carte de maille 1 n'est autre qu'une carte générale. Une carte de maille 2 est une carte *sans boucle*. Une carte de maille 3 – sans boucle, ni arête multiple – est une carte *simple* (voir Chapitres 4 et 5).

**Contraintes de connectivité.** Pour une carte planaire, on parle de  $k$ -*connectivité* lorsqu'il faut retirer au moins  $k$  sommets pour la déconnecter. On peut notamment citer les cartes planaires 3-connexes qui ont l'intéressante propriété d'être en bijection avec les graphes planaires 3-connexes, ce qui les rend particulièrement adaptées pour des algorithmes de dessin de graphes.

Tutte fut le premier à s'intéresser à l'étude énumérative des cartes planaires enracinées, dans une série d'articles fondateurs au début des années soixante [61, 60, 62]. Il introduisit à l'origine les cartes afin d'attaquer des problèmes sur les graphes (comme le théorème des quatre couleurs). En effet, contrairement aux graphes, les cartes peuvent être parcourues dans un ordre défini, du fait de l'ordre cyclique des arêtes autour de chaque sommet.

Ainsi, en partant de l'arête racine et en utilisant une approche récursive, Tutte a trouvé d'élégantes formules d'énumération pour de nombreuses familles de cartes. Ses techniques ont par la suite été largement reprises et développées. On peut citer par exemple les travaux d'Eynard qui applique ces méthodes à des cartes de genre supérieur. On retrouve alors plusieurs caractéristiques communes (voir [14] pour un traitement unifié) : la série génératrice  $y = y(x)$  d'une famille de cartes est typiquement algébrique, souvent lagrangienne (*i.e.* il existe une paramétrisation par  $\{y = Q_1(t), x = Q_2(t)\}$ , où  $Q_1(\cdot)$  et  $Q_2(\cdot)$  sont des expressions rationnelles explicites, donnant des formules simples (avec des facteurs binomiaux) pour leurs coefficients  $c_n$ , dont l'asymptotique est en  $c \gamma^n n^{-5/2}$  pour des constantes  $c > 0$  et  $\gamma > 1$ .

Grâce à ces méthodes de décomposition à la Tutte, on connaît ainsi l'expression des coefficients de la plupart des familles de cartes définies par les contraintes évoquées ci-dessus. En voici quelques unes :

- Cartes planaires enracinées à  $n$  arêtes, ou quadrangulations enracinées à  $n$  faces :

$$C_n = \frac{2 \cdot 3^n}{(n+2)(n+1)} \binom{2n}{n} = \frac{2 \cdot 3^n}{(n+2)} \text{Cat}(n)$$

- Triangulations sans boucle à  $2n$  faces :

$$T_n = \frac{2^{n+1}}{(2n+2)(2n+1)} \binom{3n}{n} = \frac{2^n}{n+1} \text{Cat}_3(n)$$

- Cartes eulériennes, ou biparties, enracinées à  $n$  arêtes :

$$E_n = \frac{3 \cdot 2^{n-1}}{(n+2)(n+1)} \binom{2n}{n} = \frac{3 \cdot 2^{n-1}}{n+2} \text{Cat}(n)$$

- Carte 2-connexes sans boucles à  $n+1$  arêtes :

$$D_n = \frac{2}{(n+1)(2n+1)} \binom{3n}{n} = \frac{2}{n+1} \text{Cat}_3(n)$$

Tutte obtint même des expressions plus précises en fixant les degrés d'un nombre donné de faces de la carte. Il s'agit de la formule connue sous le nom de formule des slicings [61], exprimant le nombre  $A[\ell_1, \dots, \ell_r]$  de cartes avec  $r$  faces ordonnées  $f_1, \dots, f_r$  de degrés respectifs  $\ell_1, \dots, \ell_r$ , chaque face portant un coin marqué, où soit toutes les faces sont de degré pair (cas biparti), soit exactement deux degrés  $\ell_i$  et  $\ell_j$  sont impairs (cas quasi-biparti) :

$$A[\ell_1, \dots, \ell_r] = \frac{(e-1)!}{v!} \prod_{i=1}^r \alpha(\ell_i), \text{ avec } \alpha(\ell) := \frac{\ell!}{\lfloor \ell/2 \rfloor! \lfloor (\ell-1)/2 \rfloor!},$$

où  $\begin{cases} e &= \sum_{i=1}^r \ell_i / 2 \\ v &= e - r + 2 \end{cases}$  représentent les nombres d'arêtes et de sommets.

#### 1.2.4 Bijections classiques sur les cartes

En étudiant de plus près les expressions des coefficients cités précédemment, on remarque qu'on voit toujours apparaître, quels que soient les types de contraintes imposés, un nombre de Catalan généralisé. Cela suggère l'existence d'un lien entre cartes planaires et arbres plans.

Ce sont Cori et Vauquelin qui en feront la première preuve bijective [29], établissant une relation entre cartes planaires pointées (*i.e.* avec un sommet marqué) et arbres *bien étiquetés*. Un arbre bien étiqueté est un arbre plan dont les sommets portent des étiquettes entières strictement positives, telles que les étiquettes de deux sommets adjacents diffèrent d'au plus un. Toutefois cette bijection repose sur une décomposition récursive, et c'est Schaeffer [56] qui en donne une reformulation directe – connue comme la bijection Cori-Vauquelin-Schaeffer – avec des *arbres bourgeonnants*.

La bijection Cori-Vauquelin-Schaeffer, reposant sur un processus de clôture d'arbre décoré, ouvrit la voie à des bijections similaires pour de nombreuses autres familles de cartes. L'une des plus importantes est la bijection de Bouttier-Di Francesco-Guitter [19] (souvent abrégée *BDG*) qui l'étend aux cartes biparties – en fait, elle fut initialement formulée pour les hypercartes. La bijection *BDG* admet de multiples spécialisations permettant de retrouver plusieurs résultats dont on ne connaissait pas encore de preuve bijective. On pourra trouver deux exemples de spécialisations de cette bijection à des familles d'hypercartes dans les Chapitres 2 (pour les cartes biparties et quasi-biparties, vues comme des 2-constellations et quasi-2-constellations) et 3 (pour les  $p$ -constellations et quasi- $p$ -constellations). On peut également citer la bijection d'Ambjørn et Budd [6], assez proche de la bijection de Cori-Vauquelin-Schaeffer, mais qui se comporte mieux vis-à-vis de la distance, et peut ainsi être utilisée pour l'étude des quadrangulations en tant qu'espace métrique.

## 1.3 Distances et convergence

### 1.3.1 Profil des distances dans les cartes

Une carte planaire peut être considérée comme un espace métrique en définissant la *distance* entre deux sommets comme la longueur minimale (en nombre d'arêtes) des chemins qui les relient. Plus précisément, pour une carte planaire enracinée  $G = (V, E)$  avec  $n$  arêtes, la distance  $d(v)$  d'un sommet  $v \in V$  (par rapport au sommet racine) est la longueur du plus court chemin de  $G$  partant de  $v$  et se terminant au sommet racine. Le rayon d'une carte  $G$  est alors la distance maximale dans  $G$  :  $r(G) = \max_{v \in V} \{d(v)\}$ . On définit également le *profil des distances* de  $G$  comme l'ensemble  $\{d(v)\}_{v \in V}$  des distances des sommets de  $G$ . Notons que d'autres distances peuvent être considérées : c'est le cas notamment dans le Chapitre 5 où l'on définira distance et profil pour les arêtes (et non les sommets) dans les cartes simples, ou encore une distance *contrainte* n'empruntant pas le plus court chemin pour les triangulations eulériennes.

L'étude des propriétés métriques des cartes planaires aléatoires est un domaine de recherche très actif depuis une dizaine d'années. Les premiers résultats majeurs furent obtenus dans l'article fondateur de Chassaing et

Schaeffer [26], où ils s'intéressaient à la classe des *quadrangulations* enracinées. Ils y démontraient que, dans une quadrangulation enracinée uniformément aléatoire  $Q_n$  avec  $n$  sommets, la distance typique est d'ordre  $n^{1/4}$  (à titre de comparaison, la distance typique dans les arbres plans aléatoires est d'ordre  $n^{1/2}$ ). De plus, ils établirent que le profil renormalisé des distances converge en loi vers une distribution de probabilité explicite liée à l'ISE –pour *Integrated SuperBrownian Excursion*, la mesure d'occupation du serpent Brownien, introduite par Aldous dans [5] comme limite naturelle du profil normalisé de certaines familles d'arbres étiquetés. Ces résultats furent ensuite généralisés à plusieurs autres classes de cartes aléatoires : cartes biparties [46], cartes enracinées avec des poids de Boltzmann sur les faces [50].

Si le profil donne le comportement des distances par rapport à un sommet fixé, il est intéressant de connaître le comportement des distances entre des sommets aléatoires. Ainsi plusieurs articles ont étudié la *fonction à deux points* [7] [18]) ou encore la *fonction à trois points* [20], qui sont les séries génératrices des cartes ayant deux ou trois sommets marqués à une distance donnée les uns des autres. Ils montrent en particulier la convergence de ces fonctions vers des fonctions d'échelle issues de modèles de gravité quantique.

### 1.3.2 Résultats de convergence

Dans la continuité des travaux cités précédemment, l'étude de la convergence des cartes elles-mêmes en tant qu'espaces métriques progresse grâce des efforts continus. Une série d'articles (dont [47], [42], [20], [48], [43]) attaquèrent le cas des quadrangulations planes à  $n$  faces  $Q_n$ , qui fut résolu indépendamment par [44] et [49], établissant que la limite, au sens de Gromov-Hausdorff, des quadrangulations planes aléatoires est un espace métrique aléatoire  $\mathfrak{B}$  appelé *carte brownienne*.

Plus précisément, on définit la distance de Hausdorff  $d_H$  entre deux sous-ensembles  $X, Y$  d'un espace métrique  $(M, d)$  par :

$$d_H(X, Y) = \max \left( \sup_{x \in X} \inf_{y \in Y} d(x, y), \sup_{y \in Y} \inf_{x \in X} d(x, y) \right)$$

Intuitivement, cela signifie que deux ensembles sont proches si tout point de l'un est proche d'au moins un point de l'autre.

La distance de Gromov-Hausdorff  $d_{GH}$  a été introduite pour pouvoir comparer deux ensembles qui ne sont pas plongés dans le même espace métrique. Soit deux espaces métriques compacts  $X, Y$  :

$$d_{GH}(X, Y) = \inf_{\substack{(M, d) \\ \text{espace métrique}}} \inf_{\substack{\phi : X \rightarrow M \\ \psi : Y \rightarrow M \\ \text{isométries}}} d_H(\phi(X), \psi(Y)).$$

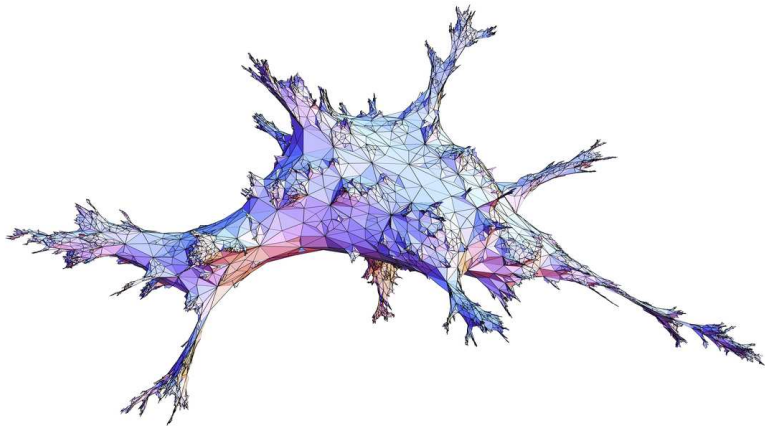


Figure 1.6: Une simulation de grande triangulation aléatoire par Nicolas Curien.

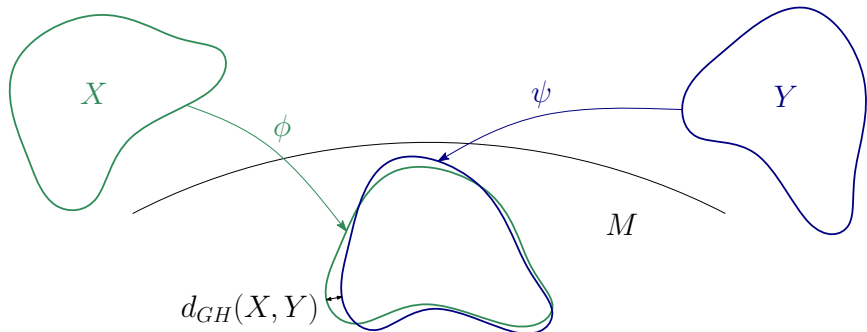


Figure 1.7: Visualisation de la distance de Gromov-Hausdorff entre deux espaces métriques  $X$  et  $Y$ .

Ainsi, si  $Q_n$  est une quadrangulation plane aléatoire à  $n$  arêtes, on obtient la convergence suivante en distribution, pour la topologie de Gromov-Hausdorff :

$$\left(\frac{8n}{9}\right)^{1/4} Q_n \xrightarrow[n \rightarrow \infty]{(d)} \mathfrak{B}$$

Cet espace aléatoire aléatoire  $\mathfrak{B}$  – qui possède presque sûrement la topologie de la sphère – a cela de remarquable qu'il est également la limite de nombreuses autres familles de cartes planaires (seule la constante de renormalisation diffère). En effet, Le Gall [44] donna également une “recette” à suivre pour prouver la convergence vers la carte brownienne, qui apparaît alors comme *limite universelle* de toute famille de cartes “raisonnables”.

Cette méthode repose essentiellement sur deux ingrédients :

- l'existence d'une bijection entre la famille de cartes et une famille d'arbres “bien” étiquetés qui convergent vers le *serpent brownien* – autre structure aléatoire – où les étiquettes encodent la distance dans la carte,
- une propriété d'invariance par réenracinement du modèle considéré.

Cette méthode fut mise en œuvre avec succès pour les triangulations et les  $2p$ -angulations par Le Gall [44], pour les cartes biparties par Abraham [1], pour les triangulations simples et les quadrangulations simples par d'Addario-Berry et Albenque [2] et pour les cartes planaires générales par Bettinelli, Jacob et Miermont [12].

## 1.4 Organisation de la thèse

### Chapitre 2 : Cartes (quasi-)biparties avec bords

Nous étudierons la famille des cartes biparties (puis quasi-biparties dans un second temps) avec des bords de longueur fixée, utilisées en physique statistique pour modéliser des surfaces avec des contraintes aux frontières. Nous chercherons à donner une interprétation bijective de formules obtenues par Eynard [33] sur ces objets.

En combinant la bijection de Bouttier-Di Francesco-Guitter sur les cartes biparties et appliquant une idée due à Pitman (établissant une correspondance entre les mobiles obtenus et des forêts de mobiles), nous donnerons une généralisation des formules d'Eynard à un nombre arbitraire de bords de longueur paire.

Dans un second temps, nous étendrons ces formules aux cartes quasi-biparties en observant l'apparition d'un chemin entre les deux bords impairs dans les mobiles associés, et en jouant sur l'existence d'une bijection entre les mobiles BDG et les arbres bourgeonnants à la Schaeffer.

Soit  $G_{\ell_1, \dots, \ell_r} := G_{\ell_1, \dots, \ell_r}(t; x_1, x_2, \dots)$  la série génératrice des cartes biparties et quasi-biparties à  $r$  bords de longueurs respectives  $\ell_1, \dots, \ell_r$  (dans le cas quasi-biparti, deux de ces longueurs sont impaires), où  $t$  marque le nombre de sommets et les  $x_i$  marquent le nombre de faces de degré  $2i$  qui ne sont pas des bords, nous obtenons la formule unifiée suivante :

$$G_{\ell_1, \dots, \ell_r} = \left( \prod_{i=1}^r \alpha(\ell_i) \right) \cdot \frac{1}{s} \cdot \frac{d^{r-2}}{dt^{r-2}} R^s,$$

$$\text{avec } \alpha(\ell) = \frac{\ell!}{[\frac{\ell}{2}]! [\frac{\ell-1}{2}]!}, \quad s = \frac{\ell_1 + \dots + \ell_r}{2},$$

où  $R := R(t; x_1, x_2, \dots)$  est la série génératrice des mobiles BDG.

Cette formule met en évidence la structure de ces cartes avec bords : un produit de binomiaux pour chaque bord, et un série génératrice qui ne dépend que de la somme des longueurs des bords. Cela permet également de retrouver la formule des slicings de Tutte, par extraction de coefficients.

### Chapitre 3 : Constellations et quasi-constellations avec bords

En considérant les  $p$ -constellations comme généralisation naturelle des cartes biparties (vues comme 2-constellations), nous utiliserons les mêmes techniques bijectives que dans le Chapitre 2 pour obtenir une décomposition de ces objets. Nous introduirons pour cela la famille des  $p$ -mobiles, images des  $p$ -constellations par la bijection BDG.

Afin de résoudre le cas des quasi- $p$ -constellations, nous étudierons l'apparition d'un chemin pondéré alternant dans les quasi- $p$ -mobiles associés. Nous établirons alors un lemme de transfert de degrés (dont on peut trouver une version plus forte dans [22]) entre les sommets correspondant aux deux bords impairs, basé sur l'existence d'une bijection entre les  $p$ -mobiles et les  $p$ -arbres bourgeonnants généralisant la définition classique.

Soit  $G_{\ell_1, \dots, \ell_r}^{(p)} := G_{\ell_1, \dots, \ell_r}^{(p)}(t; x_1, x_2, \dots)$  la série génératrices des  $p$ -constellations et quasi- $p$ -constellations avec  $r$  bords  $f_1, \dots, f_r$  de longueurs  $\ell_1, \dots, \ell_r$  (dans le cas des quasi- $p$ -constellations, deux de ces longueurs ne sont pas des multiples de  $p$ ), où  $t$  marque le nombre de sommets et les  $x_i$  marquent le nombre de faces de degré  $pi$  qui ne sont pas des bords, nous obtenons la formule unifiée suivante :

$$G_{\ell_1, \dots, \ell_r}^{(p)} = \left( \prod_{i=1}^r \alpha(\ell_i) \right) \cdot \frac{c}{s} \cdot \frac{d^{r-2}}{dt^{r-2}} R_p^s,$$

$$\text{où } \alpha(\ell) = \frac{\ell!}{[\ell/p]! (\ell - [\ell/p] - 1)!}, \quad s = \frac{p-1}{p} (\ell_1 + \dots + \ell_r),$$

$R_p$  est la série des  $p$ -mobiles,

$$\text{et } c = \begin{cases} 1, & \text{quand chaque } \ell_i \text{ est multiple de } p, \\ p-1, & \text{quand exactement deux } \ell_i \text{ ne sont pas multiples de } p. \end{cases}$$

On retrouve la formule du Chapitre 2 pour  $p = 2$ , avec la même structure, si ce n'est l'apparition d'un facteur correcteur dans le cas des quasi-constellations, dû au lemme de transfert. On peut y lire également la généralisation, proposée par Bousquet-Mélou et Schaeffer [15], de la formule des slicings de Tutte.

### Chapitre 4 : Bijection pour les cartes simples

Nous proposerons dans ce chapitre une interprétation bijective d'une formule trouvée par Noy (grâce à des méthodes de calcul formel), mettant en évidence un lien entre la famille des cartes simples à face externe triangulaire, et la famille des triangulations eulériennes.

La bijection que nous obtenons repose sur trois étapes : il faut d'abord munir la carte simple d'une *orientation canonique avec bourgeons* de ses arêtes, puis transformer les arêtes ainsi orientées en triangles sombres dirigés qui formeront les faces sombres de la triangulation eulérienne après une dernière étape de perturbation locale de ces triangles.

Exploitant finalement une bijection entre triangulations eulériennes et arbres binaires orientées (cas particulier d'un résultat de [15]), nous donnerons une version bivariée de la formule de Noy, qui s'appuie sur la possibilité de lire les sommets et les faces de la carte simple dans l'arbre orienté associé. Cela nous permettra de plus de construire un générateur de Boltzmann en taille approché pour les cartes simples en contrôlant le nombre d'arêtes et de sommets.

## Chapitre 5 : Profil des distances dans les cartes simples

Dans ce chapitre, nous nous intéressons aux propriétés asymptotiques des cartes simples en tant qu'espaces métriques, et plus particulièrement à l'étude de la mesure du profil des distances des arêtes de la carte par rapport à l'arête racine. Nous montrons que la mesure du profil renormalisé par un facteur  $(2n)^{-1/4}$  (correspondant à la distance typique dans une carte simple) converge en loi vers une mesure aléatoire liée à l'ISE.

La preuve se décompose en trois grandes parties. On démontre en premier lieu la convergence du profil des triangulations eulériennes en utilisant les techniques décrites dans [41]. Puis on remarque que dans les triangulations eulériennes, les chemins le plus à droite sont presque sûrement "proches" des plus courts chemins (ou géodésiques), adaptant ici les arguments avancés dans [2] pour les triangulations simples. Finalement on conclut en remarquant que les chemins les plus à droite sont préservés par la bijection présentée dans le Chapitre 4.

Ce résultat pour les cartes simples nous donne également la convergence du profil des cartes sans boucles (avec un facteur de renormalisation  $(\frac{4n}{3})^{-1/4}$ ) et des cartes générales (avec un facteur de renormalisation  $(\frac{8n}{9})^{-1/4}$ ). Cela jette enfin les bases pour tenter d'établir la convergence des cartes simples vers la *carte brownienne*, dont nous dressons une ébauche de preuve.

## Publications associées

Les résultats présentés dans cette thèse sont basés sur les articles suivants :

- Chapitre 2 : "A simple formula for the series of bipartite and quasi-bipartite maps with boundaries", avec Éric Fusy, *DMTCS Proceedings, 24th International Conference on Formal Power Series and Algebraic Combinatorics* (FPSAC 2012, Nagoya, Japon).
- Chapitre 2 et 3 : "A simple formula for the series of constellations

and quasi-constellations with boundaries”, avec Éric Fusy, *Electronic Journal of Combinatorics*, Volume 21, Issue 2:P2.9 (2014).

- Chapitre 4 : “A bijection for plane graphs and its applications”, avec Olivier Bernardi et Éric Fusy, *Proceedings of the Eleventh Workshop on Analytic Algorithmics and Combinatorics* (ANALCO 2014, Portland, USA).
- Chapitre 5 : “On the distance-profile of random rooted plane graphs”, avec Olivier Bernardi et Éric Fusy, *25th International Conference on Probabilistic, Combinatorial and Asymptotic Methods for the Analysis of Algorithms* (AofA 2014, Paris, France).

## Chapter 2

# Bijection for bipartite and quasi-bipartite maps

### 2.1 Introduction

In this chapter we focus on bipartite maps (all faces have even degree) and on quasi-bipartite maps (all faces have even degree except for two, which have odd degree). One of the first counting results, obtained by Tutte, is a strikingly simple formula (called formula of slicings) for the number  $A[\ell_1, \dots, \ell_r]$  of maps with  $r$  numbered faces  $f_1, \dots, f_r$  of respective degrees  $\ell_1, \dots, \ell_r$ , each face having a marked corner (for simple parity reasons the number of odd  $\ell_i$  must be even).

Solving a technically involved recurrence satisfied by these coefficients, he proved in [61] that when none or only two of the  $\ell_i$  are odd (bipartite and quasi-bipartite case, respectively), then:

$$A[\ell_1, \dots, \ell_r] = \frac{(e-1)!}{v!} \prod_{i=1}^r \alpha(\ell_i), \quad \text{with } \alpha(\ell) := \frac{\ell!}{[\ell/2]! \lfloor (\ell-1)/2 \rfloor!}, \quad (2.1)$$

where  $e = \sum_{i=1}^r \ell_i/2$  and  $v = e - r + 2$  are the numbers of edges and vertices in such maps. The formula was recovered by Cori [27, 28] (using a certain encoding procedure for planar maps); and the formula in the bipartite case was rediscovered bijectively by Schaeffer [55], based on a correspondence with so-called *blossoming trees*. Alternatively one can use a more recent bijection by Bouttier, Di Francesco and Guitter [19] (based on a correspondence with so-called *mobiles*) which itself extends earlier constructions by Cori and Vauquelin [29] and by Schaeffer [56, Sec. 6.1] for quadrangulations. The bijection with mobiles yields the following: if we denote by  $R \equiv R(t) \equiv R(t; x_1, x_2, \dots)$  the generating function specified by

$$R = t + \sum_{i \geq 1} x_i \binom{2i-1}{i} R^i. \quad (2.2)$$

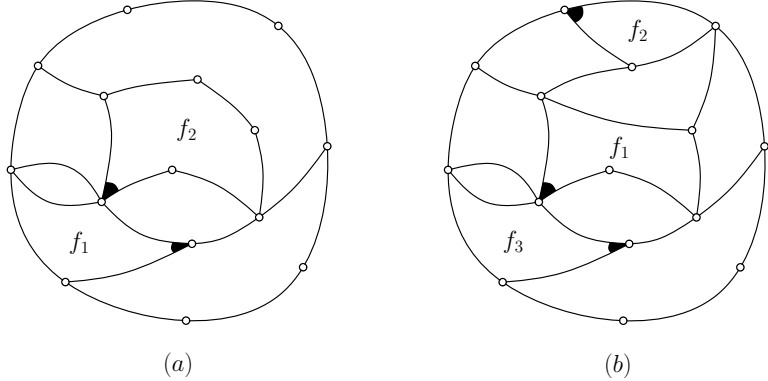


Figure 2.1: (a) A bipartite map with 2 boundaries  $f_1, f_2$  of respective degree 4, 6. (b) A quasi-bipartite map with 3 boundaries  $f_1, f_2, f_3$  of respective degree 5, 3, 4.

and denote by  $M(t) \equiv M(t; x_1, x_2, \dots)$  the generating function of rooted bipartite maps, where  $t$  marks the number of vertices and  $x_i$  marks the number of faces of degree  $2i$  for  $i \geq 1$ , then  $M'(t) = 2R(t)$ . And one easily recovers (2.1) in the bipartite case by an application of the Lagrange inversion formula to extract the coefficients of  $R(t)$ .

As we can see, maps might satisfy beautiful counting formulas, regarding *counting coefficients*<sup>1</sup>. Regarding *generating functions*, formulas can be very nice and compact as well. In his book [33], Eynard gives an iterative procedure (based on residue calculations) to compute the generating function of maps of arbitrary genus and with several marked faces, which we will call boundary-faces (or shortly boundaries). In certain cases, this yields an explicit expression for the generating function. For example, he obtains formulas for the (multivariate) generating functions of bipartite and quasi-bipartite maps with two or three boundaries of arbitrary lengths  $\ell_1, \ell_2, \ell_3$  (in the quasi-bipartite case two of these lengths are odd), where  $t$  marks the number of vertices and  $x_i$  marks the number of non-boundary faces of degree  $2i$ :

$$G_{\ell_1, \ell_2} = \gamma^{\ell_1 + \ell_2} \sum_{j=0}^{\lfloor \ell_2/2 \rfloor} (\ell_2 - 2j) \frac{\ell_1! \ell_2!}{j! (\frac{\ell_1 - \ell_2}{2} + j)! (\frac{\ell_1 + \ell_2}{2} - j)! (\ell_2 - j)!} \quad (2.3)$$

$$G_{\ell_1, \ell_2, \ell_3} = \frac{\gamma^{\ell_1 + \ell_2 + \ell_3 - 1}}{y'(1)} \left( \prod_{i=1}^3 \frac{\ell_i!}{\lfloor \ell_i/2 \rfloor! \lfloor (\ell_i - 1)/2 \rfloor!} \right). \quad (2.4)$$

In these formulas the series  $\gamma$  and  $y'(1)$  are closely related to  $R(t)$ , precisely

---

<sup>1</sup>We also mention the work of Krikun [40] where a beautiful formula is proved for the number of triangulations with multiple boundaries of prescribed lengths, a bijective proof of which is still to be found.

$\gamma^2 = R(t)$  and one can check that  $y'(1) = \gamma/R'(t)$ .

We obtain new formulas which generalize Eynard's ones to any number of boundaries, both in the bipartite and the quasi-bipartite case. For  $r \geq 1$  and  $\ell_1, \dots, \ell_r$  positive integers, an *even map* of type  $(\ell_1, \dots, \ell_r)$  is a map with  $r$  (numbered) marked faces —called *boundary-faces*—  $f_1, \dots, f_r$  of degrees  $\ell_1, \dots, \ell_r$ , each boundary-face having a marked corner, and with all the other faces of even degree. (Note that there is an even number of odd  $\ell_i$  by a simple parity argument.) Let  $G_{\ell_1, \dots, \ell_r} := G_{\ell_1, \dots, \ell_r}(t; x_1, x_2, \dots)$  be the corresponding generating function where  $t$  marks the number of vertices and  $x_i$  marks the number of non-boundary faces of degree  $2i$ . Our main result is:

**Theorem 1.** *When none or only two of the  $\ell_i$  are odd, then the following formula holds:*

$$G_{\ell_1, \dots, \ell_r} = \left( \prod_{i=1}^r \alpha(\ell_i) \right) \cdot \frac{1}{s} \cdot \frac{d^{r-2}}{dt^{r-2}} R^s, \quad (2.5)$$

$$\text{with } \alpha(\ell) = \frac{\ell!}{\lfloor \frac{\ell}{2} \rfloor! \lfloor \frac{\ell-1}{2} \rfloor!}, \quad s = \frac{\ell_1 + \dots + \ell_r}{2}, \quad \text{where } R \text{ is given by (2.2).}$$

Our formula covers all parity cases for the  $\ell_i$  when  $r \leq 3$ . For  $r = 1$ , the formula reads  $G_{2a}' = \binom{2a}{a} R^a$ , which is a direct consequence of the bijection with mobiles. For  $r = 2$  the formula reads  $G_{\ell_1, \ell_2} = \alpha(\ell_1)\alpha(\ell_2)R^s/s$  (which simplifies the constant in (2.3)). And for  $r = 3$  the formula reads  $G_{\ell_1, \ell_2, \ell_3} = \alpha(\ell_1)\alpha(\ell_2)\alpha(\ell_3)R'R^{s-1}$ . Note that (2.5) also “contains” the formula of slicings (2.1), by noticing that  $A[\ell_1, \dots, \ell_r]$  equals the evaluation of  $G_{\ell_1, \dots, \ell_r}$  at  $\{t = 1; x_1 = 0, x_2 = 0, \dots\}$ , which equals  $(\prod_{i=1}^r \alpha(\ell_i)) \cdot \frac{(s-1)!}{(s-r+2)!}$ . Hence, (2.5) can be seen as an “interpolation” between the two formulas of Eynard given above and Tutte's formula of slicings. In addition, (2.5) has the nice feature that the expression of  $G_{\ell_1, \dots, \ell_r}$  splits into two factors: (i) a *constant factor* which itself is a product of independent contributions from every boundary, (ii) a *series-factor* that just depends on the number of boundaries and the total length of the boundaries.

Even though the coefficients of  $G_{\ell_1, \dots, \ell_r}$  have simple binomial-like expressions (easy to obtain from (2.1)), it does not explain why at the level of generating functions the expression (2.5) is so simple (and it would not be obvious to guess (2.5) by just looking at (2.1)). Relying on the bijection with mobiles (recalled in Section 2.2), we give a transparent proof of (2.5). In the bipartite case, our construction (described in Section 2.3) starts from a forest of mobiles with some marked vertices, and then we aggregate the connected components so as to obtain a single mobile with some marked black vertices of fixed degrees (these black vertices correspond to the boundary-faces). The idea of aggregating connected components as we do is reminiscent of a construction due to Pitman [54], giving for instance a very simple proof (see [3, Chap. 26]) that the number of Cayley trees with  $n$  nodes

is  $n^{n-2}$ . Then we show in Section 2.4 that the formula in the quasi-bipartite case can be obtained by a reduction to the bipartite case<sup>2</sup>. This reduction is done bijectively with the help of auxiliary trees called *blossoming trees*. Let us mention that these blossoming trees have been introduced in another bijection with bipartite maps [55]. We could alternatively use this bijection to prove Theorem 1 in the bipartite case (none of the  $\ell_i$  is odd). But in order to encode quasi-bipartite maps, one would have to use extensions of this bijection [16, 17] in which the encoding would become rather involved. This is the reason why we rely on bijections with mobiles, as given in [19].

**Notation.** We will often use the following notation: for  $\mathcal{A}$  and  $\mathcal{B}$  two (typically infinite) combinatorial classes and  $a$  and  $b$  two integers, write  $a \cdot \mathcal{A} \simeq b \cdot \mathcal{B}$  if there is a “natural”  $a$ -to- $b$  correspondence between  $\mathcal{A}$  and  $\mathcal{B}$  (the correspondence will be explicit each time the notation is used) that preserves several parameters (which will be listed when the notation is used, typically the correspondence will preserve the face-degree distribution).

## 2.2 Bijection between vertex-pointed maps and mobiles

We recall here a well-known bijection due to Bouttier, Di Francesco and Guitter [19] between vertex-pointed planar maps and a certain family of decorated trees called mobiles. We actually follow a slight reformulation of the bijection given in [10]. A *mobile* is a plane tree (i.e., a planar map with one face) with vertices either black or white, with dangling half-edges — called buds — at black vertices, such that there is no white-white edge, and such that each black vertex has as many buds as white neighbours. The *degree* of a black vertex  $v$  is the total number of incident half-edges (including the buds) incident to  $v$ . Starting from a planar map  $G$  with a pointed vertex  $v_0$ , and where the vertices of  $G$  are considered as *white*, one obtains a mobile  $M$  as follows (see Figure 2.2):

- Endow  $G$  with its geodesic orientation from  $v_0$  (i.e., an edge  $\{v, v'\}$  is oriented from  $v$  to  $v'$  if  $v'$  is one unit further than  $v$  from  $v_0$ , and is left unoriented if  $v$  and  $v'$  are at the same distance from  $v_0$ ).
- Put a new black vertex in each face of  $G$ .
- Apply the following local rules to each edge (one rule for oriented edges and one rule for unoriented edges) of  $G$ :

---

<sup>2</sup>It would be interesting as a next step to search for a simple formula for  $G_{\ell_1, \dots, \ell_r}$  when four or more of the  $\ell_i$  are odd (however, as noted by Tutte [61], the coefficients do not seem to be that simple, they have large prime factors).

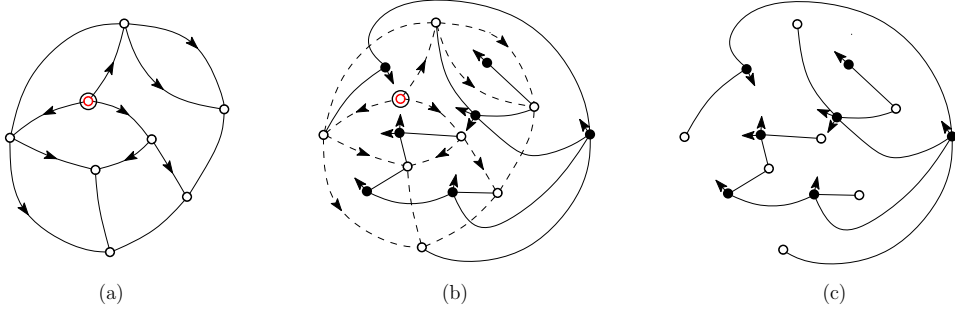
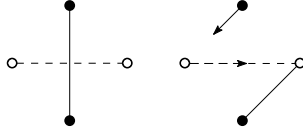


Figure 2.2: (a) A vertex-pointed map endowed with the geodesic orientation (with respect to the marked vertex). (b) The local rule is applied to each edge of the map. (c) The resulting mobile.



- Delete the edges of  $G$  and the vertex  $v_0$ .

**Theorem 2** (Bouttier, Di Francesco and Guitter [19]). *The above construction is a bijection between vertex-pointed maps and mobiles. Each non-root vertex in the map corresponds to a white vertex in the mobile. Each face of degree  $i$  in the map corresponds to a black vertex of degree  $i$  in the mobile.*

A mobile is called *bipartite* when all black vertices have even degree, and is called *quasi-bipartite* when all black vertices have even degree except for two which have odd degree. Note that bipartite (resp. quasi-bipartite) mobiles correspond to bipartite (resp. quasi-bipartite) vertex-pointed maps.

**Claim 5.** *A mobile is bipartite iff it has no black-black edge. A mobile is quasi-bipartite iff the set of black-black edges forms a non-empty path whose extremities are the two black vertices of odd degrees.*

*Proof.* Let  $T$  be a mobile and  $F$  the forest formed by the black vertices and black-black edges of  $T$ . Note that for each black vertex of  $T$ , the degree and the number of incident black-black edges have same parity. Hence if  $T$  is bipartite,  $F$  has only vertices of even degree, so  $F$  is empty; while if  $T$  is quasi-bipartite,  $F$  has two vertices of odd degree, so the only possibility is that the edges of  $F$  form a non-empty path.  $\square$

A bipartite mobile is called *rooted* if it has a marked corner at a white vertex. Let  $R := R(t; x_1, x_2, \dots)$  be the generating function of rooted bipartite mobiles, where  $t$  marks the number of white vertices and  $x_i$  marks

the number of black vertices of degree  $2i$  for  $i \geq 1$ . As shown in [19], a decomposition at the root ensures that  $R$  is given by Equation (2.2); indeed if we denote by  $S$  the generating function of bipartite mobiles rooted at a white leaf, then  $R = t + RS$  and  $S = \sum_{i \geq 1} x_i \binom{2i-1}{i} R^{i-1}$ .

For a mobile  $\gamma$  with marked black vertices  $b_1, \dots, b_r$  of degrees  $2a_1, \dots, 2a_r$ , the associated *pruned mobile*  $\hat{\gamma}$  obtained from  $\gamma$  by deleting the buds at the marked vertices (thus the marked vertices get degrees  $a_1, \dots, a_r$ ). Conversely, such a pruned mobile yields  $\prod_{i=1}^r \binom{2a_i-1}{a_i}$  mobiles (because of the number of ways to place the buds around the marked black vertices). Hence, if we denote by  $\mathcal{B}_{2a_1, \dots, 2a_r}$  the family of bipartite mobiles with  $r$  marked black vertices of respective degree  $2a_1, \dots, 2a_r$ , and denote by  $\hat{\mathcal{B}}_{2a_1, \dots, 2a_r}$  the family of pruned bipartite mobiles with  $r$  marked black vertices of respective degree  $a_1, \dots, a_r$ , we have:

$$\mathcal{B}_{2a_1, \dots, 2a_r} \simeq \prod_{i=1}^r \binom{2a_i-1}{a_i} \hat{\mathcal{B}}_{2a_1, \dots, 2a_r}.$$

### 2.3 Bipartite case

In this section, we consider the two following families:

- $\widehat{\mathcal{M}}_{2a_1, \dots, 2a_r}$  is the family of pruned bipartite mobiles with  $r$  marked black vertices of respective degrees  $a_1, \dots, a_r$ , the mobile being rooted at a corner of one of the marked vertices,
- $\mathcal{F}_s$  is the family of forests made of  $s := \sum_{i=1}^r a_i$  rooted bipartite mobiles, and where additionally  $r - 1$  white vertices  $w_1, \dots, w_{r-1}$  are marked.

**Proposition 6.** *There is an  $(r-1)!$ -to- $(r-1)!$  correspondence between the family  $\widehat{\mathcal{M}}_{2a_1, \dots, 2a_r}$  and the family  $\mathcal{F}_s$ . If  $\gamma \in \widehat{\mathcal{M}}_{2a_1, \dots, 2a_r}$  corresponds to  $\gamma' \in \mathcal{F}_s$ , then each white vertex in  $\gamma$  corresponds to a white vertex in  $\gamma'$ , and each unmarked black vertex of degree  $2i$  in  $\gamma$  corresponds to a black vertex of degree  $2i$  in  $\gamma'$ .*

*Proof.* We will describe the correspondence in both ways (see Figure 2.3). First, one can go from the forest to the pruned mobile through the following operations:

1. Group the first  $a_1$  mobiles and bind them to a new black vertex  $b_1$ , then bind the next  $a_2$  mobiles to a new black vertex  $b_2$ , and so on, to get a forest with  $r$  connected components rooted at  $b_1, \dots, b_r$ , see Figure 2.3(a).

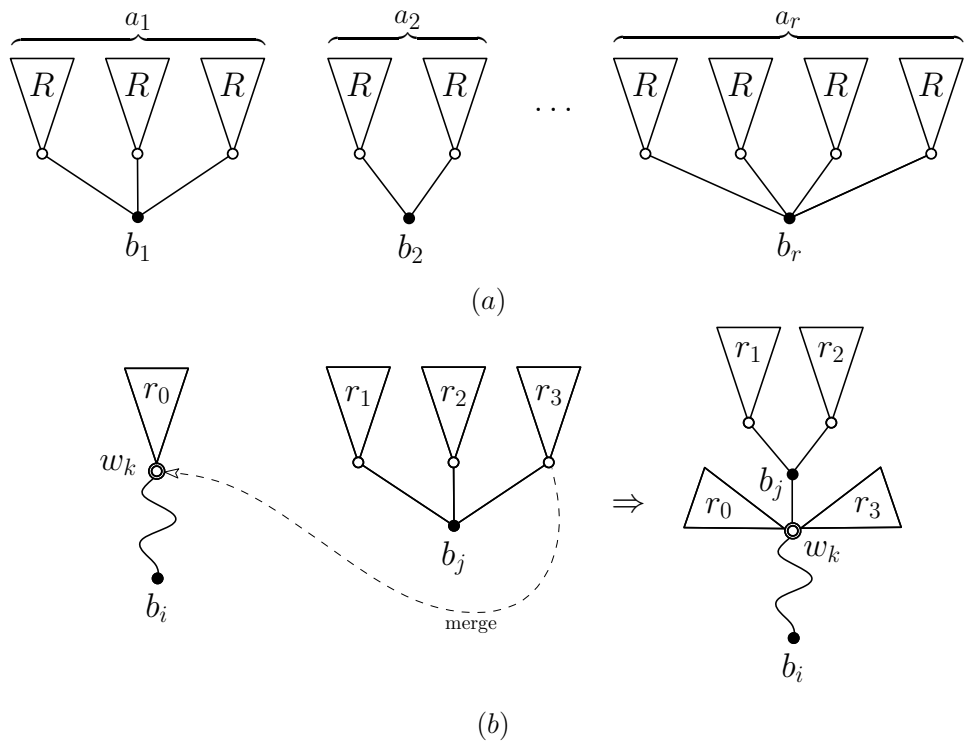


Figure 2.3: (a) From a forest with  $s = \sum_{i=1}^r a_i$  mobiles to  $r$  components rooted at black vertices  $b_1, \dots, b_r$ . (b) Merging the component rooted at  $b_j$  with the distinct component rooted at  $b_i$  containing the marked white vertex  $w_k$ .

2. The  $r - 1$  marked white vertices  $w_1, \dots, w_{r-1}$  are ordered, pick one of the  $r - 1$  components which do not contain  $w_{r-1}$ . Bind this component to  $w_{r-1}$  by merging  $w_{r-1}$  with the rightmost white neighbour of  $b_i$ , see Figure 2.3(b). Repeat the operation for each  $w_{r-i}$  to reduce the number of components to one ( $r - i$  possibilities in the choice of the connected component at the  $i$ th step), thus getting a decorated bipartite tree rooted at a corner incident to some  $b_j$ , and having  $r$  black vertices  $b_1, \dots, b_r$  without buds.

Conversely, one can go from the pruned mobile to the forest through the following operations:

1. Pick one marked black vertex  $b_k$ , but the root, and separate it as in Figure 2.3(b) read from right to left. This creates a new connected component, rooted at  $b_k$ .
2. Repeat this operation, choosing at each step ( $r - i$  possibilites at the  $i$ th step) a marked black vertex that is not the root in its connected component, until one gets  $r$  connected components, each being rooted at one of the marked black vertices  $\{b_1, \dots, b_r\}$  of respective degrees  $a_1, \dots, a_r$ .
3. Remove all marked black vertices  $b_1, \dots, b_r$  and their incident edges; this yields a forest of  $s$  rooted bipartite mobiles.

In both ways, there are  $\prod_{i=1}^{r-1} (r-i) = (r-1)!$  possibilities, that is, the correspondence is  $(r-1)!$ -to- $(r-1)!$ .  $\square$

As a corollary we obtain the formula of Theorem 1 in the bipartite case:

**Corollary 7.** *For  $r \geq 1$  and  $a_1, \dots, a_r$  positive integers, the generating function  $G_{2a_1, \dots, 2a_r}$  satisfies (2.5), i.e.,*

$$G_{2a_1, \dots, 2a_r} = \left( \prod_{i=1}^r \frac{(2a_i)!}{a_i! (a_i - 1)!} \right) \cdot \frac{1}{s} \cdot \frac{d^{r-2}}{dt^{r-2}} R^s, \quad \text{where } s = \sum_{i=1}^r a_i. \quad (2.6)$$

*Proof.* As mentioned in the introduction, for  $r = 1$  the expression reads  $G_{2a}' = \binom{2a}{a} R^a$ , which is a direct consequence of the bijection with mobiles (indeed  $G_{2a}'$  is the series of mobiles with a marked black vertex  $v$  of degree  $2a$ , with a marked corner incident to  $v$ ). So we now assume  $r \geq 2$ . Let  $B_{2a_1, \dots, 2a_r} = B_{2a_1, \dots, 2a_r}(t; x_1, x_2, \dots)$  be the generating function of  $\mathcal{B}_{2a_1, \dots, 2a_r}$ , where  $t$  marks the number of white vertices and  $x_i$  marks the number of black vertices of degree  $2i$ . Let  $\widehat{M}_{2a_1, \dots, 2a_r} = \widehat{M}_{2a_1, \dots, 2a_r}(t; x_1, x_2, \dots)$  be the generating function of  $\widehat{\mathcal{M}}_{2a_1, \dots, 2a_r}$ , where again  $t$  marks the number of white

vertices and  $x_i$  marks the number of black vertices of degree  $2i$ . By definition of  $\widehat{\mathcal{M}}_{2a_1, \dots, 2a_r}$ , we have:

$$s \cdot B_{2a_1, \dots, 2a_r} = \left( \prod_{i=1}^r \binom{2a_i - 1}{a_i} \right) \cdot \widehat{\mathcal{M}}_{2a_1, \dots, 2a_r}$$

where the factor  $s$  is due to the number of ways to place the root (i.e., mark a corner at one of the marked black vertices), and the binomial product is due to the number of ways to place the buds around the marked black vertices. Moreover, Theorem 2 ensures that:

$$G_{2a_1, \dots, 2a_r}' = \left( \prod_{i=1}^r 2a_i \right) \cdot B_{2a_1, \dots, 2a_r}$$

where the multiplicative constant is the consequence of a corner being marked in every boundary face, and where the derivative (according to  $t$ ) is the consequence of a vertex being marked in the bipartite map. Next, Proposition 6 yields:

$$\widehat{\mathcal{M}}_{2a_1, \dots, 2a_r} = \frac{d^{r-1}}{dt^{r-1}} R^s$$

hence we conclude that:

$$G_{2a_1, \dots, 2a_r}' = \frac{1}{s} \left( \prod_{i=1}^r 2a_i \binom{2a_i - 1}{a_i} \right) \cdot \frac{d^{r-1}}{dt^{r-1}} R^s,$$

which, upon integration according to  $t$ , gives the claimed formula.  $\square$

## 2.4 Quasi-bipartite case

### 2.4.1 Blossoming trees and mobiles

So far we have obtained an expression for the generating function  $G_{\ell_1, \dots, \ell_r}$  when all  $\ell_i$  are even. In general, by definition of even maps of type  $(\ell_1, \dots, \ell_r)$ , there is an even number of  $\ell_i$  of odd degree. We deal here with the case where exactly two of the  $\ell_i$  are odd. This is done by a reduction to the bipartite case, using so-called *blossoming trees* (already considered in [55]) as auxiliary structures, see Figure 2.4(a) for an example.

**Definition 3** (Blossoming trees). *A planted plane tree is a plane tree with a marked leaf; classically it is drawn in a top-down way; each vertex  $v$  (different from the root-leaf) has  $i$  (ordered) children, and the integer  $i$  is called the arity of  $v$ . Vertices that are not leaves are colored black (so a black vertex means a vertex that is not a leaf). A blossoming tree is a rooted plane tree where each black vertex  $v$ , of arity  $i \geq 1$ , carries additionally  $i-1$  dangling half-edges called buds (leaves carry no bud). The degree of such a black vertex  $v$  is considered to be  $2i$ .*

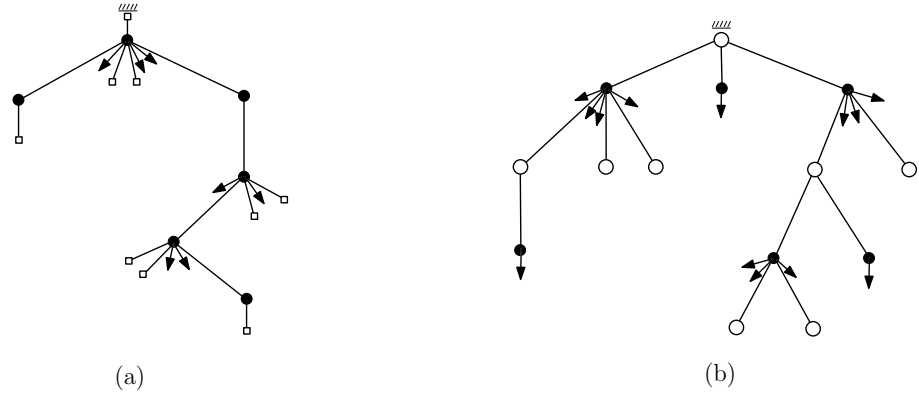


Figure 2.4: (a) A blossoming tree. (b) The corresponding rooted bipartite mobile.

By a decomposition at the root, the generating function  $T := T(t; x_1, x_2, \dots)$  of blossoming trees, where  $t$  marks the number of non-root leaves and  $x_i$  marks the number of black vertices of degree  $2i$ , is given by:

$$T = t + \sum_{i \geq 1} x_i \binom{2i - 1}{i} T^i. \quad (2.7)$$

**Claim 8.** *There is a bijection between the family  $\mathcal{T}$  of blossoming trees and the family  $\mathcal{R}$  of rooted bipartite mobiles. For  $\gamma \in \mathcal{T}$  and  $\gamma' \in \mathcal{R}$  the associated rooted bipartite mobile, each non-root leaf of  $\gamma$  corresponds to a white vertex of  $\gamma'$ , and each black vertex of degree  $2i$  in  $\gamma$  corresponds to a black vertex of degree  $2i$  in  $\gamma'$ .*

*Proof.* Note that the decomposition-equation (2.7) satisfied by  $T$  is exactly the same as the decomposition-equation (2.2) satisfied by  $R$ . Hence  $T = R$ , and one can easily produce recursively a bijection between  $\mathcal{T}$  and  $\mathcal{R}$  that sends black vertices of degree  $2i$  to black vertices of degree  $2i$ , and sends leaves to white vertices, for instance Figure 2.4 shows a blossoming tree and the corresponding rooted bipartite mobile.  $\square$

The bijection between  $\mathcal{T}$  and  $\mathcal{R}$  will be used in order to get rid of the black path (between the two black vertices of odd degrees) which appears in a quasi-bipartite mobile. Note that, if we denote by  $\mathcal{R}'$  the family of rooted mobiles with a marked white vertex (which does not contribute to the number of white vertices), and by  $\mathcal{T}'$  the family of blossoming trees with a marked non-root leaf (which does not contribute to the number of non-root leaves), then  $\mathcal{T}' \simeq \mathcal{R}'$ .

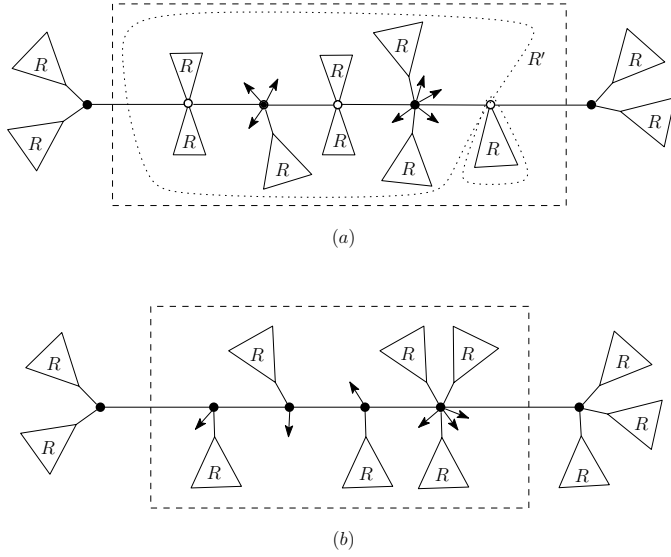


Figure 2.5: middle-parts in the bipartite case (a) and in the quasi-bipartite case (b).

#### 2.4.2 Decomposing along the middle-path

Let  $\tau$  be a mobile with two marked black vertices  $v_1, v_2$ . Let  $P = (e_1, \dots, e_k)$  be the path between  $v_1$  and  $v_2$  in  $\tau$ . If we untie  $e_1$  from  $v_1$  and  $e_k$  from  $v_2$ , we obtain 3 connected components: the one containing  $P$  is called the *middle-part*  $\tau'$  of  $\tau$ ; the edges  $e_1$  and  $e_k$  are called respectively the *first end* and the *second end* of  $\tau'$  in  $\tau$ . The vertices  $v_1$  and  $v_2$  are called *extremal*.

Let  $\mathcal{H}$  be the family of structures that can be obtained as middle-parts of quasi-bipartite mobiles where  $v_1$  and  $v_2$  are the two black vertices of odd degree (hence the path between  $v_1$  and  $v_2$  contains only black vertices). And let  $\mathcal{K}$  be the family of structures that can be obtained as middle-parts of bipartite mobiles with two marked black vertices  $v_1, v_2$ .

**Lemma 4.** *We have the following bijections:*

$$\mathcal{H} \simeq \mathcal{T}' \simeq \mathcal{R}' \quad \mathcal{K} \simeq \mathcal{R}' \times \mathcal{R}$$

Hence:

$$\mathcal{K} \simeq \mathcal{H} \times \mathcal{R}.$$

In these bijections each non-extremal black vertex of degree  $2i$  in an object on the left-hand side corresponds to a non-extremal black vertex of degree  $2i$  in the corresponding object on the right-hand side.

*Proof.* Note that any  $\tau \in \mathcal{H}$  consists of a path  $P$  of black vertices, and each vertex of degree  $2i$  in  $P$  carries (outside of  $P$ )  $i - 1$  buds and  $i - 1$  rooted mobiles (in  $\mathcal{R}$ ), as illustrated in Figure 2.5(b). Let  $\tau'$  be  $\tau$  where each rooted mobile attached to  $P$  is replaced by the corresponding blossoming tree (using the isomorphism of Claim 8), and where the ends of  $\gamma$  are considered as two marked leaves (respectively the root-leaf and a marked non-root leaf). We clearly have  $\tau' \in \mathcal{T}'$ . Conversely, starting from  $\tau' \in \mathcal{T}'$ , let  $P$  be the path between the root-leaf and the non-root marked leaf. Each vertex of degree  $2i$  on  $P$  carries (outside of  $P$ )  $i - 1$  buds and  $i - 1$  blossoming trees. Replacing each blossoming tree attached to  $P$  by the corresponding rooted mobile, and seeing the two marked leaves as the first and second end of  $P$ , one gets a structure in  $\mathcal{H}$ . So we have  $\mathcal{H} \simeq \mathcal{T}'$ .

The bijection  $\mathcal{K} \simeq \mathcal{R}' \times \mathcal{R}$  is simpler. Indeed, any  $\tau \in \mathcal{K}$  can be seen as a rooted mobile  $\gamma$  with a secondary marked corner at a white vertex (see Figure 2.5(a)). Let  $w$  (resp.  $w'$ ) be the white vertex at the root (resp. at the secondary marked corner) and let  $P$  be the path between  $w$  and  $w'$ . Each white vertex on  $P$  can be seen as carrying two rooted mobiles (in  $\mathcal{R}$ ), one on each side of  $P$ . Let  $r, r'$  be the two rooted mobiles attached at  $w'$  (say,  $r$  is the one on the left of  $w'$  when looking toward  $w$ ). If we untie  $r$  from the rest of  $\gamma$ , then  $w'$  now just acts as a marked white vertex in  $\gamma$ , so the pair  $(\gamma, r)$  is in  $\mathcal{R}' \times \mathcal{R}$ . The mapping from  $(\gamma, r) \in \mathcal{R}' \times \mathcal{R}$  to  $\tau \in \mathcal{K}$  processes in the reverse way. We get  $\mathcal{K} \simeq \mathcal{R}' \times \mathcal{R}$ .  $\square$

At the level of generating function expressions, Lemma 4 has been proved by Chapuy [22, Prop.7.5] in an even more precise form (which keeps track of a certain distance-parameter between the two extremities). We include our own proof to make this section self-contained, and because the new idea of using blossoming trees as auxiliary tools yields a short bijective proof.

Now from Lemma 4 we can deduce a reduction from the quasi-bipartite to the bipartite case (in Lemma 5 thereafter, see also Figure 2.5). Let  $a_1$  and  $a_2$  be positive integers. Define  $\mathcal{B}_{2a_1,2a_2}$  as the family of bipartite mobiles with two marked black vertices  $v_1, v_2$  of respective degrees  $2a_1, 2a_2$ . Similarly, define  $\mathcal{Q}_{2a_1-1,2a_2+1}$  as the family of quasi-bipartite mobiles with two marked black vertices  $v_1, v_2$  of respective degrees  $2a_1 - 1, 2a_2 + 1$  (i.e., the marked vertices are the two black vertices of odd degree). Let  $\widehat{\mathcal{B}}_{2a_1,2a_2}$  be the family of pruned mobiles (recall that “pruned” means “where buds at marked black vertices are taken out”) obtained from mobiles in  $\mathcal{B}_{2a_1,2a_2}$ , and let  $\widehat{\mathcal{Q}}_{2a_1-1,2a_2+1}$  be the family of pruned mobiles obtained from mobiles in  $\mathcal{Q}_{2a_1-1,2a_2+1}$ .

**Lemma 5.** *For  $a_1, a_2$  two positive integers:*

$$\widehat{\mathcal{B}}_{2a_1,2a_2} \simeq \widehat{\mathcal{Q}}_{2a_1-1,2a_2+1}.$$

*In addition, if  $\gamma \in \widehat{\mathcal{B}}_{2a_1,2a_2}$  corresponds to  $\gamma' \in \widehat{\mathcal{Q}}_{2a_1-1,2a_2+1}$ , then each non-marked black vertex of degree  $2i$  (resp. each white vertex) in  $\gamma$  corresponds*

to a non-marked black vertex of degree  $2i$  (resp. to a white vertex) in  $\gamma'$ .

*Proof.* Let  $\gamma \in \widehat{\mathcal{Q}}_{2a_1-1,2a_2+1}$ , and let  $\tau$  be the middle-part of  $\gamma$ . We construct  $\gamma' \in \widehat{\mathcal{B}}_{2a_1,2a_2}$  as follows. Note that  $v_2$  has a black neighbour  $b$  (along the branch from  $v_2$  to  $v_1$ ) and has otherwise  $a_2$  white neighbours. Let  $w$  be next neighbour after  $b$  in counter-clockwise order around  $v_2$ , and let  $r$  be the mobile (in  $\mathcal{R}$ ) hanging from  $w$ . According to Lemma 4, the pair  $(\tau, r)$  corresponds to some  $\tau' \in \mathcal{K}$ . If we replace the middle-part  $\tau$  by  $\tau'$  and take out the edge  $\{v_2, w\}$  and the mobile  $r$ , we obtain some  $\gamma' \in \widehat{\mathcal{B}}_{2a_1,2a_2}$ . The inverse process is easy to describe, so we obtain a bijection between  $\widehat{\mathcal{Q}}_{2a_1-1,2a_2+1}$  and  $\widehat{\mathcal{B}}_{2a_1,2a_2}$ .  $\square$

Lemma 5 (in an equivalent form) has first been shown by Cori [27, Theo.VI p.75] (again we have provided our own short proof to be self-contained).

As a corollary of Lemma 5, we obtain the formula of Theorem 1 in the quasi-bipartite case, with the exception of the case where the two odd boundaries are of length 1 (this case will be treated later, in Lemma 6).

**Corollary 9.** *For  $r \geq 2$  and  $a_1, \dots, a_r$  positive integers, the generating function  $G_{2a_1-1,2a_2+1,2a_3, \dots, 2a_r}$  satisfies (2.5).*

*Proof.* We first consider the case  $r = 2$ . Let  $\widehat{B}_{2a_1,2a_2} = \widehat{B}_{2a_1,2a_2}(t; x_1, x_2, \dots)$  (resp.  $B_{2a_1,2a_2} = B_{2a_1,2a_2}(t; x_1, x_2, \dots)$ ) be the generating function of  $\widehat{\mathcal{B}}_{2a_1,2a_2}$  (resp. of  $\mathcal{B}_{2a_1,2a_2}$ ) where  $t$  marks the number of white vertices and  $x_i$  marks the number of non-marked black vertices of degree  $2i$ . There are  $\binom{2a_i-1}{a_i}$  ways to place the buds at each marked black vertex  $v_i$  ( $i \in \{1, 2\}$ ), hence:

$$B_{2a_1,2a_2} = \binom{2a_1-1}{a_1} \binom{2a_2-1}{a_2} \widehat{B}_{2a_1,2a_2}.$$

In addition Theorem 2 ensures that  $G_{2a_1,2a_2}' = 2a_1 2a_2 B_{2a_1,2a_2}$  (the multiplicative factor being due to the choice of a marked corner in each boundary-face). Hence:

$$G_{2a_1,2a_2}' = 4a_1 a_2 \binom{2a_1-1}{a_1} \binom{2a_2-1}{a_2} \widehat{B}_{2a_1,2a_2}.$$

Similarly, if we denote by  $\widehat{Q}_{2a_1-1,2a_2+1} = \widehat{Q}_{2a_1-1,2a_2+1}(t; x_1, x_2, \dots)$  the generating function of the family  $\widehat{\mathcal{Q}}_{2a_1-1,2a_2+1}$  where  $t$  marks the number of white vertices and  $x_i$  marks the number of non-marked black vertices of degree  $2i$ , then we have:

$$G_{2a_1-1,2a_2+1}' = (2a_1-1)(2a_2+1) \binom{2a_1-2}{a_1-1} \binom{2a_2}{a_2} \widehat{Q}_{2a_1-1,2a_2+1}.$$

Since  $\widehat{B}_{2a_1, 2a_2} = \widehat{Q}_{2a_1-1, 2a_2+1}$  by Lemma 5, we get (with the notation  $\alpha(\ell) = \frac{\ell!}{[\ell/2]![\ell-1]/2!]}$ ):

$$\alpha(2a_1 - 1) \cdot \alpha(2a_2 + 1) \cdot G_{2a_1, 2a_2} = \alpha(2a_1) \cdot \alpha(2a_2) \cdot G_{2a_1-1, 2a_2+1}.$$

In a very similar way (by the isomorphism of Lemma 5), we have for  $r \geq 2$ :

$$\alpha(2a_1 - 1) \cdot \alpha(2a_2 + 1) \cdot G_{2a_1, 2a_2, 2a_3, \dots, 2a_r} = \alpha(2a_1) \cdot \alpha(2a_2) \cdot G_{2a_1-1, 2a_2+1, 2a_3, \dots, 2a_r}.$$

Hence the fact that  $G_{2a_1-1, 2a_2+1, 2a_3, \dots, 2a_r}$  satisfies (2.5) follows from the fact (already proved in Corollary 7) that  $G_{2a_1, 2a_2, 2a_3, \dots, 2a_r}$  satisfies (2.5).  $\square$

It remains to show the formula when the two odd boundary-faces have length 1. For that case, we have the following counterpart of Lemma 5:

**Lemma 6.** *Let  $\mathcal{B}_2$  be the family of bipartite mobiles with a marked black vertex of degree 2, and let  $\mathcal{B}'_2$  be the family of objects from  $\mathcal{B}_2$  where a white vertex is marked. Then*

$$\mathcal{Q}_{1,1} \simeq \mathcal{B}'_2.$$

*In addition, if  $\gamma \in \mathcal{B}'_2$  corresponds to  $\gamma' \in \mathcal{Q}_{1,1}$ , then each white vertex of  $\gamma$  corresponds to a white vertex of  $\gamma'$ , and each non-marked black vertex of degree  $2i$  in  $\gamma$  corresponds to a non-marked black vertex of degree  $2i$  in  $\gamma'$ .*

*Proof.* A mobile in  $\mathcal{Q}_{1,1}$  is completely reduced to its middle-part, so we have

$$\mathcal{Q}_{1,1} \simeq \mathcal{H} \simeq \mathcal{T}' \simeq \mathcal{R}'.$$

Consider a mobile in  $\mathcal{R}'$ , i.e., a bipartite mobile where a corner incident to a white vertex is marked, and a secondary white vertex is marked. At the marked corner we can attach an edge connected to a new marked black vertex  $b$  of degree 2 (the other incident half-edge of  $b$  being a bud). We thus obtain a mobile in  $\mathcal{B}'_2$ , and the mapping is clearly a bijection.  $\square$

By Lemma 6 we have  $2G_{1,1} = G''_2$ , and similarly  $2G_{1,1, 2a_3, \dots, 2a_r} = G_{2, 2a_3, \dots, 2a_r}'$ . Hence, again the fact that  $G_{1,1, 2a_3, \dots, 2a_r}$  satisfies (2.5) follows from the fact that  $G_{2, 2a_3, \dots, 2a_r}$  satisfies (2.5), which has been shown in Corollary 7.

## Chapter 3

# Extension to $p$ -constellations and quasi- $p$ -constellations

### 3.1 Introduction

In this chapter, we extend the formula of Theorem 1 to constellations and quasi-constellations, families of maps which naturally generalize bipartite and quasi-bipartite maps. Define an *hypermap* as an eulerian map (map with all faces of even degree) whose faces are bicolored —there are dark faces and light faces— such that any edge has a dark face on one side and a light face on the other side<sup>1</sup>. Define a  $p$ -*hypermap* as a hypermap whose dark faces are of degree  $p$  (note that classical maps correspond to 2-hypermaps, since each edge can be blown into a dark face of degree 2). Note that the degrees of light faces in a  $p$ -hypermap add up to a multiple of  $p$ . A  $p$ -*constellation* is a  $p$ -hypermap such that the degrees of light faces are multiples of  $p$ , and a *quasi  $p$ -constellation* is a  $p$ -hypermap such that exactly two light faces have a degree not multiple of  $p$ . By the identification with maps, 2-constellations and quasi 2-constellations correspond respectively to bipartite maps and quasi-bipartite maps.

Bouttier, Di Francesco and Guitter [19] also described a bijection for hypermaps, in correspondence with more involved mobiles (recalled in Section 3.2). When applied to  $p$ -constellations, this bijection yields the following: if we denote by  $R_p = R_p(t) = R_p(t; x_1, x_2, \dots)$  the generating function specified by

$$R_p = t + \sum_{i \geq 1} x_i \binom{pi - 1}{i} R_p^{(p-1)i}. \quad (3.1)$$

and by  $C_p(t) = C_p(t; x_1, x_2, \dots)$  the generating function of rooted  $p$ -

---

<sup>1</sup>Hypermaps have several equivalent definitions in the literature; our definition coincides with the one of Walsh [51], by turning each dark face into a star centered at a dark vertex; and coincides with the definitions of Cori and of James [59] where hypervertices are collapsed into vertices.

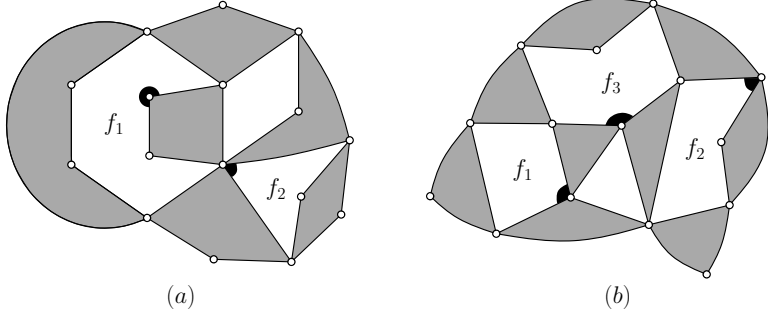


Figure 3.1: (a) A 4-constellation with 2 boundaries  $f_1, f_2$  of respective degree 8, 4. (b) A quasi-3-constellation with 3 boundaries  $f_1, f_2, f_3$  of respective degree 4, 5, 6.

constellations (*i.e.*,  $p$ -constellations with a marked corner incident to a light face) where  $t$  marks the number of vertices and  $x_i$  marks the number of light faces of degree  $pi$  for  $i \geq 1$ , then the bijection of [19] ensures that  $C'_p(t) = \frac{p}{p-1} R_p(t)$ .

We use this bijection and tools from Sections 2.3 and 2.4 to obtain the following formula for the generating function of constellations (proved in Section 3.3) and quasi-constellations (proved in Section 3.4). Let  $G_{\ell_1, \dots, \ell_r}^{(p)} := G_{\ell_1, \dots, \ell_r}^{(p)}(t; x_1, x_2, \dots)$  be the generating function of  $p$ -hypermaps with  $r$  (numbered) boundaries  $f_1, \dots, f_r$  of degrees  $\ell_1, \dots, \ell_r$ , whose non-marked faces have degrees a multiple of  $p$ , where  $t$  marks the number of vertices and  $x_i$  marks the number of non-boundary faces of degree  $pi$ . Then:

**Theorem 7.** *When none or only two of the  $\ell_i$  are not multiple of  $p$ , then the following formula holds:*

$$G_{\ell_1, \dots, \ell_r}^{(p)} = \left( \prod_{i=1}^r \alpha(\ell_i) \right) \cdot \frac{c}{s} \cdot \frac{d^{r-2}}{dt^{r-2}} R_p^s, \quad (3.2)$$

where  $\alpha(\ell) = \frac{\ell!}{[\ell/p]!(\ell - [\ell/p] - 1)!}$ ,  $s = \frac{p-1}{p}(\ell_1 + \dots + \ell_r)$ ,  $R_p$  is given by (3.1),

and  $c = \begin{cases} 1, & \text{when every } \ell_i \text{ is a multiple of } p, \\ p-1, & \text{when exactly two } \ell_i \text{ are not multiple of } p. \end{cases}$

First note that Theorem 1 is the direct application of Theorem 7 when  $p = 2$ . Moreover, this yields the following extension of Tutte's slicing formula:

**Corollary 10.** *For  $p \geq 2$ , let  $A^{(p)}[\ell_1, \dots, \ell_r]$  be the number of  $p$ -hypermaps with exactly  $r$  numbered light faces  $f_1, \dots, f_r$  of respective degrees  $\ell_1, \dots, \ell_r$ ,*

each light face having a marked corner.

When none or only two of the  $\ell_i$  are not multiple of  $p$  ( $p$ -constellations and quasi- $p$ -constellations, respectively), then:

$$A^{(p)}[\ell_1, \dots, \ell_r] = c \frac{(e - d - 1)!}{v!} \prod_{i=1}^r \alpha(\ell_i), \quad (3.3)$$

with  $\alpha(\ell) := \frac{\ell!}{\lfloor \ell/p \rfloor! (\ell - \lfloor \ell/p \rfloor - 1)!}$ , where  $e = \sum_{i=1}^r \ell_i$  is the number of edges,  $d = \frac{\sum_{i=1}^r \ell_i}{p}$  is the number of dark faces, and  $v = e - d - r + 2$  is the number of vertices, and  $c = \begin{cases} 1, & \text{when every } \ell_i \text{ is a multiple of } p, \\ p - 1, & \text{when exactly two } \ell_i \text{ are not multiple of } p. \end{cases}$

One gets (3.3) out of (3.2) by taking the evaluation of  $G_{\ell_1, \dots, \ell_r}^{(p)}$  at  $\{t = 1; x_1 = 0, x_2 = 0, \dots\}$ . The expression of the numbers  $A^{(p)}[\ell_1, \dots, \ell_r]$  when all  $\ell_i$  are multiples of  $p$  has been discovered by Bousquet-Mélou and Schaeffer [15], but to our knowledge, the expression for quasi-constellations has not been given before (though it could also be obtained from Chapuy's results [22], see the paragraphs after Lemma 4 and Lemma 11).

### 3.2 Bijection between vertex-pointed hypermaps and hypermobiles

Hypermaps admit a natural orientation by orienting each edge so as to have its incident dark face to its left. The following bijection is again a reformulation of the bijection in [19] between vertex-pointed eulerian maps and mobiles. Starting from a hypermap  $G$  with a pointed vertex  $v_0$ , and where the vertices of  $G$  are considered as *round vertices*, one obtains a mobile  $M$  as follows:

- Endow  $G$  with its natural orientation.
- Endow  $G$  with its geodesic orientation by keeping oriented edges which belong to a geodesic oriented path from  $v_0$ .
- Label vertices of  $G$  by their distance from  $v_0$ .
- Put a light (resp. dark) square in each light (resp. dark) face of  $G$ .
- Apply the following rules to each edge (oriented or not) of  $G$ :

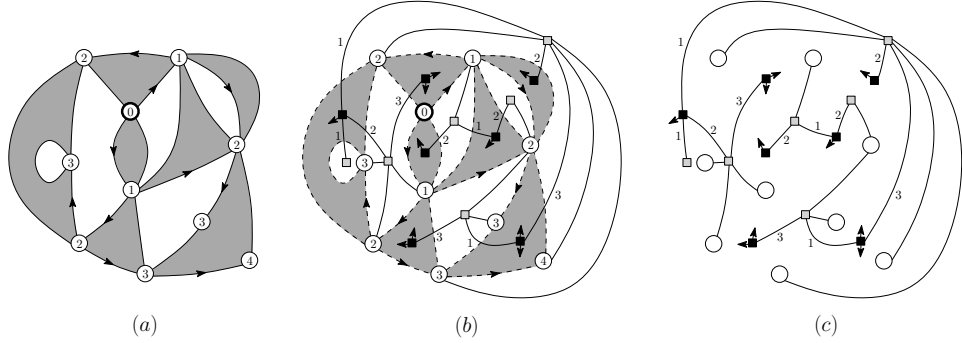
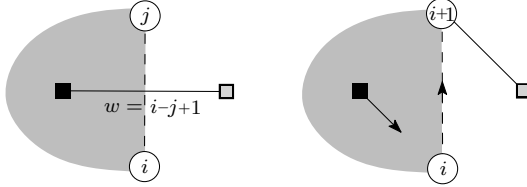


Figure 3.2: (a) A vertex-pointed hypermap endowed with its geodesic orientation (with respect to the marked vertex). (b) The local rule is applied to each edge of the hypermap. (c) The resulting hypermobile.



- Forget labels on vertices.

**Definition 8** (Hypermobiles). *A hypermobile is a tree with three types of vertices (round, dark square, and light square) and positive integers (called weights) on some edges, such that:*

- there are two types of edges: between a round vertex and a light square vertex, or between a dark square vertex and a light square vertex (these edges are called dark-light edges),
- dark square vertices possibly carry buds,
- dark-light edges carry a strictly positive weight, such that, for each square vertex (dark or light), the sum of weights on its incident edges equals the degree of the vertex.

**Theorem 9** (Bouttier, Di Francesco and Guitter [19]). *The above construction is a bijection between vertex-pointed hypermaps and hypermobiles. Each non-pointed vertex in the hypermap corresponds to a round vertex in the associated hypermobile, and each dark (resp. light) face corresponds to a dark (resp. light) square vertex of the same degree in the associated hypermobile.*

### 3.3 Proof of Theorem 7 for $p$ -constellations

For  $p \geq 2$ , hypermobiles corresponding to vertex-pointed  $p$ -constellations are called  $p$ -mobiles.

**Claim 11** (Characterization of  $p$ -mobiles [19]). *A  $p$ -mobile satisfies the following properties:*

- *dark-light edges have weight  $p$ ,*
- *each dark square vertex, of degree  $p$ , has one light square neighbour and  $p - 1$  buds (thus can be seen as a “big bud” attached to the light square neighbour),*
- *each light square vertex, of degree  $pi$  for some  $i \geq 1$ , has  $i$  dark square neighbours (i.e., carries  $i$  big buds) and  $(p - 1)i$  round neighbours.*

*Proof.* The first assertion is proved as follows. Let  $T$  be a  $p$ -mobile and  $F$  the forest formed by the edges whose weight is not a multiple of  $p$ , and their incident vertices. By construction, for each vertex of  $T$ , the degree and the sum of weights are multiple of  $p$ . Assume  $F$  is non-empty. Then  $F$  has a leaf  $v$ . Hence  $v$  has a unique incident edge whose weight is not a multiple of  $p$ , which implies that the degree of  $p$  is not a multiple of  $p$ , a contradiction. Hence  $F$  is empty and each weight in  $T$  is a multiple of  $p$ . Moreover, dark square vertices have degree  $p$ , which implies that weights are at most equal to  $p$ . Hence all weights are equal to  $p$ . Then the second and third assertion follow directly from the first one.  $\square$

Since the weights are always  $p$  they can be omitted, and seeing dark square vertices as “big buds” it is clear that in the case  $p = 2$  we recover the mobiles for bipartite maps. A *rooted  $p$ -mobile* is a  $p$ -mobile with a marked corner at a round vertex. Let  $R_p \equiv R_p(t) \equiv R_p(t; x_1, x_2, \dots)$  be the generating function of rooted  $p$ -mobiles where  $t$  marks the number of white vertices and, for  $i \geq 1$ ,  $x_i$  marks the number of light square vertices of degree  $pi$ . By a decomposition at the root (see [19]),  $R_p$  satisfies (3.1).

One can now use the same processus as in Section 2.3 to describe  $p$ -constellations with  $r$  boundaries. For a  $p$ -mobile  $\gamma$  with marked light square vertices  $b_1, \dots, b_r$  of degrees  $pa_1, \dots, pa_r$ , the associated *pruned  $p$ -mobile*  $\hat{\gamma}$  is obtained from  $\gamma$  by deleting the (big) buds at the marked vertices (thus the marked vertices get degrees  $(p - 1)a_1, \dots, (p - 1)a_r$ ). Conversely, such a pruned mobile yields  $\prod_{i=1}^r \binom{pa_i - 1}{a_i}$  mobiles (because of the number of ways to place the big buds around the marked light square vertices). Hence, if we denote by  $\mathcal{B}_{pa_1, \dots, pa_r}^{(p)}$  the family of  $p$ -mobiles with  $r$  marked light square vertices of respective degrees  $pa_1, \dots, pa_r$ , and denote by  $\hat{\mathcal{B}}_{pa_1, \dots, pa_r}^{(p)}$  the family

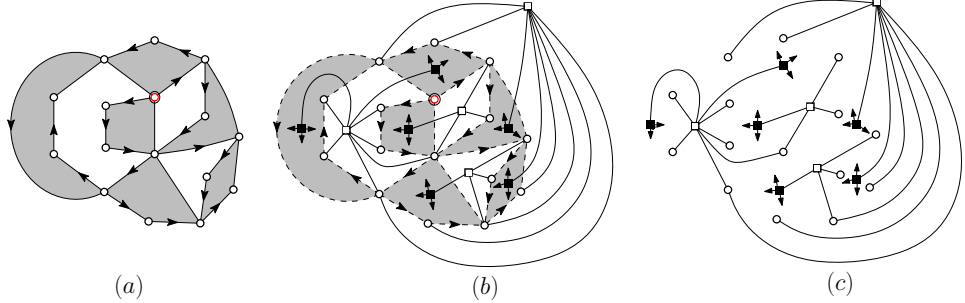


Figure 3.3: (a) A vertex-pointed  $p$ -constellation,  $p = 4$ , endowed with its geodesic orientation (with respect to the marked vertex). (b) The local rule is applied to each edge of the map. (c) The resulting  $p$ -mobile (weights on dark-light edges, which all equal  $p$ , are omitted).

of pruned  $p$ -mobiles with  $r$  marked light square vertices of respective degree  $(p - 1)a_1, \dots, (p - 1)a_r$ , we have:

$$\mathcal{B}_{pa_1, \dots, pa_r}^{(p)} \simeq \prod_{i=1}^r \binom{pa_i - 1}{a_i} \widehat{\mathcal{B}}_{pa_1, \dots, pa_r}^{(p)}$$

We consider the two following families:

- $\widehat{\mathcal{M}}_{pa_1, \dots, pa_r}^{(p)}$  is the family of pruned  $p$ -mobiles with  $r$  marked light square vertices  $v_1, \dots, v_r$  of respective degrees  $(p - 1)a_1, \dots, (p - 1)a_r$ , the mobile being rooted at a corner of one of the marked vertices,
- $\mathcal{F}_s^{(p)}$  is the family of forests made of  $s := (p - 1) \sum_{i=1}^r a_i$  rooted  $p$ -mobiles, and where additionnally  $r - 1$  round vertices  $w_1, \dots, w_{r-1}$  are marked.

**Proposition 12.** *There is an  $(r - 1)! \text{-to-} (r - 1)!$  correspondence between the family  $\widehat{\mathcal{M}}_{pa_1, \dots, pa_r}^{(p)}$  and the family  $\mathcal{F}_s^{(p)}$ . If  $\gamma \in \widehat{\mathcal{M}}_{pa_1, \dots, pa_r}^{(p)}$  corresponds to  $\gamma' \in \mathcal{F}_s^{(p)}$ , then each round vertex in  $\gamma$  corresponds to a round vertex in  $\gamma'$ , and each light square vertex of degree  $pi$  in  $\gamma$  corresponds to a light square vertex of degree  $pi$  in  $\gamma'$ .*

*Proof.* This correspondence works in the same way as in Theorem 6, where light square vertices act as black vertices and round vertices act as white vertices, and where one groups the first  $(p - 1)a_1$  components of the forest, then the following  $(p - 1)a_2$  components, and so on, and then uses the same aggregation process as in the bipartite case.  $\square$

As a corollary we obtain the formula of Theorem 7 in the case of  $p$ -constellations:

**Corollary 13.** *For  $r \geq 1$  and  $a_1, \dots, a_r$  positive integers, the generating function  $G_{pa_1, \dots, pa_r}^{(p)}$  satisfies:*

$$G_{pa_1, \dots, pa_r}^{(p)} = \left( \prod_{i=1}^r \frac{(pa_i)!}{((p-1)a_i - 1)! a_i!} \right) \cdot \frac{1}{s} \cdot \frac{d^{r-2}}{dt^{r-2}} R_p^s, \quad (3.4)$$

where  $s = (p-1) \sum_{i=1}^r a_i$ .

*Proof.* In the case  $r = 1$ , the expression reads  $G_{pa}^{(p)'} = {pa \choose a} R_p^a$ , which is a direct consequence of the bijection with  $p$ -mobiles (indeed  $G_{pa}^{(p)'} = G_{pa}$  is the series of  $p$ -mobiles with a marked light square vertex  $v$  of degree  $pa$ , with a marked corner incident to  $v$ ). So we now assume  $r \geq 2$ . The formula derives (as formula (2.6)) by combining the bijection of Theorem 9 and the correspondence of Proposition 12, upon consistent rooting and placing of the buds, and a final integration.  $\square$

### 3.4 Proof of Theorem 7 for quasi $p$ -constellations

In a similar way as for quasi bipartite maps, we prove Theorem 7 in the case of quasi  $p$ -constellations (two boundaries have length not a multiple of  $p$ ) by a reduction to  $p$ -constellations, with some more technical details. We call *quasi  $p$ -mobiles* the hypermobiles associated to quasi  $p$ -constellations by the bijection of Section 3.2, see Figure 3.4 for an example. In the following, we will refer to vertices whose degree is not a multiple of  $p$  as *non-regular vertices* and edges whose weight is not a multiple of  $p$  as *non-regular edges*.

**Claim 14** (Alternating path in a quasi- $p$ -mobile). *In a quasi- $p$ -mobile, all weights of edges are at most  $p$  (so regular edges have weight  $p$ ) and the set of non-regular edges forms a non-empty path whose extremities are the two non-regular vertices. Moreover, if the degrees of the non-regular vertices  $v_1, v_2$  are  $pi - d = p(i-1) + p - d$  and  $pj + d$ ,  $i, j \geq 1$ ,  $1 \leq d \leq p-1$  (the sum of the two degrees must be a multiple of  $p$ ), the weights along the path from  $v_1$  to  $v_2$  start with  $p-d$ , alternate between  $p-d$  and  $d$ , and end with  $d$ .*

*Proof.* The fact that the weights are at most  $p$  just follows from the fact that dark square vertices have degree  $p$ . Let  $T$  be a quasi- $p$ -mobile, and let  $F$  be the forest formed by the non-regular edges of  $T$ . Leaves of  $F$  are necessarily non-regular, hence  $F$  has only two leaves which are  $v_1, v_2$ , so  $F$  is reduced to a path  $P$  connecting  $v_1$  and  $v_2$ . Starting from  $v_1$ , the first edge of  $P$  must have weight  $p-d$ . This edge is incident to a black square vertex of degree  $p$ , so the following edge of  $P$  must have weight  $d$ . The next vertex on  $P$  is either  $v_2$  or is a regular light square vertex, in which case the next

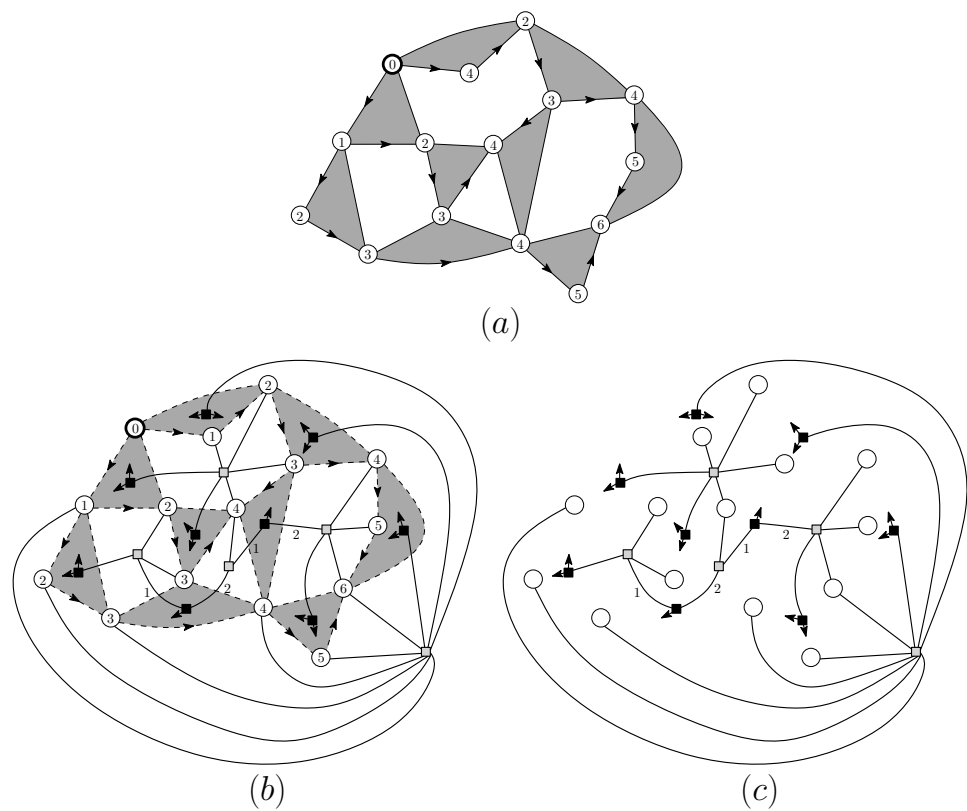


Figure 3.4: (a) A vertex-pointed quasi-3-constellation endowed with the geodesic orientation. (b) The local rule is applied to each edge of the map. (c) The resulting quasi-3-mobile, where the weights on the alternating path are  $(1, 2, 1, 2)$ .

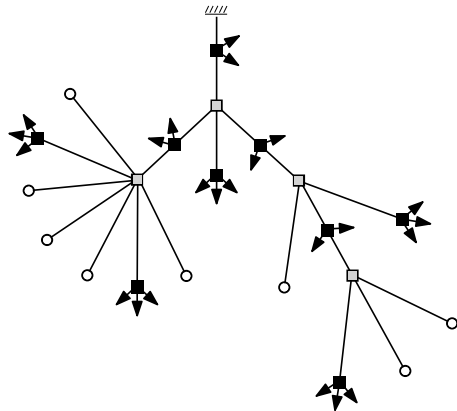


Figure 3.5: A blossoming 4-tree.

edge along  $P$  must have weight  $p - d$ . The alternation continues the same way until reaching  $v_2$  (necessarily using an edge of weight  $d$ ).  $\square$

As for  $p$ -mobiles, weights on regular edges (always equal to  $p$ ) can be omitted, and dark square vertices not on the alternating path can be seen as “big buds” (those on the alternating path are considered as “intermediate” dark square vertices). It is easy to check that regular light square vertices of degree  $pi$  are adjacent to  $i$  big buds, and non-regular light square vertices of degree  $pi + d$  (for some  $1 \leq d \leq p - 1$ ) are adjacent to  $i$  big buds.

### 3.4.1 Blossoming $p$ -trees and $p$ -mobiles

**Definition 10** (Blossoming  $p$ -trees [15]). *For  $p \geq 2$ , a planted  $p$ -tree is a planted tree (non-leaf vertices are light square, leaves are round) where the arity of internal vertices is of the form  $(p - 1)i$ . A blossoming  $p$ -tree is a structure obtained from a planted  $p$ -tree where:*

- *on each edge going down to a light square vertex, a dark square vertex (called intermediate) is inserted that additionally carries  $p - 2$  buds,*
- *at each light square vertex of arity  $(p - 1)i$  one further attaches  $i - 1$  new dark square vertices (called big buds), each such dark square vertex carrying additionally  $p - 1$  buds. (After these attachments, the light square vertex is considered to have degree  $pi$ .)*

Note that in a blossoming  $p$ -tree, dark square vertices have degree  $p$ . When  $p = 2$ , dark square vertices can be erased, and we obtain the description of a standard blossoming tree. By a decomposition at the root [15], the generating function  $T_p := T_p(t; x_1, x_2, \dots)$  of rooted blossoming  $p$ -trees,

where  $t$  marks the number of non-root (round) leaves and  $x_i$  marks the number of light square vertices of degree  $pi$ , is given by:

$$T_p = t + \sum_{i \geq 1} (p-1) \cdot x_i \binom{pi-1}{i-1} T_p^{(p-1)i} = t + \sum_{i \geq 1} x_i \binom{pi-1}{i} T_p^{(p-1)i}, \quad (3.5)$$

where the factor  $(p-1)$  in the sum represents the number of ways to place the  $(p-2)$  buds at the dark square vertex adjacent to the root.

**Claim 15.** *There is a bijection between the family  $\mathcal{T}_p$  of blossoming  $p$ -trees and the family  $\mathcal{R}_p$  of rooted  $p$ -mobiles. For  $\gamma \in \mathcal{T}_p$  and  $\gamma' \in \mathcal{R}_p$  the associated rooted  $p$ -mobile, each non-root round leaf of  $\gamma$  corresponds to a round vertex of  $\gamma'$ , each light square vertex of degree  $pi$  in  $\gamma$  corresponds to a light square vertex of degree  $pi$  in  $\gamma'$ .*

*Proof.* Note that the decomposition-equation (3.5) satisfied by  $T_p$  is exactly the same as the decomposition-equation (3.1) satisfied by  $R_p$ . Hence  $T_p = R_p$ , and one can easily produce recursively a bijection between  $\mathcal{T}_p$  and  $\mathcal{R}_p$  that sends light square vertices of degree  $pi$  to light square vertices of degree  $pi$ , and sends non-root round leaves to round vertices.  $\square$

The bijection between  $\mathcal{T}_p$  and  $\mathcal{R}_p$  will be used in order to get rid of the alternating path between the non-regular two light square vertices that appear in a quasi- $p$ -mobile. Note that, if we denote by  $\mathcal{R}'_p$  the family of rooted  $p$ -mobiles with a marked round vertex (which does not contribute to the number of round vertices), and by  $\mathcal{T}'_p$  the family of blossoming  $p$ -trees with a marked round leaf (which does not contribute to the number of round leaves), then  $\mathcal{T}'_p \simeq \mathcal{R}'_p$ .

### 3.4.2 Decomposing along the alternating middle-path

As in the (quasi-) bipartite case, for a hypermobile with two marked light-square vertices  $v_1, v_2$ , we can consider the operation of untying the two ends of the path  $P$  connecting  $v_1$  and  $v_2$ . The obtained structure (taking away the connected components not containing  $P$ ) is called the *middle-part* of the hypermobile. Let  $\mathcal{H}_p$  be the family of structures that can be obtained as middle-parts of quasi- $p$ -mobiles, where  $v_1$  and  $v_2$  are the two (ordered) non-regular vertices (thus  $P$  is the alternating path of the quasi  $p$ -mobile). And let  $\mathcal{K}_p$  be the family of structures that can be obtained as middle-parts of  $p$ -mobiles with two marked light square vertices  $v_1, v_2$ . In the case of  $\mathcal{H}_p$ , note that, according to Claim 15, the weights along the alternating path only depend on the degrees (modulo  $p$ ) of the end vertices. In particular, the shape of the middle-part and the labels along the path are independent. Hence, from now on the weights can be omitted when considering middle-parts from  $\mathcal{H}_p$ .

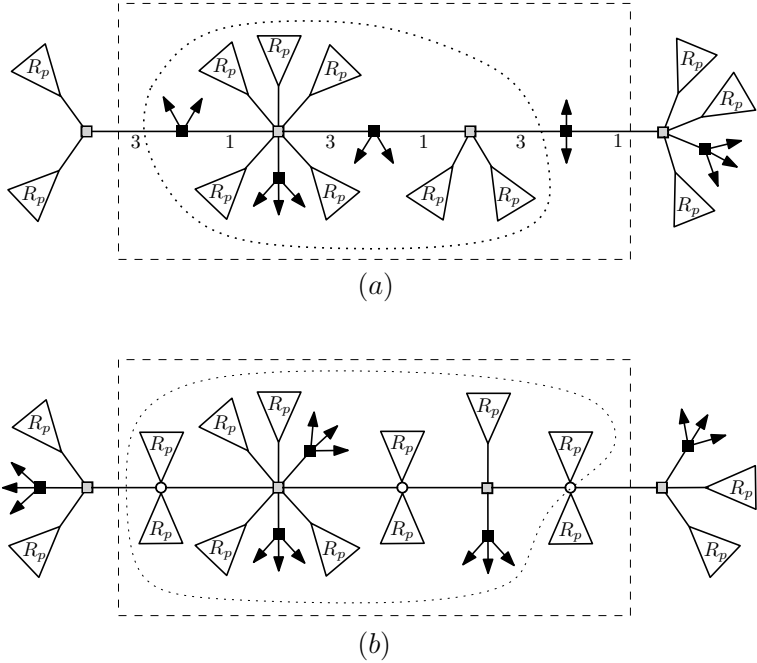


Figure 3.6: Middle-parts in a quasi-4-mobile (a), and in a 4-mobile (b).

**Lemma 11.** *We have the following bijections:*

$$\mathcal{H}_p \simeq (p-1) \cdot \mathcal{T}'_p \simeq (p-1) \cdot \mathcal{R}'_p \quad \mathcal{K}_p \simeq \mathcal{R}'_p \times \mathcal{R}_p$$

Hence:

$$(p-1) \cdot \mathcal{K}_p \simeq \mathcal{H}_p \times \mathcal{R}_p.$$

In these bijections, each light square vertex of degree  $p_i$  in an object on the left-hand side corresponds to a light square vertex of degree  $p_i$  in the corresponding object on the right-hand side.

*Proof.* For  $\mathcal{K}_p \simeq \mathcal{R}'_p \times \mathcal{R}_p$ , the proof is similar to Lemma 4, see Figure 3.6(b). To prove  $\mathcal{H}_p \simeq (p-1) \cdot \mathcal{T}'_p$  (see also Figure 3.6(a)), we start similarly as in the proof of Lemma 4, replacing each rooted  $p$ -mobile “adjacent” to the alternating path  $P$  by the corresponding blossoming  $p$ -tree. Let  $b$  be the (intermediate) dark square vertex adjacent to  $v_2$  on  $P$ . If we erase the  $p-2$  buds at  $b$ , then we naturally obtain a structure in  $\mathcal{T}'_p$  ( $b$  acts as a secondary marked leaf once its incident buds are taken out). Conversely there are  $p-1$  ways to distribute the buds at  $b$ , which gives a factor  $p-1$ .  $\square$

Again, at the level of generating function expressions, an even more precise statement (keeping track of a certain distance parameter between the two marked vertices) is given by Chapuy [22, Prop.7.5] (we include our quite shorter and completely bijective proof to make this chapter self-contained).

### 3.4.3 Degree transfer lemma

Now from Lemma 11 we reduce pruned quasi- $p$ -mobiles to pruned  $p$ -mobiles (pruned means: big buds at the marked light square vertices are taken out). Let  $a_1, a_2$  be positive integers, and  $1 \leq d \leq p - 1$ . Define  $\widehat{\mathcal{B}}_{pa_1, pa_2}^{(p)}$  as the family of pruned  $p$ -mobiles with two marked black vertices  $v_1, v_2$  of respective degrees  $(p - 1)a_1, (p - 1)a_2$ . Similarly define  $\widehat{\mathcal{Q}}_{pa_1-d, pa_2+d}^{(p)}$  as the family of pruned quasi- $p$ -mobiles with two marked black vertices  $v_1, v_2$  of respective degrees  $(p - 1)a_1 - d + 1, (p - 1)a_2 + d$  (the two marked light square vertices are the non-regular ones).

**Lemma 12.** *For  $a_1, a_2$  two positive integers, and  $1 \leq d \leq p - 1$ :*

$$(p - 1) \cdot \widehat{\mathcal{B}}_{pa_1, pa_2}^{(p)} \simeq \widehat{\mathcal{Q}}_{pa_1-d, pa_2+d}^{(p)}.$$

*In addition, if  $\gamma \in \widehat{\mathcal{B}}_{pa_1, pa_2}^{(p)}$  corresponds to  $\gamma' \in \widehat{\mathcal{Q}}_{pa_1-d, pa_2+d}^{(p)}$ , then each non-marked light square vertex of degree  $pi$  in  $\gamma$  corresponds to a non-marked light square vertex of degree  $pi$  in  $\gamma'$ .*

*Proof.* The proof is similar to Lemma 5, where we additionally have to transfer a part of the degree contribution from one end of the alternating path to the other, in order to obtain a well-formed pruned  $p$ -mobile. Let  $\gamma \in \widehat{\mathcal{Q}}_{pa_1-d, pa_2+d}^{(p)}$ , and let  $\tau$  be the middle-part of  $\gamma$ . We construct  $\gamma' \in \widehat{\mathcal{B}}_{pa_1, pa_2}^{(p)}$  as follows. Note that  $v_2$  has a dark square neighbour  $b$  (along the path from  $v_2$  to  $v_1$ ) and has otherwise  $(p - 1)a_2 + d - 1$  white neighbours. Let  $w_0, \dots, w_{d-1}$  be the  $d$  next neighbour after  $b$  in counter-clockwise order around  $v_2$ , and let  $r_0, \dots, r_{d-1}$  be the mobiles (in  $\mathcal{R}_p$ ) hanging from  $w_0, \dots, w_{d-1}$ . According to Lemma 4, the pair  $(\tau, r_0)$  corresponds to some pair  $(i, \tau')$ , where  $1 \leq i \leq p - 1$  and  $\tau' \in \mathcal{K}_p$ . If we replace the middle-part  $\tau$  by  $\tau'$  and take out the edge  $\{v_2, w_0\}$  and the mobile  $r_0$ , then transfer  $r_1, \dots, r_{d-1}$  from  $v_2$  to  $v_1$ , we obtain some  $\gamma' \in \widehat{\mathcal{B}}_{pa_1, pa_2}^{(p)}$ . We associate to  $\gamma$  the pair  $(i, \gamma')$ . The inverse process is easy to describe, so we obtain a bijection between  $\widehat{\mathcal{Q}}_{pa_1-d, pa_2+d}^{(p)}$  and  $(p - 1) \cdot \widehat{\mathcal{B}}_{pa_1, pa_2}^{(p)}$ .  $\square$

Denote by  $\mathcal{Q}_{pa_1-d_1, pa_2+d, pa_3, \dots, pa_r}$  the family of quasi  $p$ -constellations where the marked light faces are of degrees  $pa_1 - d, pa_2 + d, pa_3, \dots, pa_r$ . As a corollary of Lemma 12 (the additional factors correspond to the number of ways to place the big buds at the pruned marked vertices), we obtain

$$\binom{pa_1-1}{a_1} \binom{pa_2-1}{a_2} \mathcal{Q}_{pa_1-d, pa_2+d}^{(p)} \simeq (p-1) \cdot \binom{pa_1-d-1}{a_1-1} \binom{pa_2+d-1}{a_2} \mathcal{B}_{pa_1, pa_2}^{(p)},$$

and very similarly (since the isomorphism of Lemma 12 preserves light square

vertex degrees):

$$\begin{aligned} & \binom{pa_1 - 1}{a_1} \binom{pa_2 - 1}{a_2} \mathcal{Q}_{pa_1-d, pa_2+d, pa_3, \dots, pa_r}^{(p)} \\ & \simeq (p-1) \cdot \binom{pa_1 - d - 1}{a_1 - 1} \binom{pa_2 + d - 1}{a_2} \mathcal{B}_{pa_1, pa_2, pa_3, \dots, pa_r}^{(p)}, \end{aligned}$$

which yields Theorem 7 in the case where at least one of the two non-regular (degree not multiple of  $p$ ) light faces is of degree larger than  $p$ . In the remaining we show the formula of Theorem 7 when the two non-regular light faces are of degree smaller than  $p$ .

**Lemma 13.** *Let  $\mathcal{B}_p$  be the family of  $p$ -mobiles with a marked light square vertex of degree  $p$ , and let  $\mathcal{B}'_p$  be the family of objects from  $\mathcal{B}_p$  where a round vertex is marked. Then, for any  $d \in [1..p-1]$ ,*

$$\mathcal{Q}_{d,p-d}^{(p)} \simeq \mathcal{B}'_p.$$

*In addition, if  $\gamma \in \mathcal{B}'_p$  corresponds to  $\gamma' \in \mathcal{Q}_{d,p-d}^{(p)}$ , then each non-marked light square vertex of degree  $pi$  in  $\gamma$  corresponds to a non-marked light square vertex of degree  $pi$  in  $\gamma'$ .*

*Proof.* A mobile in  $\mathcal{Q}_{d,p-d}^{(p)}$  can be decomposed as follows: two marked light squares  $v_1, v_2$ , their incident rooted  $p$ -mobiles (one for each round neighbour) and the middle-part. Hence we have:

$$\begin{aligned} \mathcal{Q}_{d,p-d}^{(p)} & \simeq \mathcal{R}_p^{d-1} \times \mathcal{H}_p \times \mathcal{R}_p^{p-d-1} \\ & \simeq (p-1) \cdot \mathcal{T}'_p \times \mathcal{R}_p^{p-2} \\ & \simeq (p-1) \cdot \mathcal{R}'_p \times \mathcal{R}_p^{p-2}. \end{aligned}$$

If we now consider an object  $\gamma' \in \mathcal{B}'_p$ , the marked light square vertex (of degree  $p$ ) carries one big bud, and has  $p-1$  white neighbours  $w_1, \dots, w_{p-1}$ . From each white neighbour  $w_i$  hangs a rooted  $p$ -mobile  $r_i$ , and one of these rooted  $p$ -mobiles has a secondary marked round vertex (the secondary marked vertex of  $\gamma'$ ). Thus

$$\mathcal{B}'_p \simeq (p-1) \cdot \mathcal{R}'_p \times \mathcal{R}_p^{p-2},$$

where the factor  $p-1$  is due to the choice of which of the mobiles  $r_1, \dots, r_{p-1}$  carries the secondary marked round vertex.  $\square$

By Lemma 13 we have:

$$p G_{d,p-d}^{(p)} = d(p-d) (G_p^{(p)})',$$

(the additional factors are due to marking a corner in each marked light face), and similarly:

$$p G_{d,p-d,pa_3,\dots,pa_r}^{(p)} = d(p-d) G_{p,pa_3,\dots,pa_r}^{(p)}'.$$

Hence, again the fact that  $G_{d,p-d,pa_3,\dots,pa_r}^{(p)}$  satisfies (3.2) follows from the fact (already proved) that  $G_{p,pa_3,\dots,pa_r}^{(p)}$  satisfies (3.2). This concludes the proof of Theorem 7.

# Chapter 4

## A bijection for simple maps

### 4.1 Introduction

In this chapter we focus on *simple planar maps* (planar maps without loops nor multiple edges). This family of planar maps has, quite surprisingly, not been considered until fairly recently. This is probably due to the fact that loops and multiple edges are typically allowed in studies about planar maps, whereas they are usually forbidden in studies about planar graphs. At any rate, the first result about simple maps was an exact algebraic expression given in [8] (using a non-bijective substitution approach) for the generating function  $M(z)$  of rooted simple maps counted by the number of edges (a planar map is said *rooted* if it has a marked directed edge with the outer face on its right). Such generating functions expressions can be given in several forms; and recently Marc Noy [53] found a nice simplified form for  $M(z)$ :

$$M(z) = \frac{zB(z)}{1 - zB(z)}, \quad (4.1)$$

where  $B(z) = 1 + \sum_{n \geq 1} \frac{3 \cdot 2^{n-1}}{(n+2)(n+1)} \binom{2n}{n} z^n$  is the generating function of rooted bipartite maps counted by edges (including the one-vertex map). By a classical construction, rooted bipartite maps are in bijection with rooted *eulerian triangulations* (an eulerian triangulation is a planar map with triangular faces of two types, dark or light, such that the outer face is dark and each edge is incident to both a light and a dark face); and each edge of the bipartite map corresponds to a dark face of the associated eulerian triangulation. Thus  $B(z)$  is also the generating function of rooted eulerian triangulations counted by dark faces.

The identity (4.1) can be reformulated by introducing the generating function  $C(z)$  of *outer-triangular simple maps* (simple maps such that the outer face is a triangle) counted by edges. Indeed, as explained in Sec-

tion 4.3.1, it is easy to see that

$$M(z) = \frac{z(1 + C(z)/z^2)}{1 - z(1 + C(z)/z^2)}.$$

Hence (4.1) is equivalent to

$$\begin{aligned} C(z) &= z^2(B(z) - 1) \\ &= \sum_{n \geq 1} \frac{3 \cdot 2^{n-1}}{(n+2)(n+1)} \binom{2n}{n} z^{n+2}. \end{aligned} \quad (4.2)$$

We will prove this identity (and a refinement of it taking into account the number of vertices), by giving a bijection between outer-triangular simple maps with  $n + 2$  edges and eulerian triangulation with  $n$  dark triangles, followed by a bijection between eulerian triangulation with  $n$  dark triangles and some oriented plane trees. More precisely, we define an *oriented binary tree* as a plane tree with vertices of degree 1 (called *leaves*) or 3 (called *inner nodes*), where edges incident to leaves (called *legs*) are oriented toward the leaf and other edges (called *inner edges*) are oriented arbitrarily. An inner node whose 3 incident edges are all outgoing is called a *source*. We can now state our main result.

**Theorem 16.** *For  $n \geq 1$ , outer-triangular simple maps with  $n + 2$  edges are in bijection – via eulerian triangulations with  $n$  dark faces – with oriented binary trees with  $n + 2$  leaves. In addition, the inner faces of an outer-triangular simple map correspond to the sources of the associated oriented binary tree.*

As explained in Section 4.3.1, the bijection of Theorem 16 also gives an  $(n + 2)$ -to-3 correspondence between *rooted* outer-triangular simple maps with  $n + 2$  edges and *rooted* oriented binary trees with  $n + 2$  leaves. This proves (4.2) since there are clearly  $\frac{2^{n-1}}{n+1} \binom{2n}{n}$  rooted oriented binary trees with  $n + 2$  leaves. The bijection is illustrated in Figure 4.1 and described in Section 4.2. Both steps of the bijection rely crucially on the existence of certain *canonical orientations*, introduced by Bernardi and Fusy, in [10] for outer-triangular simple maps and in [11] for eulerian triangulations. In the first step of the bijection, the canonical orientation is used to define some local operations which transform the outer-triangular simple map into an eulerian triangulation; see Figure 4.3. We then apply a special case of a bijection by Bousquet-Mélou and Schaeffer [15] (reformulated in [11] in terms of canonical orientations) in order to obtain an oriented binary tree; see Figure 4.7.

Our bijection keeps track of the number of edges and faces, hence also vertices by the Euler formula. We then use classical generating function techniques (and the easy correspondence between embeddings in the plane and on the sphere) to obtain the following asymptotic counting result:

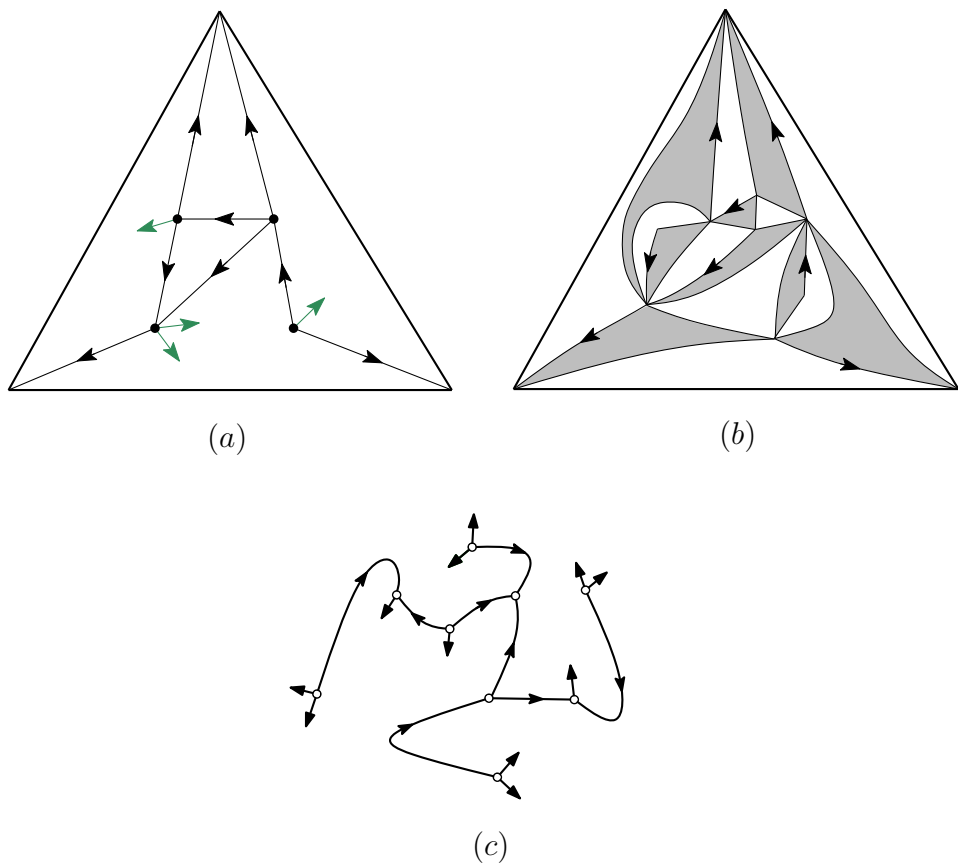


Figure 4.1: (a) An outer-triangular simple map with 11 edges and 5 inner faces, endowed with its canonical orientation, (b) the corresponding eulerian triangulation with 9 dark faces (including the outer one) endowed with its canonical orientation, and (c) the corresponding oriented binary tree with 11 leaves and 5 sources.

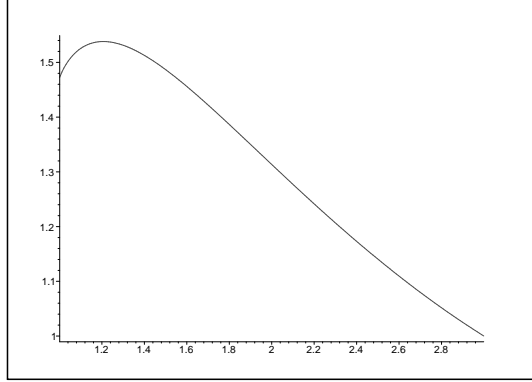


Figure 4.2: The plot of  $b(\mu)$ , which is the growth rate of the expected number of embeddings of random planar graphs with  $n$  vertices and  $\lfloor \mu n \rfloor$  edges.

**Theorem 17.** *Let  $g_{n,m}$  be the number of unrooted, vertex-labeled, simple maps embedded on the sphere, with  $n$  vertices and  $m$  edges. Then, for each fixed  $\mu \in (1, 3)$ , there are analytically computable positive constants  $c(\mu)$  and  $\gamma(\mu)$  such that*

$$g_{n,\lfloor \mu n \rfloor} \sim n! c(\mu) \cdot \gamma(\mu)^n n^{-4}.$$

An asymptotic estimate of the same form—with some other constants  $\tilde{c}(\mu)$  and  $\tilde{\gamma}(\mu)$ —has been proved by Giménez and Noy [39] for the number  $\tilde{g}_{n,m}$  of connected vertex-labeled planar graphs with  $n$  vertices and  $m$  edges. Since the expected number  $E_{n,m}$  of embeddings on the sphere of a (uniformly) random connected planar graph with  $n$  vertices and  $m$  edges is  $g_{n,m}/\tilde{g}_{n,m}$ , we get:

**Corollary 18.** *For each fixed  $\mu \in (1, 3)$  there are analytically computable constants  $a(\mu)$  and  $b(\mu)$  such that the expected number of embeddings satisfies:*

$$E_{n,\lfloor \mu n \rfloor} \sim a(\mu) b(\mu)^n.$$

The plot of  $b(\mu)$  is shown in Figure 4.2. As expected, when  $\mu \rightarrow 1$ ,  $b(\mu)$  tends to  $4/e$  (indeed the number of labeled plane trees with  $n$  vertices is  $\frac{n!}{n(2n-2)} \binom{2n-2}{n-1} = \Theta(n! 4^n n^{-5/2})$ , while the number of Cayley trees with  $n$  vertices is  $n^{n-2} = \Theta(n! e^n n^{-5/2})$ ), and when  $\mu \rightarrow 3$ ,  $b(\mu)$  tends to 1 (indeed, at the limit  $\mu \rightarrow 3$ , we have planar triangulations, which have an essentially unique embedding by Whitney’s theorem). Interestingly  $b(\mu)$  does not decrease from  $4/e \approx 1.4715$  to 1, but instead starts increasing (with a positive slope equal to  $4/e$  at  $\mu = 1$ ) up to the critical value  $\mu_0 \approx 1.2065$ , where  $b(\mu_0) \approx 1.5381$ , after which  $b(\mu)$  decreases (on the interval  $[\mu_0, 3]$ ) toward 1.

As a byproduct of our bijection we also obtain efficient random samplers for rooted simple maps according to the number of edges (univariate), and according to the number of vertices and the number of edges (bivariate). While the univariate sampler is elementary (see Section 4.4), the bivariate sampler relies on *Boltzmann sampling*, as was the case for the random sampler for planar graphs given in [37]. However the sampler for simple maps given here is much simpler to describe and implement. In particular, we can sample *exactly at the singularity*, which was not the case for the sampler for planar graphs in [37] (due to an extensive use of rejection).

**Bijective link with 1342-avoiding permutations.** As observed by Marc Noy [53], the expression  $M(z) = (zB(z))/(1 - zB(z))$  coincides with the expression discovered and proved bijectively by Bona [13] for the generating function of 1342-avoiding permutations. Thus, Theorem 16, combined with Bona’s proof, yields a bijection between 1342-avoiding permutations of size  $n$  and rooted simple maps with  $n$  edges.

**Relation with existing bijections.** There is now a rich literature on bijections for various families of planar maps, with some very general constructions [56, 57, 19, 11, 4] at hand. These bijections typically associate a tree (decorated in a certain way) to a map with specific constraints (e.g., no loops, no multiple edges, a restriction on the face-degrees). In particular, a different bijection for outer-triangular simple maps was given in [10], relying on the same canonical orientations as the ones used here, but not going through eulerian triangulations. The bijection in [10] is more precise than the one of Theorem 16 in the sense that the corresponding decorated trees, called *mobiles*, keep track of the face-degree distribution of the outer-triangular simple maps. However, the price to pay is that the mobiles in [10] are significantly more complicated than the oriented binary trees appearing in Theorem 16. It suggests that, when forgetting the precise face-degrees (and recording just the number of edges and faces), the mobiles in [10] should simplify into oriented binary trees. Such a simplification does not seem easy to define on tree-structures. Instead the strategy adopted here is to use another family of maps (eulerian triangulations) as intermediate structures used to simplify the output tree-structure. So the simplification occurs conveniently (and quite mysteriously) at the “map-level” rather than at the “tree-level”<sup>1</sup>.

---

<sup>1</sup>In a similar spirit, a recent bijection due to Ambjørn and Budd [6] makes it possible to simplify the shape of the tree containing the information on the distance-profile of a map, using quadrangulations as intermediate structures.

## 4.2 The bijection

### 4.2.1 Canonical orientations for outer-triangular simple maps.

An *orientation with buds* of a planar map is an orientation of its edges, with some additional outgoing half-edges called *buds* attached to corners of the map. A *3-orientation with buds* of an outer-triangular simple map is an orientation of the inner edges (the outer edges are left unoriented) with buds, such that each outer vertex has outdegree 0, each inner vertex has outdegree 3 (buds contribute to the outdegree), and each inner face of degree  $d + 3$  has  $d$  incident buds. The following holds:

**Theorem 19** ([10]). *A planar map  $G$  with a triangular outer face admits a 3-orientation with buds iff  $G$  is simple. Moreover each outer-triangular plane  $G$  graph has a unique 3-orientation with buds satisfying the following properties (see Figure 1.a):*

- *Outer-accessibility: from any vertex, there is an oriented path toward the outer boundary.*
- *Minimality: there is no clockwise circuit.*
- *Local property at buds: the next half-edge after each bud in clockwise order around the incident vertex is either a bud or an outgoing edge. In particular, if a vertex carries two buds, they must be adjacent.*

*This orientation is called the canonical 3-orientation with buds of  $G$ .*

In an outer-triangular simple map endowed with its canonical 3-orientation with buds, an inner vertex with  $i$  ( $0 \leq i \leq 2$ ) buds is called a vertex of *type  $i$* .

### 4.2.2 Canonical orientations for eulerian triangulations.

A *1-orientation* of an eulerian triangulation is a partial orientation without buds such that outer edges are unoriented, each outer vertex has outdegree 0, each inner vertex has outdegree 1, and each inner dark triangle has one edge oriented counterclockwise while the other two are unoriented. The following holds:

**Theorem 20** ([15, 11]). *Each eulerian triangulation has a unique 1-orientation with no circuit (this is easily seen to be equivalent to an outer-accessibility property, i.e., the existence of an oriented path to the outer boundary from each inner vertex). We call it the canonical 1-orientation.*

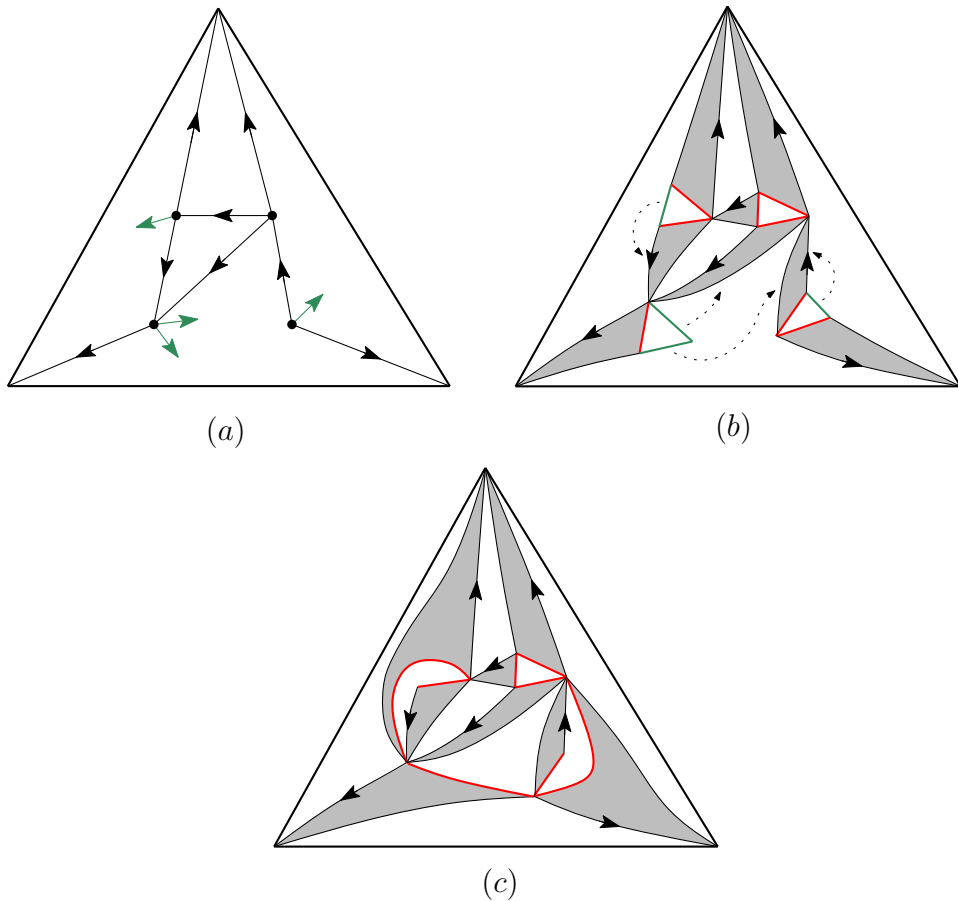


Figure 4.3: (a) An outer-triangular simple map endowed with its canonical 3-orientation with buds, (b) after inflation and (c) after merging, the resulting eulerian triangulation endowed with its canonical 1-orientation.

In an eulerian triangulation endowed with its canonical 1-orientation, we call *base-edge* (drawn in red on figures) of a dark inner triangle  $f$  the edge following the unique oriented edge of  $f$  in clockwise order around  $f$ . A light triangle with  $i \in \{0, 1, 2, 3\}$  incident non-base edges is called a light triangle of type  $i$ .

#### 4.2.3 Bijection between outer-triangular simple maps and eulerian triangulations.

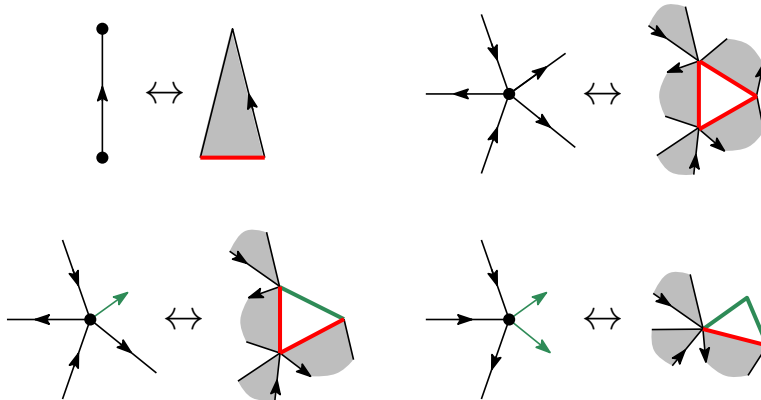
We use the canonical orientations to derive the main bijective result of this chapter:

**Theorem 21.** *There is a bijection between outer-triangular simple maps*

and eulerian triangulations. Each inner edge of the simple map corresponds to an inner dark triangle. Each inner vertex of type  $i \in \{0, 1, 2\}$  of the simple map corresponds to a light triangle of type  $i$ , and each inner face corresponds to a light triangle of type 3.

*Proof.* Let  $C$  be an outer-triangular simple map endowed with its canonical 3-orientation with buds. Inner edges and inner vertices will be inflated in the following way:

- Each inner edge becomes a dark triangle whose basis is the origin of the edge,
- each inner vertex becomes a light triangle whose edges come from its former outgoing half-edges (including buds).



After inflation, former inner faces of degree  $d + 3$  ( $d \geq 0$ ) have now degree  $2d + 3$  (the  $d$  incident buds have turned into edges). Considering edges coming from buds as opening parenthesis, and remaining edges as closing parenthesis, one can form a clockwise parenthesis system leaving 3 edges unmatched, see Figure 4.4. Hence, after merging the matched edges, the 3 unmatched edges form a light triangle. This ensures that each face is a triangle in the resulting map. Moreover, the edges created by the inflation are incident to a dark and a light faces, except for edges coming from buds, which are incident to two light faces. After merging, these edges are necessarily incident to a dark face as well. Therefore the triangulation is properly bicolored and is an eulerian triangulation (the outer face, which is left unchanged, is colored dark).

The resulting eulerian triangulation itself is endowed with an orientation (without buds). After inflation, each inner dark triangle carries one counterclockwise oriented edge, and the vertex at the right extremity of the base-edge has outdegree 1. Other vertices (coming from buds) have no outgoing edge before merging. The merging ensures that these vertices are

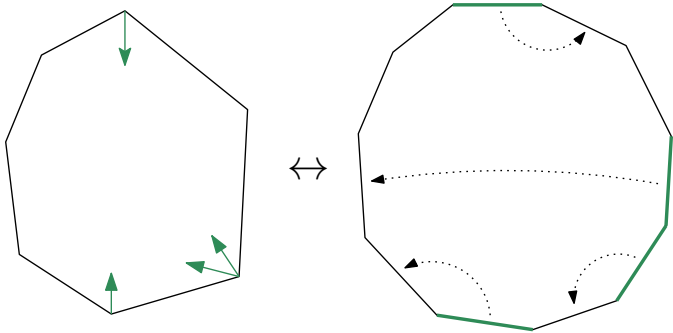


Figure 4.4: Generic situation in a face of degree  $4 + 3$ .

merged with vertices of outdegree 1, without creating any circuit, and preserving oriented paths from inner vertices to the outer boundary. Therefore we obtain the canonical 1-orientation for eulerian triangulations.

Conversely, starting from an eulerian triangulation endowed with its canonical 1-orientation, each transformation can be easily reversed. Edges that have been merged are exactly the non-base edges in light triangles of type 1 or 2. Let a *dark peak* incident to a vertex be the two consecutive edges of a single dark triangle incident to this vertex. Notice that, in clockwise order around a vertex, a dark peak can be either black-black, red-black or black-red. Moreover, there is exactly one red-black peak around a vertex since each vertex has outdegree 1.

In a first step, at each light triangle of type 1 or 2, untie a black-red dark peak as in Figure 4.5 (these operations have to be thought as done *simultaneously* at each light triangle of type 1 or 2):

In the resulting *untied* map, light triangles of type 3 have become light faces of degree  $2d + 3$  (for some  $d \geq 0$ ), while other triangles are left unchanged. It is easy to check that the light triangles of type 0, 1 or 2 are vertex-disjoint (this follows from the fact that, in a 1-orientation, around any inner vertex  $v$ , there is just one corner incident to  $v$  in a light face such that the clockwise-most edge of the corner is a base-edge). Hence light triangles of type 0, 1 or 2 can be contracted independently into vertices of the same type, and inner dark triangles into oriented edges, which yields an outer-triangular simple map endowed with a 3-orientation with buds.

Untied edges were all unoriented, thus accessibility is preserved in the untied map for any vertex but for those duplicated in the separation process. When dark triangles are contracted, those vertices are merged with the ones having an outgoing edge, which guarantees outer-accessibility. The local property at buds is also readily checked to be satisfied (see Figure 4.5). It remains to show that the orientation is minimal. Suppose it is not. Then by outer-accessibility, it must have a clockwise cycle  $C$  that such that any

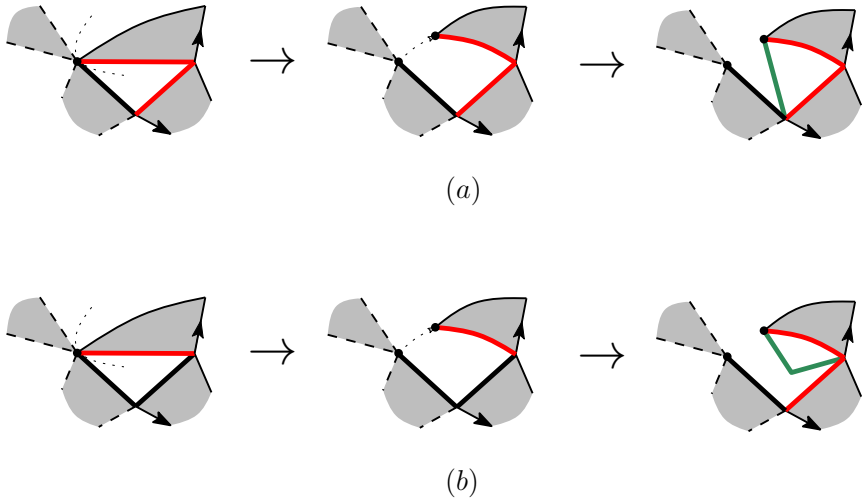


Figure 4.5: Separation in (a) a light triangle of type 1, and (b) a light triangle of type 2.

edge incident to  $C$  from the inside of  $C$  is directed out of  $C$ . Clearly such a cycle  $C$  had to be already present in the untied map ( $C$  has not been affected by the contraction step), and also before the separation process, a contradiction. Therefore the output is an outer-triangular simple map endowed with its canonical 3-orientation with buds.  $\square$

#### 4.2.4 Bijection with oriented binary trees.

In this subsection, we follow the reformulation given in [11] of the bijection for eulerian triangulations due to Bousquet-Mélou and Schaeffer [15] (their construction applies actually to more general objects called constellations). We then make some simplifications.

Starting from an eulerian triangulation  $T$ , where vertices are drawn as circles, one obtains a binary tree as follows:

- Endow  $T$  with its canonical 1-orientation.
- Put a dark square vertex in each inner dark triangle, and a light square vertex in each light triangle.
- Apply the local rule indicated in Figure 4.6 to each edge of  $T$ .
- Remove every edge of  $T$ , and the 3 outer vertices.

**Claim 22** ([15, 11]). *The above construction is a bijection between eulerian triangulations and unrooted binary trees with*

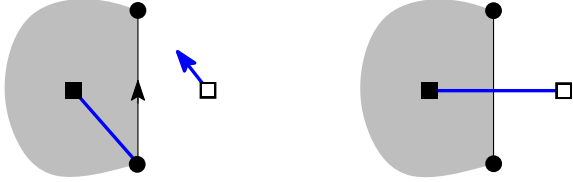


Figure 4.6: Local rule of the bijection between eulerian triangulations and binary trees.

- *two types of leaves:* round leaves and (*extremities of*) buds,
- *two types of inner nodes:* dark squares (*adjacent to one round leaf and two light squares*) and light squares (*adjacent to buds and dark squares*),
- *and such that each dark square is adjacent to two light squares and one round leaf.*

*Each inner dark triangle corresponds to a dark square of the binary tree, and each light triangle to a light square. Each inner edge corresponds to an edge (excluding buds) of the binary tree, and each inner vertex to a round leaf.*

This kind of binary tree can be further simplified thanks to the particular neighborhood of each dark square: one can replace each dark square and its adjacent round leaf by an oriented edge as represented in Figure 4.8. After simplification, one obtains a binary tree with only light square inner nodes and whose leaves are the former buds, hence an oriented binary tree. The full process is illustrated in Figure 4.7. This gives the following result, which together with Theorem 21 implies Theorem 16.

**Theorem 23** ([15] reformulated in [11]). *There is a bijection between eulerian triangulations and oriented binary trees. Each inner dark triangle corresponds to an inner edge of the binary tree. Each light triangle of type  $0 \leq i \leq 3$  corresponds to an inner node of outdegree  $i$ .*

## 4.3 Counting results

### 4.3.1 Exact counting.

Let  $C$  be an outer-triangular simple map,  $E$  the corresponding eulerian triangulation and  $T$  the corresponding oriented binary tree. Looking at the local rules (see Figures 4.6 and 4.8), one sees that each inner dark face of  $E$  yields an oriented inner edge and a leaf in  $T$  —these are considered as

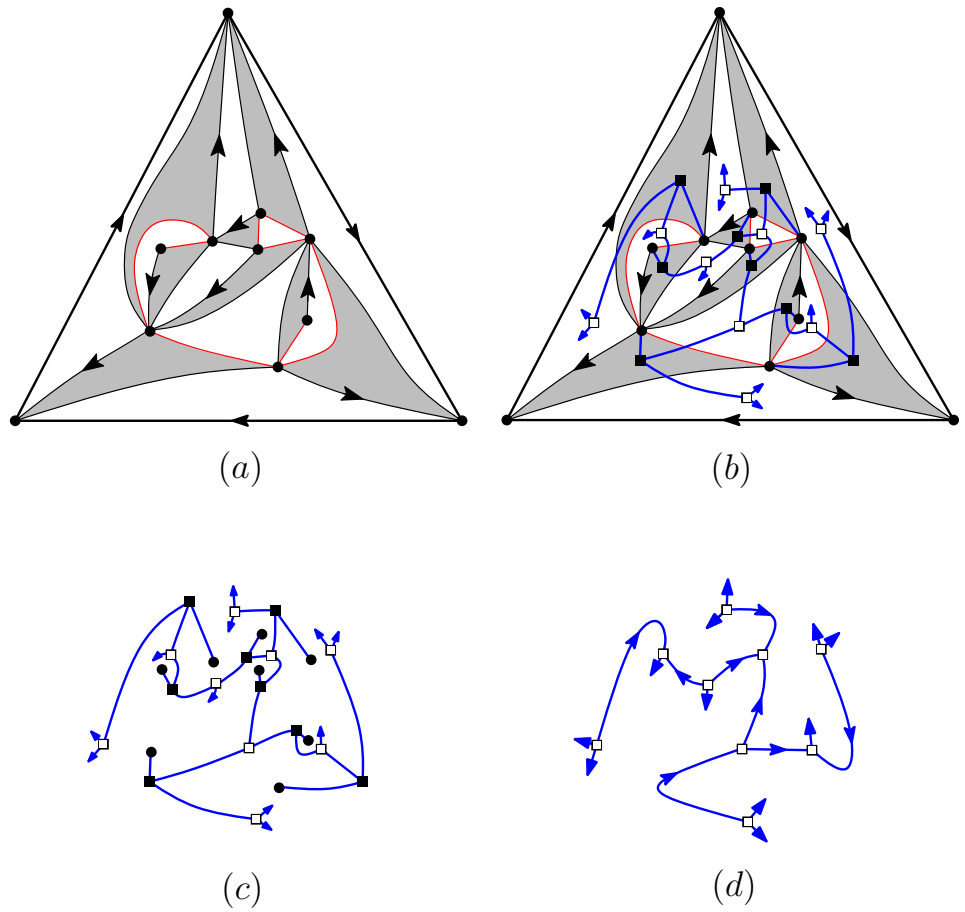


Figure 4.7: (a) An eulerian triangulation endowed with its canonical 1-orientation, (b) applying the local rule, (c) the resulting bicolored binary tree and (d) the simplified oriented binary tree.

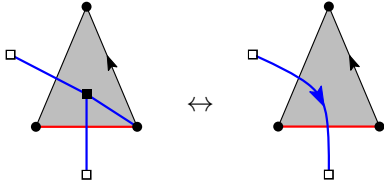


Figure 4.8: Simplification of the binary trees.

*matched*—, and each of the 3 outer edges of  $E$  yields a leaf (no inner edge) in  $T$ . These 3 special leaves of  $T$  are called *exposed*, the other ones (non-exposed) being matched with the inner edges of  $T$ . The 3 exposed leaves naturally correspond to each of the 3 outer edges of  $E$ , which are also the 3 outer edges of  $C$ . Hence, by Theorem 16, rooted outer-triangular simple maps with  $n$  edges and  $i$  inner faces ( $n - i - 2$  inner vertices) are in bijection with oriented binary trees rooted at an exposed leaf, with  $n$  leaves and  $i$  sources ( $n - i - 2$  non-source inner nodes).

Let  $\mathcal{U}$  be the family of oriented binary trees rooted at a leaf, and let  $\mathcal{V}$  be the family of oriented binary trees rooted at a leaf, with the edge incident to the root-leaf reversed (thus the inner node adjacent to the leaf is never a source, moreover the root-leaf is not considered as a source). Let  $U \equiv U(x, z)$  (resp.  $V \equiv V(x, z)$ ) be the generating function of  $\mathcal{U}$  (resp.  $\mathcal{V}$ ) where  $x$  marks the number of non-source inner nodes and  $z$  marks the number of non-root leaves. By a classical decomposition at the root (into a left subtree and a right subtree),  $U$  and  $V$  are given by

$$\begin{cases} U = (z + V)^2 + 2xU(z + V) + xU^2, \\ V = x(z + U + V)^2. \end{cases} \quad (4.3)$$

Notice that, for  $x = 1$ , by symmetry we have  $U = V$  and thus  $U = (z + 2U)^2$ , which gives  $U = \sum_{n \geq 1} \frac{2^{n-1}}{n+1} \binom{2n}{n} z^{n+1}$ .

**Proposition 24.** *Let  $\mathcal{C}$  be the family of rooted outer-triangular simple maps, and let  $C \equiv C(x, z)$  be the generating function of  $\mathcal{C}$  where  $x$  marks the number of inner vertices (all vertices except the 3 outer ones) and  $z$  marks the number of edges. Then we have the two following expressions:*

$$\frac{\partial C}{\partial z} = 3U, \quad C = zU - UV, \quad (4.4)$$

where  $U$  and  $V$  are given by (4.3).

*Proof.* The first expression is just a consequence of the fact that among the  $n$  leaves of an oriented binary tree, 3 are exposed, so that  $C = 3 \int U dz$ . The second expression follows from the property that, in an oriented binary tree, the non-exposed leaves are matched with the inner edges, and from the fact

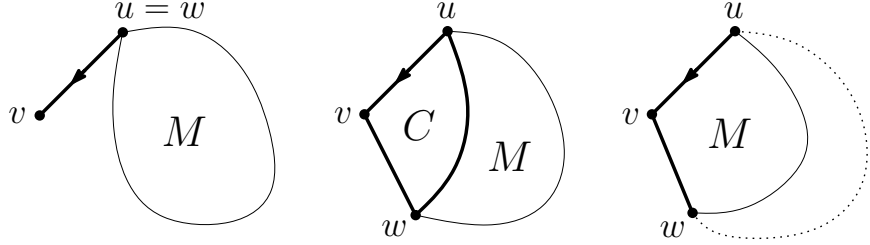


Figure 4.9: Decomposition of a simple map along the root: 3 cases.

that  $UV$  is clearly the generating function of oriented binary trees with a marked inner edge. Thus, since  $zU$  is the generating function of oriented binary trees rooted at a leaf, we conclude that  $zU - UV$  is the generating function of oriented binary trees rooted at an exposed leaf.  $\square$

Let  $\mathcal{M}$  be the family of rooted simple maps (with at least one edge), and let  $M \equiv M(x, z)$  be the generating function of  $\mathcal{M}$ , where  $x$  marks the number of vertices and  $z$  marks the number of edges. We can now easily express  $M(x, z)$  from  $C(x, z)$ . Consider a rooted simple map  $\gamma$ , call  $u$  the origin of the root-edge,  $v$  the end of the root-edge, and  $w$  the next vertex after  $v$  in counterclockwise order around the root-face. Three cases can happen, as shown in Figure 4.9:

1.  $u = w$ , i.e., the root edge is a pending leg (with  $v$  of degree 1), and there is a rooted simple map  $\gamma'$  (possibly reduced to a vertex) hanging at  $u$ ;
2.  $u$  and  $w$  are not equal but are adjacent in  $\gamma$ , then  $\gamma$  naturally decomposes (cutting along the edge  $\{u, w\}$ ) into a map in  $\mathcal{C}$  and a map in  $\mathcal{M}$ ;
3.  $u$  and  $w$  are not equal nor adjacent, in which case  $\gamma$  is uniquely obtained from some  $\gamma' \in \mathcal{C}$  by deleting the outer edge that follows the root-edge in a clockwise walk around the outer face.

This yields

$$\begin{aligned} M &= xz(x + M) + xz^{-1}CM + x^3z^{-1}C \\ \Rightarrow M &= \frac{x^2z(1+xC/z^2)}{1-xz(1+C/z^2)}, \end{aligned} \tag{4.5}$$

and by Proposition 24 we obtain:

**Proposition 25.** *The generating function  $M \equiv M(x, z)$  of rooted simple maps by the number of vertices and the number of edges is expressed as*

$$M = \frac{x^2z + x^3U \cdot (1 - V/z)}{1 - xz - xU \cdot (1 - V/z)}, \tag{4.6}$$

where  $U$  and  $V$  are given by (4.3).

### 4.3.2 Asymptotic counting.

This section gives asymptotic estimates for the number of rooted simple maps (and labeled connected graphs embedded on the sphere), which follow rather directly from the expressions in Section 4.3.1 and the application of suitable lemmas from singularity analysis (taken from [31], the terminology used here is taken from [24, Sec. 2]). For a bivariate series  $f(x, z)$ , for each  $x > 0$ , let  $\rho(x)$  be the radius of convergence of  $z \rightarrow f(x, z)$ . Then  $\rho(x)$  is called the *singularity function* of  $f(x, z)$  with respect to  $z$ . A point  $(x_0, z_0)$  such that  $z_0 = \rho(x_0)$  is called a *singular point* of  $f(x, z)$ . Let  $(x_0, z_0)$  be a singular point of  $f(x, z)$  such that  $\rho'(x_0) \neq 0$  and  $\rho(x)$  is analytically continuable to a complex neighborhood of  $x_0$ . Then, for  $\alpha$  a positive half-integer,  $f(x, z)$  is said to admit a *singular expansion* of order  $\alpha$  around  $(x_0, z_0)$  with leading variable  $z$ , if there exist functions  $g(x, z)$  and  $h(x, z)$  analytic around  $(x_0, z_0)$ , with  $h(x_0, z_0) \neq 0$ , such that, in a complex neighborhood of  $(x_0, z_0)$ ,

$$f(x, z) = g(x, z) + h(x, z) \cdot (1 - z/\rho(x))^\alpha.$$

The singular expansion is called *strong* if  $f(x, z)$  is analytically continuable to a complex domain of the form  $\Omega = \{(x, z) \mid |x| \leq x_0 + \delta, |z| \leq z_0 + \delta\} \setminus \{1 - z/\rho(x) \in \mathbf{R}_{\leq 0}\}$  for some  $\delta > 0$ . It can be shown (see [31]) that then  $f(x, z)$  also has a strong singular expansion at  $(x_0, z_0)$  with leading variable  $x$ , hence it is not necessary to mention which variable is taken as the leading variable.

A first task for us is to determine the singular points of  $U(x, z)$ . It is easy to see that the singular points are the same for  $U(x, z)$  as for  $V(x, z)$ . We have  $U = x(z+U+V)^2 + (1-x)(z+V)^2 = V + (1-x)(z+V)^2$ , so that  $V = x(z+2V+(1-x)(z+V)^2)^2$ , so we have an explicit polynomial equation of the form  $H(x, z, V) = 0$ , satisfied by  $V \equiv V(x, z)$ . Hence we classically have to look for solutions in  $\{x, z\}$  of the system  $\{H(x, z, V), \frac{\partial H}{\partial V}(x, z, V) = 0\}$ . With the help of a computer algebra system (to take the resultant of the two equations according to  $V$ ), we find and check that the singular points cover the curve parametrized by

$$\begin{cases} x = \frac{(u+1)(u-1)^3}{u^3(u-2)} \\ z = \frac{(2u+1)(u-2)u^3}{4(u+1)(u-1)} \end{cases} \quad \text{over } u \in (0, 1). \quad (4.7)$$

**Lemma 26.** *The generating functions  $U(x, z)$  and  $V(x, z)$  have a strong singular expansion of order  $1/2$  around any of their singular points, which are parametrized by (4.7).*

*Proof.* There are general conditions, given in [30], under which a bivariate (more generally a multivariate) generating function  $f(x, z)$  that appears in a positive equation-system has a strong singular expansion of order  $1/2$  at any singular point  $(x_0, z_0)$ . These conditions (irreducibility, aperiodicity,...) are readily checked to be satisfied by (4.3).  $\square$

We will use the following lemma from [31] (see also [24, Sec.2]):

**Lemma 27.** *Let  $f(x, z)$  be a bivariate generating function that admits a strong singular expansion of order  $\alpha$  at a singular point  $(x_0, z_0)$ . Then the generating function  $\int f(x, z)dz$  admits a strong singular expansion of order  $\alpha + 1$  at  $(x_0, z_0)$ .*

**Lemma 28.** *The generating functions  $C(x, z)$  and  $M(x, z)$  have the same singular points as  $U(x, z)$ . In addition, at any singular point  $(x_0, z_0)$ ,  $C(x, z)$  and  $M(x, z)$  admit a strong singular expansion of order  $3/2$ .*

*Proof.* For  $C(x, z)$  it is a direct consequence of  $C = \int U dz$  and of Lemmas 26 and 27. We now consider  $M(x, z)$ . We have (where the symbol  $\preceq$  means “coefficient-wise smaller”):

$$x^3 C(x, z) \preceq M(x, z) \preceq x^3 C(x, z)/z^2,$$

the lower bound is due to  $\mathcal{C}$  being a subfamily of  $\mathcal{M}$ , and the upper bound is due to the fact that, for an object in  $\mathcal{M}$ , the operation of adding a vertex of degree 2 in the outer face connected to the two extremities of the root-edge yields an object in  $\mathcal{C}$ . These bounds and the fact that  $M(x, z)$  has a specific rational expression (4.5) in terms of  $C(x, z)$ ,  $x$  and  $z$  easily imply that  $M(x, z)$  “inherits” from  $C(x, z)$  the property of having a strong singular expansion of order  $3/2$  at  $(x_0, z_0)$ .  $\square$

We now turn our attention to embeddings on the sphere. Let  $g_{i,n}$  be the number of connected graphs embedded on the sphere with  $n$  edges and  $i$  vertices, the vertices having distinct labels in  $[1..i]$ . And let  $G(x, z) = \sum_{i,n} \frac{1}{i!} g_{i,n} x^i z^n$  be the corresponding (exponential) generating function. Let  $m_{i,n}$  be the number of rooted simple maps with  $i$  vertices and  $n$  edges. There are  $i!$  distinct ways to label the vertices of a rooted simple map with  $i$  vertices; and there are  $2n$  ways to root a connected labeled graph embedded on the sphere (one takes the face on the right of the root-edge as the outer face). Since these are two ways to construct the same objects (rooted labeled) we have  $i! m_{i,n} = 2n g_{i,n}$ , hence

$$2z \frac{\partial G}{\partial z}(x, z) = M(x, z). \quad (4.8)$$

Hence, by Lemmas 27 and 28 we obtain:

**Lemma 29.** *The generating function  $G(x, z)$  has the same singular points as  $U(x, z)$ . In addition, at any singular point  $(x_0, z_0)$ ,  $G(x, z)$  admits a strong singular expansion of order  $5/2$ .*

From this we can obtain asymptotic estimates for the coefficients of  $G(x, z)$  (as well as  $C(x, z)$  and  $M(x, z)$ ) using the following transfer lemma [34]:

**Lemma 30.** *Let  $f(x, z)$  be a generating function that admits a strong singular expansion of order  $\alpha$  at any singular point, and let  $\rho(z)$  be the singularity function of  $f(x, z)$  with respect to  $x$ . Then for any  $z_0 > 0$  (in particular  $z_0 = 1$ ) the coefficient  $f_n(z_0) = [x^n]f(x, z_0)$  satisfies*

$$f_n(z_0) \sim c n^{-\alpha-1} \gamma^n.$$

where  $\gamma = 1/\rho(z_0)$  and  $c$  is some (analytically computable) positive constant.

Assume that  $\mu(z) := -z\rho'(z)/\rho(z)$  is strictly increasing, and define  $a = \lim_{z \rightarrow 0} \mu(z)$  and  $b = \lim_{z \rightarrow +\infty} \mu(z)$ . For any fixed  $\mu \in (a, b)$  let  $z_0$  be the positive value where  $\mu(z_0) = \mu$  and let  $\gamma(\mu) = 1/\rho(z_0)$ . Then there is a positive (analytically computable) constant  $c(\mu)$  such that the coefficients  $f_{n,m} := [x^n z^m]f(x, z)$  satisfy

$$f_{n,\lfloor \mu n \rfloor} \sim c(\mu) n^{-\alpha-3/2} \gamma(\mu)^n \quad \text{when } n \rightarrow \infty.$$

In our case (singularity function of  $U(x, z)$ ), we easily check (with a computer algebra system) that  $a = 1$  and  $b = 3$ . Together with Lemma 29, the second part of Lemma 30 yields Theorem 17; while the first part ensures for instance that the number  $c_n$  of connected graphs embedded on the sphere and having  $n$  (labeled) vertices satisfies asymptotically  $c_n \sim n! c n^{-7/2} \gamma^n$ , where  $c$  and  $\gamma$  are computable,  $\gamma \approx 34.2672$ . This is to be compared with the asymptotic number  $\tilde{c}_n$  of connected *planar graphs* with  $n$  vertices given in [39], which is asymptotically  $\tilde{c}_n \sim n! \tilde{c} n^{-7/2} \tilde{\gamma}^n$ , with  $\tilde{\gamma} \approx 27.2269$ . Hence, the expected number of embeddings on the sphere of a random planar graph with  $n$  (labeled) vertices is asymptotically  $a \cdot b^n$ , with  $b \approx 1.2586$ .

## 4.4 Application to random generation of simple maps

### 4.4.1 Sampling rooted simple maps by edges.

We first give an easy uniform random sampler for the family  $\mathcal{M}_m$  of rooted simple maps with  $m$  edges.

Let  $\mathcal{C}_m$  be the set of rooted outer-triangular simple maps with  $m$  edges. As explained in Section 4.3.1, the bijection of Theorem 16 can be formulated as an  $m$ -to-3 correspondence between  $\mathcal{C}_m$  and the family  $\mathcal{U}_m$  of rooted oriented binary trees with  $m$  leaves. Uniform sampling in  $\mathcal{U}_m$  can classically be done in linear time (generate a rooted binary tree *via* recursive method and flip a coin at each inner edge to choose the orientation). Hence, composing with the bijection of Theorem 16 (seen as an  $m$ -to-3 correspondence) yields a linear-time uniform random sampler for  $\mathcal{C}_m$ .

Now, let  $\tilde{\mathcal{C}}_m \subset \mathcal{C}_m$  be the set of rooted outer-triangular simple maps with  $m$  edges such that the outer vertex opposite to the root-edge has degree 2.

For  $C \in \tilde{\mathcal{C}}_{m+2}$ , let  $\phi(C) \in \mathcal{M}_m$  be the rooted simple map obtained from  $C$  by deleting the outer vertex opposite to the root-edge (and its two incident edges). Clearly,  $\phi$  is a bijection between  $\tilde{\mathcal{C}}_{m+2}$  and  $\mathcal{M}_m$ . Hence a uniform random sampler for  $\mathcal{M}_m$  is obtained by repeatedly calling the sampler for  $\mathcal{C}_{m+2}$  until the generated object  $C$  is in  $\tilde{\mathcal{C}}_{m+2}$ , and then returning  $\phi(C)$ .

**Proposition 31.** *The above procedure yields a uniform random sampler for rooted simple maps with  $m$  edges in expected time  $O(m)$ .*

*Proof.* At each trial the probability of success (of being in  $\tilde{\mathcal{C}}_{m+2}$ ) is  $|\tilde{\mathcal{C}}_{m+2}|/|\mathcal{C}_{m+2}| = |\mathcal{M}_m|/|\mathcal{C}_{m+2}|$ . The expressions of  $C(z)$  and  $M(z)$  yield (using transfer lemmas) asymptotic estimates of the form  $c8^m m^{-5/2}$  for both  $|\mathcal{C}_{m+2}|$  and  $|\mathcal{M}_m|$ . Thus, the probability of success tends to a positive constant as  $m \rightarrow \infty$  (hence is bounded from below uniformly in  $m$ ). Moreover, by an elementary probability identity, the expected complexity of the sampler for  $\mathcal{M}_m$  equals the expected complexity of the sampler for  $\mathcal{C}_{m+2}$  (which is  $O(m)$ ) divided by the probability of success.  $\square$

#### 4.4.2 Sampling rooted simple maps by vertices and edges.

We now explain how to generate rooted simple maps by vertices and edges. Our generator relies on the methodology of Boltzmann sampling [32]. This is similar to the sampler developed for planar graphs in [37], but the sampler described here is much simpler and one can sample *exactly at the singularity*. We denote  $\mathcal{U} = \bigcup_m \mathcal{U}_m$ ,  $\mathcal{C} = \bigcup_m \mathcal{C}_m$ , and  $\tilde{\mathcal{C}} = \bigcup_m \tilde{\mathcal{C}}_m$ . Let  $\Gamma U(x, z)$  be the *Boltzmann sampler* for the class  $\mathcal{U}$  of oriented binary trees according to the number of non-source inner nodes and the number of leaves. As explained in [32], a grammar specification such as (4.3) can be automatically translated into a Boltzmann sampler  $\Gamma U(x, z)$ , such that the complexity of generating a tree  $T \in \mathcal{U}$  is linear in  $m$ . Via the  $m$ -to-3 correspondence between  $\mathcal{U}_m$  and  $\mathcal{C}_m$ ,  $\Gamma U(x, z)$  yields a random generator  $\Gamma C(x, z)$  where each  $C \in \mathcal{C}$  is drawn with probability proportional to  $mx^n z^m$ , where  $n$  is the number of vertices and  $m$  is the number of edges, and the cost is linear in  $m$ .

From this generator  $\Gamma C(x, z)$  we can easily obtain random samplers for rooted plane graphs, either in the form of an *exact-size* or an *approximate-size* random sampler (in the first case, the “target-domain” for the pair  $(\#vertices, \#edges)$  is a singleton  $(n, m)$ , in the second case, the target-domain is of the form  $[n(1-\epsilon), n(1+\epsilon)] \times [m(1-\epsilon), m(1+\epsilon)]$ ). As explained in [32], by appropriately tuning  $x$  and  $z$  in  $\Gamma C(x, z)$ , and using early-abort technique, one can obtain efficient exact- and approximate-size samplers. Indeed, let  $\mu := m/n$  and let  $z_0$  be the value of  $z$  associated to  $\mu$  as explained in the second part of Lemma 30, and let  $x_0$  be the value such that  $(x_0, z_0)$  is a singular point of  $U(x, z)$ . We consider the random sampler that consists in calling  $\Gamma C(x_0, z_0)$  until the generated simple map  $G = (V, E)$  is in  $\tilde{\mathcal{C}}$  and the pair  $(n, m)$  given by  $n := |V|-1, m := |E|-2$  is in the target-domain

(each call to  $\Gamma C(x_0, z_0)$  is aborted as soon as these numbers are already too large), and then returning  $G' = \phi(G)$ , which has  $n$  vertices and  $m$  edges.

**Proposition 32.** *When  $m/n$  is bounded away from 1 and 3 (by a fixed positive constant  $c > 0$ ), the expected cost of the random sampler for rooted simple maps is  $O(n^{5/2})$  in exact-size sampling and is  $O(n/\epsilon)$  in approximate-size sampling. (The constant in the big O depends on  $c$ .)*

As in [37] it is also possible to get an exact-size (target-domain  $n$ ) and approximate-size (target-domain  $[n(1 - \epsilon), n(1 + \epsilon)]$ ) random sampler according to the number of vertices, with no target domain for the number of edges. The technique is similar except that one has to call the Boltzmann sampler  $\Gamma C(x_0, 1)$  —with  $x_0$  the value such that  $(x_0, 1)$  is singular— until the rooted simple map obtained is in  $\tilde{\mathcal{C}}$  and the number of vertices is in the target-domain (again each call to  $\Gamma C(x_0, 1)$  is aborted as soon as the number of vertices is too large). In this case, the expected cost is  $O(n^2)$  for exact-size sampling and  $O(n/\epsilon)$  for approximate-size sampling.

## 4.5 A simpler formulation of the mapping from oriented binary trees to simple maps

In order to get a simpler and more efficient random sampler, we describe here a more direct reformulation of the bijection from oriented binary trees to outer-triangular simple maps. While the previous bijection involved some simultaneous untyings in the whole map, the new formulation can be performed with only local operations. It is thus easier to implement, and clearly yields an algorithm of linear complexity.

Starting from an oriented binary tree, first place a dangling *leg* at the left of each inner edge. Considering leaves as opening parenthesis, and legs as closing parenthesis, one can form a clockwise parenthesis system leaving 3 leaves unmatched, called *exposed leaves* (drawn in black in Figure 4.11). Connect each matched pair with an edge (drawn in purple in Figure 4.11). This results in a map with two types of vertices (former vertices of the tree, and vertices on the middle of each edge of tree) where each vertex has degree 3. Notice that, if the 3 exposed leaves were to be connected to an additional vertex, this would yield the pointed bicubic map associated to the oriented binary tree, dual of the corresponding eulerian triangulation.

**Remark 33.** *Rooting the tree on one of the exposed leaves results in a balanced eulerian tree as defined in [56].*

Now the 3 exposed leaves split the infinite face of the map into 3 sections (delimited by dashed lines in Figure 4.11(b)). Place a new vertex in each section. Each inner edge of the former tree spans an inner edge of the

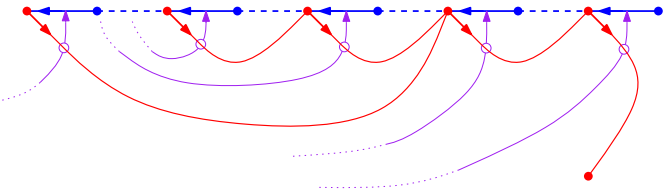


Figure 4.10: Drawing the edges of the simple map (in red) for some oriented edges of the tree.

simple map as follows. The left corner at the end of an inner edge is called a *darting corner*. Place a *dart*, an outgoing half-edge, coming from each darting corner. Connect this dart to the next darting corner along the counter-clockwise contour of the tree (or to the new vertex in the section if there is none), such that the new edge crosses exactly one edge of the bicubic map (see Figure 4.10).

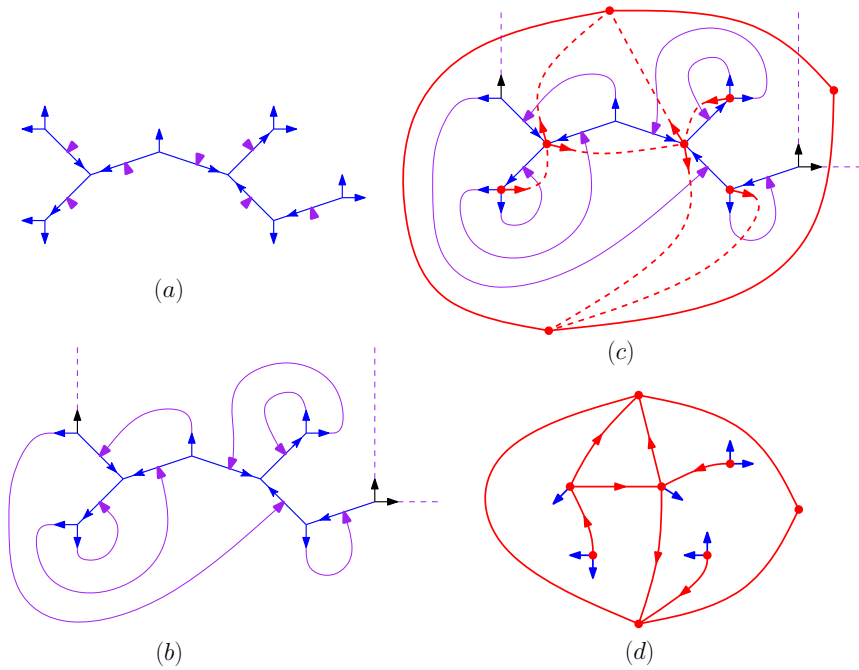


Figure 4.11: (a) An oriented binary tree with dangling legs, (b) its corresponding (almost) bicubic map, (c) applying the rule to each inner edge of the tree and (d) the resulting outer-triangular simple map and its 3-orientation with buds.

Then erase edges of the tree and the bicubic map, and disconnected vertices. Finally connect the 3 outer vertices to obtain the outer-triangular simple map. One can also recover the canonical 3-orientation with buds

by orienting each edge according to its dart, and by adding a bud for each outgoing edge (including bud) on non-source vertices of the tree.



# Chapter 5

## Distance-profile in random rooted simple maps

### 5.1 Introduction

In this chapter, we prove the convergence of the distance profile for rooted simple maps, that is, maps without loops nor multiple edges. We also show that it implies the same type of result for the class of loopless maps, and for the class of all maps. We now give a few definitions in view of stating our main result. For a rooted planar map  $G = (V, E)$  with  $n$  edges, the *distance*  $d(e)$  of an edge  $e \in E$  (with respect to the root) is the length of a shortest path of  $G$  starting at (an extremity of)  $e$  and ending at the root-vertex, the *distance-profile* of  $G$  is the  $n$ -set  $\{d(e)\}_{e \in E}$  (notice that we consider a distance-profile at edges, not at vertices). Let us now give some terminology for the type of convergence results to be obtained. We denote by  $\mathcal{M}_1$  the set of probability measures on  $\mathbf{R}$ , endowed with the *weak topology* (that is, the topology given by the convergence in law). For  $\mu \in \mathcal{M}_1$ , we denote by  $F_\mu(x)$  the cumulative function of  $\mu$ ,  $\inf(\mu) := \inf\{x : F_\mu(x) > 0\}$  and  $\sup(\mu) := \sup\{x : F_\mu(x) < 1\}$ , and define the *width* of  $\mu$  as  $\sup(\mu) - \inf(\mu)$ . We also define the *nonnegative shift* of  $\mu$  as the probability measure (with support in  $\mathbf{R}_+$ ) whose cumulative function is  $x \mapsto F_\mu(x + \inf(\mu))$ .

The *Integrated SuperBrownian excursion* (or *ISE* for short) is a random probability measure on  $\mathbf{R}^d$  ( $d > 0$ ) introduced by Aldous [5] as the continuum limit of rescaled random distributions of mass on discrete trees embedded in the lattice  $\mathbf{Z}^d$ . In this chapter, we will consider the case  $d = 1$  of the one-dimensional ISE, following the setting of [26]. First take an unembedded discrete rooted tree (as a Cayley tree) with  $n$  vertices from the uniform distribution. Then this tree can be randomly embedded in  $\mathbf{Z}$  as follows: give length 1 to each edge, place the root at 0 and fold the tree by mapping edges of the tree with edges of the lattice. By assigning a unit mass to each leaf of the tree, one obtains a random distribution of mass

on  $\mathbf{Z}$ . Then, upon scaling the lattice by  $n^{1/4}$ , these random distributions admit, when  $n$  tends to infinity, a continuum limit  $\mathcal{I}$  which is the random probability measure called ISE.

**Definition 34.** We denote by  $\mu_{\text{ISE}}$  a random variable with ISE law (as defined in [5]), and by  $\mu_{\text{ISE}}^{\text{shift}}$  its non-negative shift; these are random variables taking values in  $\mathcal{M}_1$ . A sequence  $\mu^{(n)}$  of random variables taking values in  $\mathcal{M}_1$  is said to satisfy the ISE limit property if the following properties hold:

- $\mu^{(n)}$  converges in law to  $\mu_{\text{ISE}}^{\text{shift}}$  (for the weak topology on  $\mathcal{M}_1$ ).
- $\sup(\mu^{(n)})$  converges in law to  $\sup(\mu_{\text{ISE}}^{\text{shift}})$  (i.e., the width of  $\mu_{\text{ISE}}$ ).

For  $\mu \in \mathcal{M}_1$ , we denote by  $X(\mu)$  a real random variable with distribution given by  $\mu$ . It is easy to see that if a sequence  $\mu^{(n)}$  of random variables taking values in  $\mathcal{M}_1$  converges in law to  $\mu$ , then  $X(\mu^{(n)})$  converges in law to  $X(\mu)$ . It is known that  $X(\mu_{\text{ISE}}^{\text{shift}})$  is distributed as  $\sup(\mu_{\text{ISE}})$  (whose cumulative function has an explicit expression, see [18]). Hence, if  $\mu^{(n)}$  has the ISE limit property, then  $X(\mu^{(n)})$  converges in law to  $\sup(\mu_{\text{ISE}})$ .

For an  $n$ -set  $\mathbf{x} = \{x_1, \dots, x_n\}$  of nonnegative values, and for  $a > 0$ , define  $\mu_a(\mathbf{x})$  as the probability measure

$$\mu_a(\mathbf{x}) = \frac{1}{n} \sum_{i=1}^n \delta_{x_i/(an)^{1/4}},$$

where  $\delta_x$  denotes the Dirac measure at  $x$ . Our main result is the following:

**Theorem 35.** For  $n \geq 1$ , let  $\pi_n$  be the distance-profile of the uniformly random rooted simple maps with  $n$  edges. Then  $\mu_2(\pi_n)$  satisfies the ISE limit property.

We mention that much less is known on the distance profile of *unembedded* planar graphs, the most precise result known at the moment, shown by [25], is that the diameter is  $n^{1/4+o(1)}$  in probability.

We close this section by recalling a useful classical result. For  $\mu$  and  $\nu$  two elements of  $\mathcal{M}_1$ , the *linear Wasserstein distance* between  $\mu$  and  $\nu$  is defined as

$$W_1(\mu, \nu) = \int_{\mathbf{R}} |F_\mu(x) - F_\nu(x)| dx,$$

which endows  $\mathcal{M}_1$  with a metric structure. Another characterization of  $W_1(\mu, \nu)$  is to be the infimum of  $\mathbf{E}(|X - Y|)$  over all couplings  $(X, Y)$  where the law of  $X$  is  $\mu$  and the law of  $Y$  is  $\nu$ . It is known that if a sequence  $\mu^{(n)}$  of elements of  $\mathcal{M}_1$  converges to  $\mu$  for the metric  $W_1$ , then  $\mu^{(n)}$  also converges to  $\mu$  for the weak topology on  $\mathcal{M}_1$ . Hence the following claim:

**Claim 36.** Let  $\mu^{(n)}$  and  $\nu^{(n)}$  be two sequences of random variables in  $\mathcal{M}_1$  (i.e., each variable is a random probability measure), living in the same probability space. Assume that  $\mu^{(n)}$  satisfies the ISE limit property and that, for each fixed  $\epsilon > 0$ ,  $P(W_1(\mu^{(n)}, \nu^{(n)}) \geq \epsilon)$  converges to 0 and  $P(|\sup(\mu^{(n)}) - \sup(\nu^{(n)})| \geq \epsilon)$  converges to 0. Then  $\nu^{(n)}$  satisfies the ISE limit property.

## 5.2 Bijection between outer-triangular simple maps and eulerian triangulations, and transfer of canonical paths

In this section we recall a bijection established in Chapter 4 between outer-triangular simple maps and eulerian triangulations, and establish a crucial property for canonical paths.

A rooted simple map  $C$  is said to be *outer-triangular* if its outer face (that is, the root face, drawn as the infinite face in the planar representation of  $C$ ) has degree 3. Given an outer-triangular simple map  $G$ , a *3-orientation with buds* of  $G$  is an orientation of the inner edges of  $G$  (outer edges are left unoriented), with additional outgoing half-edges at inner vertices, called *buds*, such that each inner (resp. outer) vertex has outdegree 3 (resp. 0), and each inner face of degree  $d + 3$  has  $d$  incident buds<sup>1</sup>. It is shown in [10] that each rooted outer-triangular simple map  $G$  admits a unique 3-orientation with buds, called the *canonical 3-orientation*, satisfying the following properties:

- *Outer-accessibility*: there is a directed path from any inner vertex to a vertex of the outer face.
- *Minimality*: There is no clockwise circuit.
- *Local property at buds*: the first edge following each bud in clockwise order must be outgoing<sup>2</sup>.

Figure 5.1.(a) shows such an outer-triangular simple map endowed with its canonical 3-orientation.

Let  $C$  be an outer-triangular rooted simple map. For each inner edge  $e$ , we define its *canonical path*  $P(e)$  to be the directed path in the canonical 3-orientation of  $C$  starting at  $e$  and following the rightmost (with respect to the previous edge on the path) outgoing edge until reaching a vertex of the outer face ( $P(e)$  exist because the canonical 3-orientation is minimal and outer-accessible).

A *rooted eulerian triangulation* is a rooted planar map (which may have multiple edges) where each face has degree 3 and each vertex has even degree. Hence faces can be properly bicolored (in light or dark) such that each light (resp. dark) face is adjacent only to dark (resp. light) faces. By convention (since there are exactly two possible colorings), the root face is dark. Given a rooted eulerian triangulation  $G$ , a *1-orientation* of  $G$  is an orientation of some inner edges (outer edges are left unoriented), such that each dark inner face has one directed edge, which is counterclockwise, and each inner (resp. outer) vertex has outdegree 1 (resp. 0). As shown in [15],  $G$  has a

---

<sup>1</sup>When  $G$  is a maximal simple map, 3-orientations have no bud, and correspond to the well-known Schnyder structures, introduced in [58].

<sup>2</sup>This condition implies that an inner vertex has no more than 2 buds.

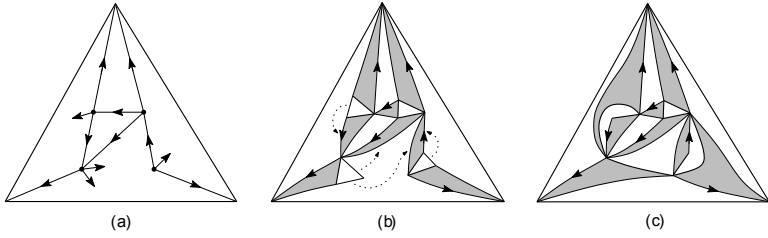


Figure 5.1: (a) An outer-triangular simple map endowed with its canonical 3-orientation with buds, (b) after inflation and (c) after merging, the resulting eulerian triangulation endowed with its canonical 1-orientation.

unique 1-orientation, called its *canonical 1-orientation*, which satisfies *outer-accessibility*; see Figure 5.1(c). The oriented edges form a spanning forest of 3 trees (one rooted at each of the outer vertices), and accordingly each vertex has a *canonical (oriented) path* reaching an outer vertex.

For each inner edge  $e$  of an outer-triangular rooted simple map  $C$ , we denote by  $\sigma(e)$  the inner vertex in the associated rooted eulerian triangulation  $G$  which is the origin of  $e$  after inflating  $e$  into a dark triangle.

**Proposition 37.** *Let  $C$  be an outer-triangular rooted simple map and  $G$  be the associated eulerian triangulation. The mapping  $\sigma$  gives a bijection between the edges of  $C$  and the inner vertices of  $G$ . Moreover the canonical path of an edge  $e$  of  $C$  has the same length as the canonical path of the vertex  $\sigma(e)$  of  $G$ .*

*Proof.* The canonical 3-orientation of  $C$  gives a partial orientation  $\Omega$  of  $G$ . It is not hard to see that  $\Omega$  is a 1-orientation, therefore  $\sigma$  gives a bijection between the edges of  $C$  and the inner vertices of  $G$ . Moreover all the canonical paths of  $C$  are directed paths in the orientation  $\Omega$  (that is, they are preserved by the inflation process), thus  $\Omega$  is outer-accessible. Thus  $\Omega$  is the canonical 1-orientation of  $G$ , and the canonical path of  $e$  becomes the canonical path of  $\sigma(e)$ . This completes the proof.  $\square$

**Remark 38.** *Beside the bijection between outer-triangular simple maps and eulerian triangulations, we will also use the following mapping from rooted outer-triangular simple maps to rooted simple triangulations. Given a rooted outer-triangular simple map  $C$  endowed with its canonical 3-orientation, every inner face of degree  $d+3$  contains  $d$  buds. We consider the triangulation  $T$  obtained from  $C$  by triangulating each inner face by completing the buds into complete edges and gluing these edges in counter-clockwise order around each inner face; see Figure 5.2. The 3-orientation of  $C$  gives a 3-orientation of  $T$  (which implies that  $T$  is simple) and we contend that it is the canonical 3-orientation of  $T$ . This follows easily from the fact that the canonical paths*

of  $C$  are canonical paths in  $T$  (because of the local property at buds) and therefore no clockwise circuit exists.

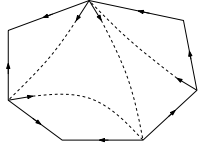


Figure 5.2: Generic situation in a face of degree 7 with its 4 incident buds, and its canonical triangulation (dashed lines).

### 5.3 The profile of random rooted eulerian triangulations

#### 5.3.1 Profile with respect to the root-vertex

Let  $T$  be a rooted eulerian triangulation with  $n + 1$  vertices, let  $V$  be the vertex-set and let  $v_0$  be the root-vertex. Recall that the faces of  $T$  are properly bicolored with the outer face being dark. A path  $P$  from a vertex  $v$  to a vertex  $v'$  is called *admissible* if each traversed edge of  $P$  has a dark face on its left. Let  $\ell(v)$  be the length of a shortest admissible path from  $v$  to  $v_0$ . The  $n$ -set  $\{\ell(v)\}_{v \in V \setminus v_0}$  is called the *root-vertex profile* of  $T$ .

**Proposition 39.** *Let  $\pi_n$  be the root-vertex profile of a uniformly random rooted eulerian triangulation with  $n + 1$  vertices. Then  $\mu_2(\pi_n)$  satisfies the ISE limit property.*

*Proof.* It is shown in [19] that random rooted eulerian triangulations with  $n + 1$  vertices are in bijection with so-called *very well-labelled trees* with  $n$  nodes, i.e., rooted plane trees with  $n$  nodes, each node having a positive label such that adjacent node labels differ by 1 in absolute value, and the root is at a node of label 1. In addition the root-vertex profile of the eulerian triangulation corresponds to the  $n$ -set of labels of the corresponding tree. Hence  $\pi_n$  is distributed as the  $n$ -set of labels of the random very well-labelled tree with  $n$  nodes. The results in [41] imply<sup>3</sup> that  $\mu_2(\pi_n)$  satisfies the ISE limit property.  $\square$

**Remark 40.** *Alternatively one could prove Proposition 39 by recycling the combinatorial arguments from Sections 4.4 and 4.5 in [26]. This would require a detour via a model of “blossoming trees” (actually the one used in [15]) in order to drop the condition that the labels are positive.*

---

<sup>3</sup>See in particular Theorem 8.2 where the methodology is applied to the very close model where adjacent node labels differ by at most 1 in absolute value.

### 5.3.2 Profile with respect to the outer face

Let  $T$  be a rooted eulerian triangulation, and let  $V$  be its set of inner vertices. For  $v \in V$ , we denote by  $\tilde{d}(v)$  the length of the canonical path of  $v$ . The set  $\{\tilde{d}(v)\}_{v \in V}$  is called the *root-face profile* of  $T$ . Then it is proved in [15] that  $\tilde{d}(v)$  is the length of a shortest admissible path from  $v$  to (a vertex of) the root-face. Hence  $\ell(v) - 2 \leq \tilde{d}(v) \leq \ell(v)$ . Thus Proposition 39 immediately gives (via Claim 36) the following result.

**Proposition 41.** *Let  $\pi_n$  be the root-face profile of a uniformly random rooted eulerian triangulation with  $n$  inner vertices. Then  $\mu_2(\pi_n)$  satisfies the ISE limit property.*

## 5.4 The profile of random rooted simple maps

### 5.4.1 Profile of random rooted outer-triangular simple maps

Let  $G$  be a rooted outer-triangular simple map, and let  $E_i$  be its set of inner edges. For  $e \in E_i$  we denote by  $\tilde{d}(e)$  the length of the canonical path of  $e$ , and by  $d(e)$  the length of a shortest path starting at (an extremity of)  $e$  and ending at (a vertex of) the root-face. The set  $\{\tilde{d}(e)\}_{e \in E_i}$  is called the *canonical path profile* of  $G$ , and the set  $\{d(e)\}_{e \in E_i}$  is called the *distance-profile at inner edges* of  $G$ . By Proposition 37 the canonical path profile of  $G$  coincides with the root-face profile of the rooted eulerian triangulation associated with  $G$  by the bijection of Section 5.2. Thus Proposition 41 gives:

**Proposition 42.** *Let  $\pi_n$  be the canonical path profile of a uniformly random rooted outer-triangular simple map with  $n + 3$  edges. Then  $\mu_2(\pi_n)$  satisfies the ISE limit property.*

We will now prove that with high probability the canonical path profile is close to the distance-profile using the following (non-random) result from [2].

**Lemma 43** ([2]). *There exist positive constants  $k_1, k_2$  such that the following holds. Let  $G$  be a rooted simple triangulation, let  $e$  be an inner edge of  $G$ , let  $P$  be the canonical path of  $e$  (for the canonical 3-orientation of  $G$ ), and let  $Q$  be another path in  $G$  from the origin of  $e$  to the root-face. If the length  $d$  of  $P$  is greater than the length  $d'$  of  $Q$ , then there exists a cycle  $C$  contained in  $P \cup Q$  of length a most  $k_1 d' / (d - d')$  such that each of the two parts of  $G$  resulting from cutting along  $C$  contains a (consecutive) subpath of  $Q$  of length at least  $k_2(d - d')$ .*

This implies the following (non-random) statement for rooted outer-triangular simple maps, where the *diameter*  $\text{Diam}(G)$  of a graph  $G$  is the maximal distance between pairs of vertices.

**Lemma 44.** *The statement of Lemma 43 also holds if one replaces “simple triangulation” by “outer triangular simple map”. Consequently, for any  $\Delta > 0$ , if  $G$  is a rooted outer-triangular simple map, and  $e$  is an inner edge such that  $d(e) \leq \tilde{d}(e) - \Delta$ , then  $G$  has a cycle  $C$  of length at most  $k_1 d(e)/\Delta$  such that the two parts  $G_\ell, G_r$  resulting from cutting along  $C$  each have diameter at least  $k_2 \Delta$ .*

*Proof.* Let  $G$  be a rooted outer triangular simple map. We consider its canonical 3-orientation with buds. As explained in Remark 38, there is a canonical way to complete the buds of  $G$  into complete edges so as to triangulate each inner face of  $G$  and obtain a simple triangulation  $\hat{G}$  endowed with its canonical 3-orientation. Moreover, for any inner edge  $e$  of  $G$ , the canonical path of  $e$  is the same in  $G$  as in  $\hat{G}$ . This proves the first statement. The second statement is a simple consequence obtained by considering the canonical path  $P$  of an edge  $e$  of  $G$  and a geodesic path  $Q$ . In this case  $G$  has a cycle  $C$  of length at most  $k_1 d(e)/(\tilde{d}(e) - d(e)) \leq k_1 d(e)/\Delta$  such that the two parts  $G_\ell, G_r$  resulting from cutting along  $C$  each have a subpath of  $Q$  of length at least  $k_2(\tilde{d}(e) - d(e)) \geq k_2 \Delta$ . Since a subpath of a geodesic path is geodesic, we conclude that each of  $G_\ell, G_r$  has diameter at least  $k_2 \Delta$ .  $\square$

**Definition 45.** *A sequence  $X_n$  of real random variables is said to have the uniform exponential decay property if there exist constants  $a, b > 0$  such that for all  $n$ ,  $P(X_n \geq x) \leq a \exp(-bx)$ .*

**Lemma 46.** *Let  $H_n$  be the uniformly random rooted outer-triangular simple map with  $n+3$  edges. Then  $\text{Diam}(H_n)/n^{1/4}$  satisfies the uniform exponential decay property.*

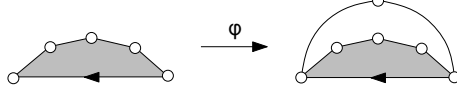
*Proof.* The property is inherited from eulerian triangulations. Precisely, let  $\pi_n$  denote the root-vertex profile of the uniformly random rooted eulerian triangulation. The calculations done in Section 6.2 of [26] for well-labeled trees (which correspond to rooted quadrangulations) can be adapted verbatim to very well-labelled trees (which correspond to rooted eulerian triangulations) in order to show that  $\sup(\mu_2(\pi_n))$  has the uniform exponential decay property. Hence, if  $\pi'_n$  denotes the root-face profile of the uniformly random rooted eulerian triangulation with  $n$  vertices, then  $\sup(\mu_2(\pi'_n))$  has the uniform exponential decay property. This is in turn transferred (bijectively) to  $\sup(\mu_2(\pi''_n))$ , where  $\pi''_n$  is the canonical path profile of  $H_n$ . Since  $d(e) \leq \tilde{d}(e)$ , the property is also satisfied by  $\sup(\mu_2(\pi'''_n))$ , where  $\pi'''_n = \{d(e)\}_{e \in E_i}$  is the distance-profile at inner edges of  $H_n$ . Since  $\text{Diam}(H_n) \leq 2 \cdot \max_{e \in E_i}(d(e)) + 2$ , we conclude that  $\text{Diam}(H_n)/n^{1/4}$  satisfies the uniform exponential decay property.  $\square$

For  $n \geq 0$  we denote by  $\mathcal{M}_n$  the set of rooted simple maps with  $n$  edges, and  $\mathcal{C}_n$  the subset of outer-triangular simple maps in  $\mathcal{M}_n$ . It was shown in

Chapter 3 that

$$|\mathcal{C}_n| = 3 \cdot 2^{n-1} \frac{(2n)!}{n! (n+2)!} = O(8^n n^{-5/2}). \quad (5.1)$$

Observe that there is an injective map  $\phi$  from  $\mathcal{M}_n$  to  $\mathcal{C}_{n+2}$  as shown in the figure below.



Thus  $|\mathcal{M}_n| \leq |\mathcal{C}_{n+2}| = O(8^n n^{-5/2})$ . Moreover  $\text{Diam}(\phi(G)) - \text{Diam}(G) \in \{0, 1\}$ . Thus (observing that  $\frac{|\mathcal{M}_n|}{|\mathcal{C}_{n+2}|} \geq \frac{|\mathcal{C}_n|}{|\mathcal{C}_{n+2}|}$  is bounded away from 0) Lemma 46 implies the following.

**Corollary 47.** *Let  $G_n$  be the uniformly random rooted simple map with  $n$  edges. Then  $\text{Diam}(G_n)/n^{1/4}$  satisfies the uniform exponential decay property. Therefore there exist constants  $a, b > 0$  such that for all  $n \geq 0$  and  $x > 0$  the number of elements in  $\mathcal{M}$  of diameter at least  $xn^{1/4}$  is at most  $a8^n n^{-5/2} \exp(-bx)$ .*

**Lemma 48.** *Let  $\epsilon > 0$  and let  $G_n$  be the random rooted outer-triangular simple map with  $n+3$  edges. Let  $\mathcal{E}_{n,\epsilon}$  be the event that  $G_n$  has an inner edge  $e$  for which  $d(e) \leq \tilde{d}(e) - \epsilon n^{1/4}$ . Then  $\lim_{n \rightarrow \infty} P(\mathcal{E}_{n,\epsilon}) = 0$ .*

*Proof.* We first show the statement for the event  $\mathcal{E}_{n,\epsilon,A} = \mathcal{E}_{n,\epsilon} \cap \{\text{Diam}(G_n) \leq An^{1/4}\}$ , where  $A$  is an arbitrary fixed positive constant. Let  $U_n$  be the set of rooted outer-triangular simple maps with  $n$  edges of diameter at most  $An^{1/4}$  having an inner edge  $e$  for which  $d(e) \leq \tilde{d}(e) - \epsilon n^{1/4}$ . By (5.1), it suffices to show that  $|U_n| = o(8^n n^{-5/2})$ . By Lemma 44 (applied to  $\Delta = \epsilon n^{1/4}$ ), any map in  $U_n$  has a cycle of length  $c \leq k_1 d(e)/\epsilon n^{1/4} \leq k_1 A/\epsilon$  separating two maps of diameter at least  $k_2 \epsilon n^{1/4}$ . We now fix a positive integer  $c$ , and denote by  $V_n^c$  the set of pairs  $(G, C)$  where  $G$  is a rooted outer-triangular simple map with  $n$  edges and  $C$  is a cycle of  $G$  of length  $c$  such that the two parts of  $G$  obtained by cutting along  $C$  each have diameter at least  $k_2 \epsilon n^{1/4}$ . It suffices to prove that  $|V_n^c| = o(8^n n^{-5/2})$ . Let  $w_{i,n}$  be the number of maps in  $\mathcal{M}_i$  of diameter at least  $k_2 \epsilon n^{1/4}$ . By Corollary 47 there are constants  $a, b' > 0$  such that  $w_{i,n} \leq a8^i i^{-5/2} \exp(-b'(n/i)^{1/4})$ . Decomposing pairs  $(G, C) \in V_n^c$  into two maps gives

$$|V_n^c| \leq \sum_{i+j=n+c} 2n \cdot w_{i,n} w_{j,n}$$

where the factor  $2n$  accounts for choosing the position of the root edge of  $G$ . Let  $S$  be the above sum restricted to  $\{i > n/(\log(n)^8)\} \cap \{j > n/(\log(n)^8)\}$  and  $S'$  the sum of the other terms. Since  $w_{i,n} \leq a8^i i^{-5/2}$ ,

$$S \leq (n+c) \cdot 2n \cdot a^2 8^{n+c} (n/\log(n)^8)^{-5} = o(8^n n^{-5/2}).$$

And since  $w_{i,n} \leq a8^i \exp(-b'(n/i)^{1/4})$ ,

$$S' \leq 2n/(\log(n)^8) \cdot 2n \cdot a^2 8^{n+c} \exp(-b'(\log(n))^2) = o(8^n n^{-5/2}).$$

Hence  $|V_n^c| = o(8^n n^{-5/2})$  and this completes the proof that for any  $A > 0$ ,  $\lim_{n \rightarrow \infty} P(\mathcal{E}_{n,\epsilon,A}) = 0$ . Thus for all  $A > 0$ ,

$$\begin{aligned} \lim_{n \rightarrow \infty} P(\mathcal{E}_{n,\epsilon}) &\leq \lim_{n \rightarrow \infty} (P(\mathcal{E}_{n,\epsilon,A}) + P(\text{Diam}(G_n) > An^{1/4})) \\ &\leq \sup_n P(\text{Diam}(G_n) > An^{1/4}). \end{aligned}$$

And since by Lemma 46,  $\lim_{A \rightarrow \infty} \sup_n P(\text{Diam}(G_n) > An^{1/4}) = 0$ , we get  $\lim_{n \rightarrow \infty} P(\mathcal{E}_{n,\epsilon}) = 0$ .  $\square$

**Remark 49.** A result similar to Lemma 48 is given in [2] for random rooted simple triangulations. However, we could not deduce Lemma 48 from that result and instead had to start from Lemma 43 above.

We can now prove the main result of this section.

**Proposition 50.** Let  $\pi_n$  be the distance-profile at inner edges of a uniformly random rooted outer-triangular simple map with  $n+3$  edges. Then  $\mu_2(\pi_n)$  satisfies the ISE limit property.

*Proof.* Let  $G_n$  be the uniform random rooted outer-triangular simple map with  $n$  inner edges, and let  $E_i$  be the set of inner edges. We consider the  $n$ -sets  $\mathbf{d} = \{d_e\}_{e \in E_i}$  and  $\tilde{\mathbf{d}} = \{\tilde{d}(e)\}_{e \in E_i}$ . When  $\mathcal{E}_{n,\epsilon}$  does not hold, then  $W_1(\mu_2(\mathbf{d}), \mu_2(\tilde{\mathbf{d}})) \leq \epsilon/2^{1/4}$ , and  $|\sup(\mu_2(\mathbf{d})) - \sup(\mu_2(\tilde{\mathbf{d}}))| \leq \epsilon/2^{1/4}$ . Hence, the result follows from Proposition 42 and Lemma 48, using Claim 36.  $\square$

#### 5.4.2 Profile of random rooted simple maps

We now transfer our result for outer-triangular simple maps to general simple maps. For this we exploit an easy decomposition (already described in Chapter 3) of rooted simple maps in terms of rooted outer-triangular simple maps. Let  $\mathcal{M}$  be the family of rooted simple maps, and let  $\mathcal{C}$  be the family of rooted outer-triangular simple maps. Let  $p$  be the rooted simple map with two edges meeting at a point, which is the root-vertex, and let  $\mathcal{D} = \mathcal{C} \cup \{p\}$ . For an element of  $\mathcal{D}$ , the *right-edge* is the edge following the root-edge in counterclockwise order around the root-face. It is shown in [9] that each graph  $\gamma \in \mathcal{M}$  is uniquely obtained from a sequence  $\gamma_1, \dots, \gamma_k$  of elements of  $\mathcal{D}$  where the following operations are performed:

- (i) for  $i \in [1..k-1]$ , merge the right-edge of  $\gamma_i$  with the root-edge of  $\gamma_{i+1}$  (identifying the root-vertices),
- (ii) delete the right-edge of  $\gamma_k$ .

In the decomposition,  $\gamma_i$  (if it exists, i.e., if  $i \leq k$ ) is called the  $i$ th component. This decomposition also ensures that the generating functions  $M(z)$  of  $\mathcal{M}$  and  $C(z)$  of  $\mathcal{C}$  (according to the number of edges) are related by

$$M(z) = \sum_{k \geq 1} (z + C(z)/z)^k = \frac{D(z)}{1 - D(z)}, \quad \text{where } D(z) := z + C(z)/z.$$

Let  $G_n$  be the random rooted simple map with  $n$  edges, and for  $i, j \geq 1$ , let  $\mathcal{E}_n^{(i,j)}$  be the event that, in the decomposition  $\gamma_1, \dots, \gamma_k$  of  $G_n$ , the  $i$ th component  $\gamma_i$  exists (i.e.,  $i \leq k$ ) and has  $n - j + 1$  edges. And let  $\pi_n^{(i,j)}$  be the probability that  $\mathcal{E}_n^{(i,j)}$  occurs.

**Lemma 51.** *For any  $i, j \geq 1$ , there exists a non-negative constant  $\pi^{(i,j)}$  such that  $\pi_n^{(i,j)}$  converges to  $\pi^{(i,j)}$ . In addition  $\sum_{i,j} \pi^{(i,j)} = 1$ .*

*Proof.* Let  $m_n$  be the number of rooted simple maps with  $n$  edges,  $m_n^{(i,j)}$  the number of rooted simple maps with  $n$  edges for which  $\mathcal{E}_n^{(i,j)}$  occurs (note that  $\pi_n^{(i,j)} = m_n^{(i,j)}/m_n$ ), and  $d_n$  be the number of elements of  $\mathcal{D}$  with  $n$  edges. From  $C(z) = \sum_{n \geq 1} \frac{3 \cdot 2^{n-1} (2n)!}{n! (n+2)!} z^{n+2} = \frac{z^2 (-1 + 12z + \sqrt{1-8z})}{(1+\sqrt{1-8z})^2}$ . one finds that  $D(z)$  and  $M(z)$  have the following singular expansion at  $z = 1/8$ , with the notation  $Z = \sqrt{1-8z}$  and with  $d := 5/32$  and  $e = 1/4$ :

$$\begin{aligned} D(z) &= d + eZ^3 - 9Z^2/32 + O(Z^4), \\ M(z) &= \frac{d}{1-d} + \frac{e}{(1-d)^2} Z^3 - 32Z^2/81 + O(Z^4). \end{aligned}$$

Now, let  $M^{(i,j)}(z) = \sum_n m_n^{(i,j)} z^n$ . It is easy to see that  $M^{(i,j)}(z) = a^{(i,j)} z^j D(z)$ , where  $a^{(i,j)} = [z^j] \frac{D(z)^{i-1}}{1-D(z)}$  counts the number of possibilities for the components  $\gamma_s$  for  $s \neq i$ . Hence  $M^{(i,j)}(z)$  has a singular expansion of the form  $M^{(i,j)}(z) = d^{(i,j)} + e^{(i,j)} Z^{3/2} + g^{(i,j)} Z^2 + O(Z^4)$ , with  $e^{(i,j)} = a^{(i,j)} \cdot e \cdot 8^{-j}$ . By classical transfer lemmas of singularity analysis in [34],

$$m_n \sim \frac{1}{\sqrt{\pi}} \frac{e}{(1-d)^2} 8^n n^{-5/2}, \quad m_n^{(i,j)} \sim \frac{1}{\sqrt{\pi}} a^{(i,j)} \cdot e \cdot 8^{-j} \cdot 8^n n^{-5/2}.$$

Hence  $\pi_n^{(i,j)} = m_n^{(i,j)}/m_n$  converges to  $\pi^{(i,j)} := (1-d)^2 8^{-j} [z^j] \frac{D(z)^{i-1}}{1-D(z)}$ . We have for each  $i \geq 1$ ,  $\sum_j \pi^{(i,j)} = (1-d)^2 \cdot D(1/8)^{i-1} / (1 - D(1/8)) = (1-d)^2 \cdot d^{i-1} / (1-d)$ , hence  $\sum_{i,j} \pi^{(i,j)} = 1$ .  $\square$

**Lemma 52.** *For  $i, j \geq 1$  fixed, let  $\pi_n^{(i,j)}$  be the profile of the random rooted simple map  $G_n^{(i,j)}$  with  $n$  edges conditioned on  $\mathcal{E}_n^{(i,j)}$ . Then  $\mu_2(\pi_n^{(i,j)})$  satisfies the ISE limit property.*

*Proof.* Let  $E$  be the set of edges of  $G_n^{(i,j)}$  and let  $E_i$  be the set of inner edges of  $\gamma_i$ . Let  $\mathbf{d} = \{d_e\}_{e \in E}$  be the  $n$ -set of distances of the edges of  $G_n^{(i,j)}$  from

the root-vertex, and let  $\mathbf{d}' = \{d_e\}_{e \in E_i}$  be the  $(n - j - 2)$ -set of distances of inner edges of  $\gamma_i$  from the root-vertex of  $\gamma_i$  (which is also the root-vertex of  $G_n^{(i,j)}$ ). It is easy to see that there exists a constant  $A > 0$  (depending only on  $i$  and  $j$ ) such that, for any rooted simple map with  $n$  edges and satisfying  $\mathcal{E}_n^{(i,j)}$ ,

$$W_1(\mu_2(\mathbf{d}), \mu_2(\mathbf{d}')) \leq A \cdot \frac{\text{Diam}(\gamma_i)}{n}.$$

Since  $\gamma_i$  is a uniformly random rooted outer-triangular simple map with  $n - j + 1$  edges, Lemma 46 ensures that  $\text{Diam}(\gamma_i)/n^{1/4}$  satisfies the uniform exponential decay property, hence

$$P(W_1(\mu_2(\mathbf{d}), \mu_2(\mathbf{d}')) \geq A/\sqrt{n}) = O(\exp(-\Omega(n^{1/4}))).$$

Similarly

$$P(|\sup(\mu_2(\mathbf{d})) - \sup(\mu_2(\mathbf{d}'))| \geq A/\sqrt{n}) = O(\exp(-\Omega(n^{1/4}))).$$

Since  $\mu_2(\mathbf{d}')$  satisfies the ISE limit property according to Proposition 50, we conclude from Claim 36 that  $\mu_2(\mathbf{d})$  also satisfies the ISE limit property.  $\square$

*Proof of Theorem 35.* Let  $\eta > 0$ . Let  $k$  be the smallest value such that  $\sum_{i \leq k, j \leq k} \pi^{(i,j)} > 1 - \eta$ , and let  $\mathcal{E}_{n,\eta}$  be the event that  $\mathcal{E}_n^{(i,j)}$  holds for some  $i \leq k$  and  $j \leq k$ . By Lemma 52, conditioned on  $\mathcal{E}_{n,\eta}$ , the random rooted simple map with  $n$  edges satisfies the ISE limit property. Note that, as  $n \rightarrow \infty$  the probability that  $\mathcal{E}_{n,\eta}$  holds converges to  $c_\eta := \sum_{i \leq k, j \leq k} \pi^{(i,j)}$  (because for  $n$  large enough two events  $\mathcal{E}_n^{(i,j)}$  and  $\mathcal{E}_n^{(i',j')}$  do not intersect), hence for  $n$  large enough, the probability that  $\mathcal{E}_{n,\eta}$  holds is at least  $1 - \eta$ . Taking  $\eta$  arbitrarily small, we conclude that  $G_n$  satisfies the ISE limit property.  $\square$

We define the *radius*  $r(G)$  of a planar map  $G$  as the largest possible distance of a vertex of  $G$  from the root-vertex.

**Proposition 53.** *Let  $R_n$  be the radius of the random rooted simple map  $G_n$  with  $n$  edges. Then  $R_n/(2n)^{1/4}$  converges in law to the width of  $\mu_{\text{ISE}}$ , and the convergence also holds for the moments.*

*Proof.* The convergence in law follows from Theorem 35. The convergence of the moments then follows from the uniform exponential decay property of  $R_n/(2n)^{1/4}$  which is given by Corollary 47.  $\square$

## 5.5 Further results

### 5.5.1 The profile of random rooted loopless and general maps

It is known that any loopless map decomposes along multiple edges into a tree of components of two types: simple maps and multi-edges, see e.g. [36,

Sec2.1] for a description of the decomposition in the quadrangulated case. In addition, denoting by  $L_n$  the uniformly random rooted loopless map of size  $n$ , it has been shown in [38, 8] that, when  $n$  gets large, the (decomposition-) tree of  $L_n$  has almost surely a unique “giant component”  $S$ , which is a uniformly random simple map whose size is concentrated around  $2n/3$ , and the second largest component has size  $O(n^{2/3+\delta})$  for any  $\delta > 0$ . Hence  $L_n$  can be seen as a random simple map  $S$  of size  $\sim 2n/3$  whose edges are possibly substituted by “small” random rooted loopless maps. Based on this, it can be deduced from Theorem 35 that  $\mu_{4/3}(\pi(L_n))$  satisfies the ISE limit property ( $\pi(M)$  denotes the distance-profile of a map  $M$ ). The scaling constant  $4/3$  that appears here can be thought of as  $2 \cdot (2/3)$ , indeed it combines the effects of the scaling constant  $2$  applied to the giant simple map  $S$ , and of the fact that the size of  $S$  is asymptotically  $2/3$  of the size of  $L_n$ .

Similarly, any general map decomposes along loops into a tree of components that are loopless maps (the edges of the tree corresponding to the loops of the map). Again, denoting by  $M_n$  the random rooted map with  $n$  edges, it has been shown in [38, 8] that when  $n$  gets large, the (decomposition-) tree of  $M_n$  has almost surely a unique “giant component”  $L$ , which is a uniformly random loopless map whose size is concentrated around  $2n/3$ , and the second largest component has size  $O(n^{2/3+\delta})$  for any  $\delta > 0$ . Based on this, it can be shown that  $\mu_{8/9}(\pi(M_n))$  satisfies the ISE limit property. We recover here a known result, which alternatively follows from the study by [26] of the profile of random rooted quadrangulations, combined with the recent profile-preserving bijection in [6] between quadrangulations and maps.

### 5.5.2 Towards convergence to the Brownian map

We give again (after the one of Section 4.4.1) a reformulation of the mapping from oriented binary trees to outer-triangular simple maps, this time based on a canonical labelling of the corners of the tree. This gives a reformulation that is reminiscent of the Schaeffer bijection from well-labelled trees to pointed quadrangulations, which has been used to show the convergence of the random quadrangulation with  $n$  faces to the Brownian map. In a work in progress with Marie Albenque, Olivier Bernardi, and Éric Fusy, we will actually show that this reformulation gives a way to prove convergence of the random simple map with  $n$  edges to the Brownian map, using similar ingredients as in [12], which is merely sketched in the following. Let us now give the reformulation.

An oriented binary tree admits a canonical labelling of its inner corners which is defined as follows. Both corners incident to one of the 3 exposed leaves have label 0. One can read the label of each remaining corner by following the counter-clockwise contour of the tree: a leaf (except exposed leaves) increases labels by 1 while a leg decreases labels by 1 (see Figure 5.3).

Each label is then a nonnegative integer.

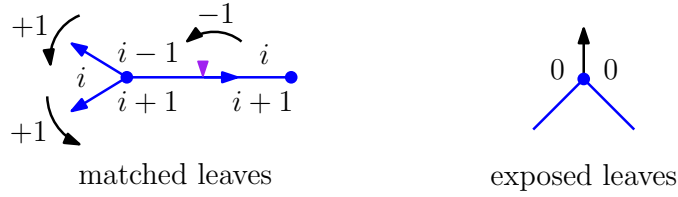


Figure 5.3: Reading labels along the contour of the oriented binary tree.

**Remark 54.** Let the infinite face have depth 0, then the label of a corner reads as the depth of its incident face in the associated bicubic map (with respect to the infinite face, and where the tree acts like a wall and cannot be crossed over). By duality, the depth of a face in the bicubic map corresponds to the depth of the dual vertex in the oriented forest of the dual eulerian triangulation. Finally the depth of a vertex in the oriented forest of an eulerian triangulation corresponds to the length of the rightmost path of an oriented edge in the corresponding simple map, as seen in Section 5.2 – which is almost surely the geodesic distance, upon a negligible error.

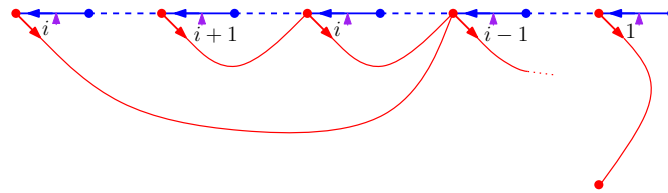


Figure 5.4: Drawing the edges of the simple map (in red) for some oriented edges of the tree.

Once the oriented binary tree is labelled, place a vertex into each section delimited by the exposed leaves. Each inner edge spans an inner edge of the simple map as follows. Once again, place a *dart* coming from each darting corner of label  $i$  ( $i \geq 0$ ) and connect this dart to:

- the next darting corner of label  $i - 1$  if  $i \geq 1$ ,
- the vertex in the incident section of the infinite face if  $i = 1$ .

Erasing edges and source vertices (which have no incident darts) of the tree, and connecting the 3 outer vertices, we then obtain the outer-triangular simple map as in the original bijection. One can even recover the canonical 3-orientation with buds of the simple map by orienting each inner edge according to its dart, and by adding a bud on a vertex for each outgoing edge (including leaves). Furthermore, if one labels an inner edge of the

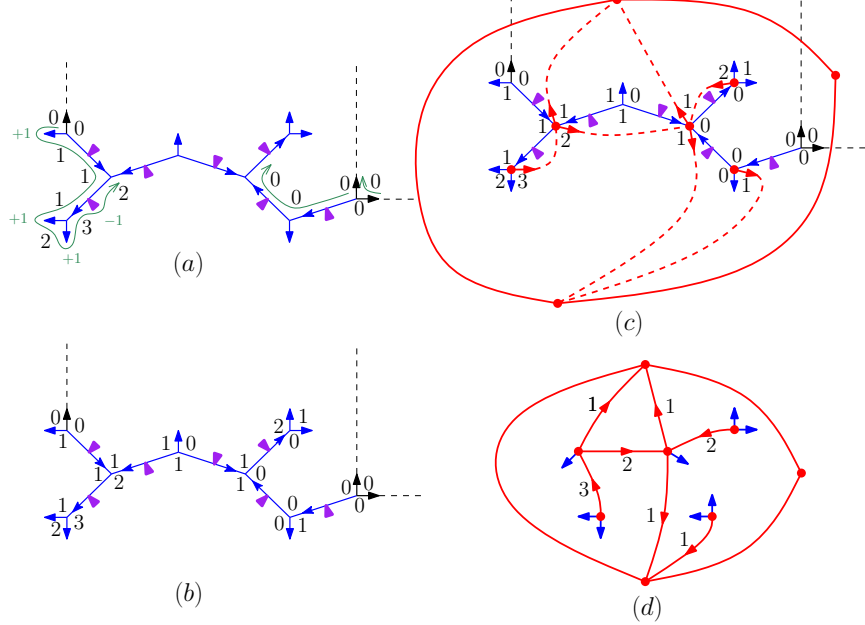


Figure 5.5: (a) An oriented binary tree, (b) its labelling, (c) applying the local rule to draw the edges of the simple map, and (d) the resulting outer-triangular simple map with its canonical 3-orientation with buds.

simple map with the label of the darting corner it comes from, the label of an edge is the length of the rightmost path to the outer face (see Remark 54).

It can be readily checked that this is merely a labelled version of the bijection presented in Section 4.5. Closing a dart of label  $i$  onto the next darting corner of label  $i - 1$  is equivalent, by Remark 54, to closing a dart onto the next darting corner after crossing an edge (thus decreasing by 1 the depth of the incident face) of the bicubic map. This closure of darting corners is reminiscent of the closure of (every) corners in the Schaeffer's well-labelled trees. Although labels are carried by the vertices in well-labelled trees, one can indeed associate to any corner the label of its incident vertex. The label constraints along the contour of the tree is then quite similar to ours, as two consecutive labels must differ by at most 1.

Moreover, for a rooted (at a leaf) oriented binary tree, there is also a canonical labelling of the corners, slightly differently defined: the corner to the left of the root is labelled 0, and turning around the tree, increase label by 1 when crossing a leaf —this time even an exposed one— and decrease label by 1 when crossing a leg. Notice that labels can now become negative, and that, shifting the labels of the rooted tree by the minimum label, one recovers the labels in the unoriented case, up to an error bounded by 3. Then notice that at each inner node the labels of the 3 incident corners

from left to right are of the form  $i, i + 1, i + 2$ . One can label such a node by  $i$ , then erase all leaves and legs, this way one obtains the so-called *shape* of the oriented binary tree.

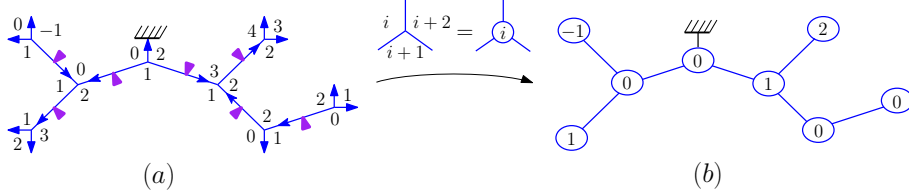


Figure 5.6: (a) The non-conditionned vertex-labelling of a rooted oriented binary tree, (b) its vertex-labelled tree-shape.

Such labelled tree-shapes fit in the criteria of [45] and thus one can show that the pair formed by the contour of the tree-shape and the labels around the tree-shape, rescaled by  $(2n)^{1/4}$ , converges to the head of the *Brownian snake*, from which is built the Brownian map. While the factor  $n^{1/4}$  is universal for planar maps, the constant factor depends on the family we are considering, and is derived from both the shape of the associated tree and the behaviour of the labels along its contour.

Hence with some more work, one will be able to show that, if  $M_n$  denotes the random rooted simple map with  $n$  edges, then the random metric space  $\left(M_n, \frac{d_{gr}}{(2n)^{1/4}}\right)$  converges to the Brownian map.



# Chapter 6

## Conclusion et perspectives

Les résultats présentés dans cette thèse viennent illustrer la richesse et la polyvalence de la méthode bijective pour l'étude des cartes planaires. En construisant peu à peu un vaste dictionnaire permettant de naviguer entre différents objets, la méthode bijective aide à comprendre leur structure sous-jacente. Ainsi, afin de résoudre un problème sur une famille donnée, il suffira de se ramener à une famille plus adaptée pour en simplifier l'étude.

### 6.1 Cartes avec bords

Dans les chapitres 2 et 3, une suite d'opérations bijectives nous permet d'élaborer des preuves transparentes de résultats énumératifs exacts sur les cartes planaires à bords. Nous retrouvons ainsi des formules de Tutte, de Bousquet-Mélou et Schaeffer sur les coefficients, des formules d'Eynard sur les séries génératrices, et de plus, en mettant à jour la structure de ces cartes à bords, nous obtenons une généralisation de ces résultats.

Toutefois nous nous heurtons à la même difficulté qu'avait rencontrée Tutte lorsqu'il s'agit d'étendre ces formules pour un nombre de bords non-réguliers supérieur à deux : bords de longueur impaire pour les cartes biparties, ou de longueur non multiple de  $p$  pour les  $p$ -constellations. En effet, pour traiter les bords non-réguliers, nous isolons un chemin formé par les arêtes non-régulières dans les mobiles associés. Quand le nombre de bords non-réguliers augmente, l'ensemble formé par ces arêtes non-régulières devient plus complexe : il prend une structure arborescente, ou peut se décomposer en plusieurs composantes connexes. Les coefficients qui apparaissent alors ne sont plus aussi simples (de grands facteurs premiers apparaissent), suggérant l'absence de formules aussi élégantes que celles présentées dans ce mémoire.

On peut néanmoins espérer une généralisation de ces formules aux cartes de genre supérieur. En effet, Eynard [33] a obtenu des expressions explicites en genre 1 et 2, et de manière plus générale, sa méthode fonctionne en

genre quelconque. De plus, la bijection de Bouttier-Di Francesco-Guitter sur laquelle nous nous appuyons s'étend naturellement en genre supérieur (voir les travaux de Chapuy [23]).

Enfin Bouttier et Guitter ont eux-mêmes obtenu un raffinement de nos résultats aux cartes biparties  $d$ -irréductibles [21], *i.e.* ayant des contraintes sur la longueur de leurs cycles. Il serait donc intéressant d'étudier si leurs travaux peuvent se voir étendus à des constellations avec contraintes de maille.

## 6.2 Cartes simples et distances

En exploitant l'existence de bijections entre les cartes simples et de nombreux autres objets, nous parvenons à en faire l'énumération exacte et asymptotique, mais également à produire des générateurs aléatoires efficaces. En outre, bien choisir les bijections utilisées permet de garder la trace de paramètres intéressants comme le nombre de sommets, de faces, d'arêtes, ou encore la distance. Cela donne alors accès à des générateurs aléatoires plus fins, ou encore à la structure des cartes en tant qu'espaces métriques.

Le résultat de convergence du profil des distances s'inscrit dans le vaste mouvement initié par les travaux de Chassaing et Schaeffer visant à comprendre la forme des grandes cartes aléatoires. Si nous donnons également dans ce mémoire une ébauche de la preuve de la convergence vers la carte Brownienne, d'autres questions restent en suspens. En effet, le profil des distances ne donne qu'une réponse partielle au comportement de la métrique dans les cartes. Afin d'avoir accès à des informations plus fines, il faudrait s'intéresser aux fonctions à deux points, à trois points, pour lesquelles on connaît des expressions pour certaines familles de cartes.

La bijection que nous présentons, entre les cartes simples (ou cartes de maille 3) à face externe triangulaire et les triangulations eulériennes, admet une extension aux cartes de maille  $d$  à face externe  $d$ -angulaire, qui s'envoient alors sur une sous-famille de  $d$ -constellations. Si cette sous-famille est moins aisée à définir que celle des triangulations eulériennes, il pourrait toutefois s'avérer intéressant d'étudier plus en détail cette transformation et les informations qu'elle nous donne sur les distances dans ces cartes.

# Bibliography

- [1] C. Abraham. Rescaled bipartite planar maps converge to the brownian map, 2013. In preparation.
- [2] L. Addario-Berry and M. Albenque. The scaling limit of random simple triangulations and random simple quadrangulations, 2013. arXiv:1306.5227.
- [3] M. Aigner and G. M. Ziegler. *Proofs from the book, 3rd edition.* Springer, 2004.
- [4] M. Albenque and D. Poulalhon. Generic method for bijections between blossoming trees and planar maps. arXiv:1305.1312, 2013.
- [5] D. J. Aldous. Tree-based models for random distribution of mass. *J. Stat. Phys.*, pages 625–641, 1993.
- [6] J. Ambjørn and T.G. Budd. Trees and spatial topology change in causal dynamical triangulations. *J. Phys. A: Math. Theor.*, 46(31):315201, 2013.
- [7] J. Ambjørn and Y. Watabiki. Scaling in quantum gravity. *Nucl.Phys.*
- [8] C. Banderier, P. Flajolet, G. Schaeffer, and M. Soria. Random maps, coalescing saddles, singularity analysis, and Airy phenomena. *Random Structures Algorithms*, 19(3/4):194–246, 2001.
- [9] O. Bernardi, G. Collet, and É. Fusy. A bijection for plane graphs and its applications. In *Proceedings of the 11th Workshop on Analytic Algorithmics and Combinatorics (ANALCO)*, pages 52–61, 2014.
- [10] O. Bernardi and É. Fusy. Unified bijections for maps with prescribed degrees and girth. *J. Combin. Theory Ser. A*, 119(6):1352–1387, 2012.
- [11] O. Bernardi and É. Fusy. A master bijection for planar hypermaps with general girth constraints. In preparation, 2013.
- [12] J. Bettinelli, E. Jacob, and G. Miermont. The scaling limit of uniform random plane maps, via the Ambjørn Budd bijection, 2013. arXiv:1312.5842.

- [13] M. Bona. Exact enumeration of 1342-avoiding permutations; a close link with labeled trees and planar maps. *J. Combin. Theory Ser. A*, 80:257–272, 1997.
- [14] M. Bousquet-Mélou and A. Jehanne. Polynomial equations with one catalytic variable, algebraic series, and map enumeration. *J. Combin. Theory Ser. B*, 96:623–672, 2005.
- [15] M. Bousquet-Mélou and G. Schaeffer. Enumeration of planar constellations. *Adv. in Appl. Math.*, 24(337–368), 2000.
- [16] M. Bousquet-Mélou and S. Schaeffer. The degree distribution in bipartite planar maps: applications to the ising model, 2002.
- [17] J. Bouttier, P. Di Francesco, and E. Guitter. Census of planar maps : from the one-matrix. model solution to a combinatorial proof. *Nucl. Phys.*, B 645:477–499, 2002.
- [18] J. Bouttier, P. Di Francesco, and E. Guitter. Geodesic distance in planar graphs. *Nucl. Phys.*, B663:535–567, 2003.
- [19] J. Bouttier, P. Di Francesco, and E. Guitter. Planar maps as labeled mobiles. *Electron. J. Combin.*, 11(1), 2004.
- [20] J. Bouttier and E. Guitter. The three-point function of planar quadrangulations. *J. Stat. Mech. Theory Exp.*, 7:7–22, 2008.
- [21] J. Bouttier and E. Guitter. A note on irreducible maps with several boundaries. *Electronic J. Combin.*, 21:1, 2014.
- [22] G. Chapuy. Asymptotic enumeration of constellations and related families of maps on orientable surfaces. *Combinatorics, Probability, and Computing*, 18 (4):477–516, 2009.
- [23] G. Chapuy. *Combinatoire bijective des cartes de genre supérieur*. PhD thesis, École Polytechnique, 2009.
- [24] G. Chapuy, É. Fusy, O. Giménez, B. Mohar, and M. Noy. Asymptotic enumeration and limit laws for graphs of fixed genus. *J. Combin. Theory Ser. A*, 118(3):748–777, 2011.
- [25] G. Chapuy, É. Fusy, O. Giménez, and M. Noy. On the diameter of random planar graphs. In *DMTCS Proceedings, 21st International Meeting on Probabilistic, Combinatorial, and Asymptotic Methods in the Analysis of Algorithms (AofA '10)*, 2010.
- [26] P. Chassaing and G. Schaeffer. Random Planar Lattices and Integrated SuperBrownian Excursion. *Probab. Theory Related Fields*, 128(2):161–212, 2004.

- [27] R. Cori. Un code pour les graphes planaires et ses applications. *Astérisque*, 27:1–169, 1975.
- [28] R. Cori. Planarité et algébricité. *Astérisque*, 38–39:33–44, 1976.
- [29] R. Cori and B. Vauquelin. Planar maps are well labeled trees. *Canad. J. Math.*, 33(5):1023–1042, 1981.
- [30] M. Drmota. Systems of functional equations. *Random Structures Algorithms*, 10(1-2):103–124, 1997.
- [31] M. Drmota, O. Giménez, and M. Noy. Vertices of given degree in series-parallel graphs. *Random Structures Algorithms*, 36(3):273–314, 2010.
- [32] P. Duchon, P. Flajolet, G. Louchard, and G. Schaeffer. Boltzmann samplers for the random generation of combinatorial structures. *Combin. Probab. Comput.*, 13(4–5):577–625, 2004. Special issue on Analysis of Algorithms.
- [33] B. Eynard. *Counting surfaces*. Springer, 2011.
- [34] P. Flajolet and R. Sedgewick. *Analytic combinatorics*. Cambridge University Press, 2009.
- [35] P. Flajolet, P. Zimmerman, and B. Van Cutsem. A calculus for the random generation of labelled combinatorial structures. *Theoretical Computer Science*, 132(1-2).
- [36] É. Fusy. Counting unrooted maps using tree-decomposition. *Séminaire Lotharingien de Combinatoire*, B54A1, 2007.
- [37] É. Fusy. Uniform random sampling of planar graphs in linear time. *Random Struct. Algorithms*, 35(4):464–522, 2009.
- [38] J. Gao and N. Wormald. The size of the largest components in random planar maps. *SIAM J. Discrete Math.*, 12(2):217–228, 1999.
- [39] O. Giménez and M. Noy. Asymptotic enumeration and limit laws of planar graphs. *J. Amer. Math. Soc.*, 22:309–329, 2009.
- [40] M. Krikun. Explicit enumeration of triangulations with multiple boundaries. *Electronic J. Combin.*, v14 R61, 2007.
- [41] J.-F. Le Gall. A conditional limit theorem for tree-indexed random walk. *Stochastic Process. Appl.*, 116:539–567, 2006.
- [42] J.-F. Le Gall. The topological structure of scaling limits of large planar maps. *Invent. Math.*, 169(3):621–670, 2007.

- [43] J.-F. Le Gall. Geodesics in large planar maps and in the brownian map. *Acta Math.*, 205(2):2088–2960, 2010.
- [44] J.-F. Le Gall. Uniqueness and universality of the Brownian map. *Ann. Probab.*, 41:2880–2960, 2013.
- [45] J.-F. Marckert. The lineage process in galton-watson trees and globally centered discrete snakes. *Annals of Applied Probability*, 2008.
- [46] J.-F. Marckert and G. Miermont. Invariance principles for random bipartite planar maps. *Ann. Probab.*, 35(5):1642–1705, 2007.
- [47] J.-F. Marckert and A. Mokkadem. Limit of normalized random quadrangulations: the brownian map. *Ann. Probab.*, 34(6):2144–2202, 2006.
- [48] G. Miermont. An invariance principle for random planar maps. In *Fourth Colloquium on Mathematics and Computer Sciences CMCS’06*.
- [49] G. Miermont. The Brownian map is the scaling limit of uniform random plane quadrangulations. *Acta Math.*, 210:319–401, 2013.
- [50] G. Miermont and M. Weill. Radius and profile of random planar maps with faces of arbitrary degrees. *Electron. J. Probab.*, 13:79–106, 2008.
- [51] R. Nedela. Maps, hypermaps and related topics, 2007.
- [52] A. Nijenhuis and H. S. Wilf. *Combinatorial algorithms*. Academic Press, 1978.
- [53] M. Noy. Private communication, Sept. 2012.
- [54] J. Pitman. Coalescent random forests. *J. Comb. Theory, Ser. A*, 85(2):165–193, 1999.
- [55] G. Schaeffer. Bijective census and random generation of Eulerian planar maps with prescribed vertex degrees. *Electron. J. Combin.*, 4(1):14 pp., 1997.
- [56] G. Schaeffer. *Conjugaison d’arbres et cartes combinatoires aléatoires*. PhD thesis, Université Bordeaux I, 1998.
- [57] G. Schaeffer. Random sampling of large planar maps and convex polyhedra. In *Proceedings of the ACM Symposium on Theory of Computing*, pages 760–769. ACM, New York, 1999.
- [58] W. Schnyder. Planar graphs and poset dimension. *Order*, 5:323–343, 1989.

- [59] D. Singerman and J. Wolfart. Cayley graphs, cori hypermaps, and dessins d'enfants. *Ars Mathematica Contemporanea*, Vol 1, No 2:144–153, 2008.
- [60] W. T. Tutte. A census of planar triangulations. *Canad. J. Math.*, 14:21–38, 1962.
- [61] W. T. Tutte. A census of slicings. *Canad. J. Math.*, 14:708–722, 1962.
- [62] W. T. Tutte. A census of planar maps. *Canad. J. Math.*, 15:249–271, 1963.

## Résumé

La combinatoire bijective est un domaine qui consiste à étudier les propriétés énumératives de familles d'objets mathématiques en exhibant des bijections (idéalement explicites) qui préservent ces propriétés entre de telles familles et des objets déjà connus. Cela permet alors d'appliquer tous les outils de la combinatoire analytique à ces nouveaux objets, afin d'en obtenir une énumération explicite, des propriétés asymptotiques, ou encore d'en faire la génération aléatoire.

Dans cette thèse, nous nous intéresserons aux cartes planaires qui sont des graphes dessinés dans le plan sans croisement d'arêtes. Dans un premier temps, nous retrouverons une formule simple – établie par Eynard – pour la série génératrice des *cartes biparties* et *cartes quasi-biparties* avec des bords de longueurs définies, et nous en donnerons la généralisation naturelle aux *p-constellations* et *quasi-p-constellations*. Dans la seconde partie de cette thèse, nous présenterons une bijection originale pour les *cartes simples* – sans boucles, ni arêtes multiples – à *face externe triangulaire* et les *triangulations eulériennes*, nous permettant notamment de faire la génération aléatoire des cartes simples enracinées en contrôlant le nombre de sommets et d'arêtes. Grâce à cette bijection, nous étudierons également les propriétés métriques des cartes simples en démontrant la convergence du *profil normalisé des distances* vers une mesure aléatoire explicite liée au *serpent brownien*.

## Abstract

Bijective combinatorics is a field which consists in studying the enumerative properties of some families of mathematical objects, by exhibiting bijections (ideally explicit) which preserve these properties between such families and already known objects. One can then apply any tool of analytic combinatorics to these new objets, in order to get explicit enumeration, asymptotics properties, or to perform random sampling.

In this thesis, we will be interested in planar maps – graphs drawn on the plane with no crossing edges. First, we will recover a simple formula – obtained by Eynard – for the generating series of *bipartite maps* and *quasi-bipartite maps* with boundaries of prescribed lengths, and we will give a natural generalization to *p-constellations* and *quasi-p-constellations*. In the second part of this thesis, we will present an original bijection for *outer-triangular simple maps* – with no loops nor multiple edges – and *eulerian triangulations*. We then use this bijection to design random samplers for rooted simple maps according to the number of vertices and edges. We will also study the metric properties of simple maps by proving the convergence of the rescaled *distance-profile* towards an explicit random measure related to the *Brownian snake*.